The influence of weathering on the engineering soil profile:

a study of low relief basalts in South Africa

by

HAM van Rensburg

2018

The influence of weathering on the engineering soil profile:

a study of low relief basalts in South Africa

by

HAM van Rensburg

Submitted in fulfilment of the requirements for the degree

Magister Scientiae in Engineering and Environmental Geology

in the Faculty of Natural and Agricultural Sciences

University of Pretoria
Pretoria

2018

ABSTRACT

The high relief or mountainous basalt in and around the regions of Lesotho has extensive information on the nature and properties of the basalts, as a result of several developments on these basalts such as the Lesotho Highlands Water Project. This resulted in a wide variety of research conducted and published. In contrast, less published research is conducted on the lower relief or flat lying basalts leading to fewer available information on the nature and properties of low relief basalt deposits.

Five flat lying basalt sites were investigated in order to gather data on low relief/flat lying basalts. The two main sites of this investigation were researched in the Kruger National Park (KNP) on the southern basalts (Nhlowa) a high rainfall area, and on the northern basalts (Mooiplaas) a low rainfall area. These are two of four research supersites created in the Kruger National Park in order to create cross-disciplinary data rich sites. A mineralogical and chemical analysis for comparison of the parent rock and soil profiles between these two sites were undertaken. The Sibasa Formation basalts at Siloam and the Springbok Flats basalts at Roedtan and Codrington are three additional low relief basalt sites, in different rainfall areas. These sites were investigated to compare to each other and to the KNP sites.

XRF and XRD data were used together with profile development in their respective different climatic environments and basalt origins to determine the weathering progression and characteristic of low relief basalts. This was done by studying the depletion and enrichment of major and trace elements (Fe, Ca, Mg, Na, K, Ti, Y, Zr) through the profile from basaltic rock to residual soil. Furthermore, identifying the breakdown of primary minerals, such as Augite and Plagioclase, to secondary Smectite minerals further supports the identification of weathering progression in low relief basaltic rock. This can potentially aid in pre-planning of engineering geological investigations on residual basaltic soils. Additional information on the Atterberg Limits will also be presented in order to start to determine the effect low relief basalt weathering has on the engineering properties of the residual basalt soils.

In setting out to determine the influence different climatic conditions contribute to the weathering process and soil profile development of low relief basalts, it became clear that research of a specific rock type in a single setting is not sufficient. In order to truly understand the behaviour of basalt weathering, a combination of low relief, mountainous other settings in variable climatic conditions are necessary. This study shows the significant effect a moderate shift in climatic conditions such as rainfall and evaporation intensity have on the development of residual soils on low relief basalts, such as pedocrete and secondary mineral formations.

The influence of weathering on the engineering soil profile:

a study of low relief basalts in South Africa

TABLE OF CONTENTS

Page

LIST OF FIGURES

LIST OF TABLES

The influence of weathering on the engineering soil profile:

a study of low relief basalts in South Africa

1. INTRODUCTION

Extensive geotechnical data exist for the high relief or mountainous basalts in and around Lesotho, due to the development of dams and roads of large projects such as the Lesotho Highlands Water Project. Only sporadic data are available on the low relief or flat lying basalts scattered across South Africa, such as the Lebombo basalts present in the Kruger National Park (KNP), the Sibasa basalts at the foot and in the valleys of the Soutpansberg and the Springbok Flats basalts between Gauteng and Limpopo.

The low relief basalts are believed to experience deeper in-situ weathering and therefore have thicker residual soils than the mountainous basalt in and around Lesotho. The data available for these high relief basalts with intersecting valleys are not representative of the low relief basalts. This research study set out to investigate these low relief basalt sites in order to add to the sparse data of this subject. The main focus of this study revolves around two of the four Research Supersites created in the Kruger National Park, specifically the northern (Mooiplaas) and southern (Nhlowa) basalt sites falling in different rainfall intensity zones. Three other low relief basalt sites outside the pristine conditions of the KNP were also studied. These additional sites were at Siloam underlain by the Sibasa Formation basalts in the Soutpansberg, and the Springbok Flats basalts, of the Karoo Supergroup, at Roedtan and Codrington. These sites were also chosen based on different climatic conditions and availability of data.

These five sites were used to investigate the weathering and residual profile development of basaltic rock, based on the different climate circumstances of variable rainfall and evaporation. In order to determine and indicate progression of weathering from rock to residual material, X-Ray Fluorescence (XRF) and X-Ray Diffraction (XRD) analyses were utilized to determine the rock and soil chemistry. This also aided to indicate the different elemental exchanges that occur between high and low rainfall areas. Specifically portraying the depletion and enrichment of main elements such as Calcium and Iron between sites in the profile, which may lead to the formation of either ferricrete or calcrete. A distinct difference of ferricrete or calcrete formation was noticed between sites with different climatic environments.

A look at previously believed immobile elements such as Titanium (Ti) and the trace elements Yttrium (Y) and Zirconium (Zr) was also done in order to portray progression of weathering on an elemental scale.

Therefore, the aim of this study is to determine the influence different climatic environments have on the weathering and soil development of the scarce researched topic of low relief basalts.

In pursuit of the aim the objectives of the study are as follows:

- Add data and knowledge to the engineering geology of low relief basalts;
- Provide chemical and mineralogical data of low relief basalts in different climatic environments;
- Indicate the differences in weathering products and chemical changes occurring during weathering in the various low relief basalts in different climatic environments;
- Indicate the climatic effect and influence of basalt mineralogy on pedocrete formation.

2. LITERATURE REVIEW

2.1 Basaltic rock

Basaltic rock is the most abundant volcanic rock on Earth, creating the upper layer of the oceanic basins, forming large lava flows in many regions on the continental crust as well as forming islands from many well-known volcanos such as Hawaii and Iceland (Klein and Dutrow, 2007). Basalt is a dark coloured extrusive (being exposed to the cold atmosphere) igneous rock resulting in a fine-grained rock texture as opposed to the coarser grained intrusive gabbro equivalent. Basalt is classified as a mafic rock due to it being rich in magnesium (Mg) and iron (Fe) and poor in silica (SiO_2) as opposed to its felsic counterpart, Rhyolite, which is high in Si and alkali metals and poorer in Fe and Mg. The common major mineral assemblages in Basalt are pyroxene (ortho- and clinopyroxene) and calcium rich plagioclase such as anorthite. Olivine and augite are also frequently present with olivine mostly as phenocrysts, and augite present as both phenocrysts and the groundmass (Klein and Dutrow, 2007).

A basaltic rock can be created from a mafic magma series which can be divided into two possible groups *viz.*, alkaline and subalkaline, where the subalkaline group is further divided into tholeiitic and calc-alkaline basalt. The calc-alkaline series is mostly restricted to complex convergent plate boundaries (Winter, 2001) although also dominated by continental arcs (Tatsumi and Suzuki, 2009). Tholeiitic basalts are typically generated at mid-oceanic ridges, intra-oceanic arcs and scattered intra-plate volcanic occurrences, whereas alkaline basalts are constrained to intra-plate incidences (Winter, 2001 and Tatsumi and Suzuki, 2009). A summary of the characteristics of tholeiitic basalt from the subalkaline group and alkaline group can be seen below in **Figure 1**.

	Tholeiitic Basalt	Alkaline Basalt
Groundmass	Usually fine-grained, intergranular	Usually fairly coarse, intergranular to ophitic
	No olivine	Olivine common
	Clinopyroxene = augite (plus possibly pigeonite)	Titaniferous augite (reddish)
	Orthopyroxene (hypersthene) common, may rim ol.	Orthopyroxene absent
	No alkali feldspar	Interstitial alkali feldspar or feldspathoid may occur
	Interstitial glass and/or quartz common	Interstitial glass rare, and quartz absent
Phenocrysts	Olivine rare, unzoned, and may be partially resorbed or show reaction rims of orthopyroxene	Olivine common and zoned
	Orthopyroxene uncommon	Orthopyroxene absent
	Early plagioclase common	Plagioclase less common, and later in sequence
	Clinopyroxene is pale brown augite	Clinopyroxene is titaniferous augite, reddish rims

after Hughes (1982) and McBirney (1993).

Figure 1: Characteristic summary of Tholeiitic and Alkaline basalts (Winter, 2001).

The alkaline basalts are also characterized by a low silica content (silica-undersaturated) and higher contents of alkalis such as sodium (Na_2O) and potassium (K_2O) than the tholeiitic basalt series. The tholeiitic basalt series contain higher iron (Fe) content whereas the calc-alkaline comprises of more magnesium (Mg) and alkalis (Na_2O+K_2O) than tholeiitic basalt, as portrayed by the AFM diagram in

Figure 2.

The most distinct difference between tholeiitic and calc-alkaline magma series is the redox state the magma has crystalized from. Tholeiitic magma is mostly formed from a reduced magma state and calc-alkaline magmas from an oxidized state.

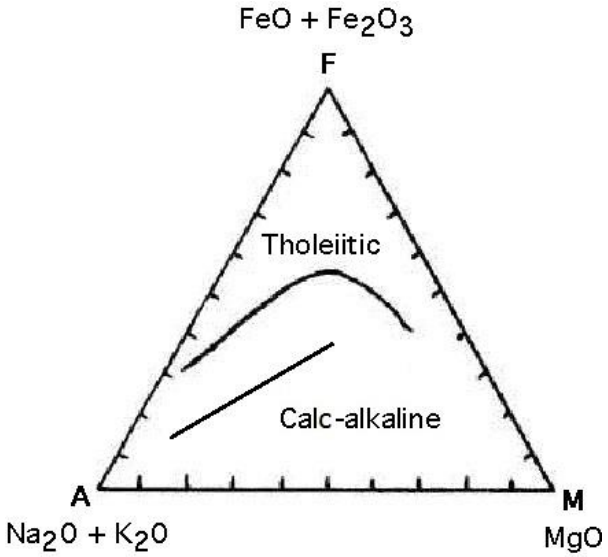

Figure 2: AFM diagram showing element abundance between Tholeiitic and calc-alkaline basalts (adapted from Winter, 2001).

This creates an excess of iron in the melt as iron poor minerals are depleted. The oxidized state of a calc-alkaline melt produces enough magnetite (containing iron oxide) to keep the iron content in the magma steady as it cools (Winter, 2001). Picritic basalt is basaltic rock which contains high amounts of magnesium rich olivine as phenocrysts together with pyroxene and augite.

The AFM diagram in

Figure 2 above portrays this formation of magnesium/iron rich minerals. As the tholeiitic magma series cools and preferentially create Mg rich minerals, the Mg content in the melt decreases. This results in the melt to progress to a higher iron concentration, whereby Fe rich minerals are then preferentially created. After the iron content reserves have also been exhausted the melt progresses to an alkali concentration to form alkali rich minerals. In this process some Mg and Fe rich minerals get re-melted and get used in the alkali mineral formation. In contrast to this, due to the calc-alkaline magma precipitating magnetite, the ratio between Fe to Mg remains constant as they are depleted evenly, therefore the melt concentration progresses in a straight line towards the alkali corner. The preferential crystallization of magnesium rich silicate minerals can occur

within the tholeiitic melt if not re-melted. Tholeiitic and calc-alkaline rocks have been found together indicating a differential fractional crystallization of a magma series to create both rock types (Tatsumi and Suzuki, 2009).

2.2 South African Basalts

An account of most basalt appearances across South Africa in geological chronology will follow. Significant occurrences of Groups/Subgroups/Formations will be elaborated on where lesser or smaller Formations/Beds will only be mentioned.

The oldest account of a basaltic type rock in South Africa is in the Lower Onverwacht Group, Barberton Supergroup and dates back 3 600 to 3 200million years (Ma). These are referred to as komatiites (also termed komatiitic basalts) which are similar to basalt although has different chemical compositions, noticeably a much higher magnesium (Mg) content. These rocks were first discovered in the Komati River valley east of Badplaas, Mpumalanga Province. The Upper Onverwacht Group overlays the Lower Onverwacht Group and consists of basalt and dacite separated by a sedimentary Middle Marker. These volcanic rocks as well as sedimentary rocks overlying them has a dark green colour and are collectively referred to as the greenstone belt. In this specific area it is termed the Barberton Greenstone Belt (BGB), situated south and southeast of Nelspruit occupying and area of 120 x 50km (McCarthy and Rubidge, 2005 and Brandl et al., 2006). The area south of the BGB has a number of greenstone belt fragments of different sizes. Such as the greenstone belt fragment in northern Kwazulu-Natal containing the Nondweni fragment/Group which created the southern boundary of the Kaapvaal Craton 60km north of the Tugela thrust front. The Nondweni Group also comprise of komatiitic basalt, basalt and basalt andesites in the Magongolozi and Witkop Formations (Brandl et al., 2006).

The Nsuze Group of the Pongola Supergroup consists mainly of volcanic rocks (basalt/andesite) which are interlayered with clastic sedimentary beds dating to around 3 074Ma (McCarthy and Rubidge, 2005 and Gold, 2006). A ~250m thick basalt layer is present in the Crown Formation of the Jeppestown Subgroup from the West Rand Group, as well as in the Bird Reef member of the Krugersdorp Formation in the Johannesburg Subgroup from the Central Rand Group. They fall collectively under the Witwatersrand

Supergroup which was dominated by sedimentation and contains mostly sedimentary rocks. These rocks date back to approximately 2 910Ma (McCarthy and Rubidge, 2005 and McCarthy, 2006).

The extended sedimentation period of the Witwatersrand Supergroup was terminated as a result of intense uplift which resulted in the rupture of the Kaapvaal Craton. This uplift created large fractures to form in the crust leading to vast amounts of very low viscous basalt to erupt and flow across the land surface, approximately 2 714Ma (McCarthy and Rubidge, 2005). This created a unique volcanic-sedimentary supercrustal record forming the Ventersdorp Supergroup. The majority of the extruded mafic lava form part of the Klipriviersberg Group (the bottom section of the Ventersdorp Supergroup) and is described as mainly tholeiitic basalts with a mild calc-alkaline affinity. Komatiitic basalts are found at the base of the Klipriviersberg Group in the Meredale Member of the Westonaria Formation (van der Westhuizen et al., 2006). At 2 700Ma the Zimbabwe Craton in the north and the Kaapvaal Craton in the south collided creating the Limpopo Belt. As a result of this collision the Kaapvaal Craton developed numerous fractures and fissures from where a bimodal assemblage of mafic and felsic lavas poured. Before and between eruption events erosion and sedimentation were dominant due to the elongated valleys created by the collapse of the highlands of the Central Rand Group, this caused the development of the Platberg Group of the Ventersdorp Supergroup. The basaltic and basaltic andesites are in minority in this group compared to the more dominant rhyolitic and sedimentary rock sequences. The Ventersdorp Supergroup ended with periodic eruptions of mafic lava creating the Allenridge Formation of the Pniel Group (McCarthy and Rubidge, 2005 and van der Westhuizen et al., 2006).

After a period of stability another crustal stretching and rifting event occurred around 2 650Ma, leading to the deposition of sand and mud in these rifts with occasional basaltic lava eruptions. This created the Wolkberg Group forming part of the Blyde River Canyon. Thermal subsidence of the Kaapvaal Craton followed this new rifting event whereby most of the landmass subsided below the sea level to create a new continental shelf. This led to large deposits of sedimentation which created the Transvaal Supergroup dominated by sedimentary and dolomitic rocks with occasional basaltic eruptions. These eruptions include the Hekpoort formation containing basaltic andesite (rather better

known and termed the Hekpoort andesites) as well as tholeiitic basalt in the Silverton Formation (McCarthy and Rubidge, 2005 and Eriksson et al., 2006).

The deposition of the Transvaal Supergroup ceased 2 060Ma ago and was followed by the largest layered intrusion known in the world, namely the Bushveld Igneous Complex (BIC). This volcanic event extruded a range of mafic to felsic lavas creating three distinct components known as the Rooiberg Group, the Rustenburg Layered Suite (RLS) and the Lebowa Granite Suite. The lowest unit of the Rooiberg Group the Dullstroom Formation predominantly consists of basalt and basaltic andesite which intruded and overlies the Pretoria Group. Near Stoffberg, Mpumalanga Province, this formation is also present both above and below the Rustenburg Layered Suite. The Dullstroom Formation is only basaltic to basaltic andesitic at the base and becomes more felsic upward also containing pyroclastic and arenaceous layers. Basalt does not occur in any other layers in the Bushveld Igneous Complex with the Rustenburg Layered Suite primarily made up of a range of rock types such as dunite, pyroxenite, norite, gabbro, anorthosite and magnetite to apatite rich diorite. These rocks are mostly the intrusive equivalent of basalt with some chemical and mineralogical differences. The position of the RLS in the central part of the BIC resulted in a longer time for the magma to cool and therefore sufficient time for crystal growth. The Lebowa Granite Suite as the name suggests is comprised of acid igneous rocks (McCarthy and Rubidge, 2005 and Cawthorn et al., 2006).

A couple of hundred million years after the deposition of the Transvaal Supergroup the Waterberg and the Soutpansberg Groups were deposited in an environment showing first accounts of an atmosphere with free oxygen. This resulted in the oxidation of the iron in the rocks to iron oxide creating a red colouration to the sediments. The Waterberg Group predominantly consists of sedimentary rocks with some interlayered granites from the Bushveld Igneous Complex as well as more mafic lavas in the Nelspruit Subgroup (McCarthy and Rubidge, 2005 and Barker et al., 2006).

The lower units of the Soutpansberg Group contain more basaltic rock occurrences which forms the Sibasa basalt Formation which erupted approximately 1 769Ma ± 34Ma ago with repetitive and cyclical eruptions, slightly exposed to air. Therefore, zones of lenticular pyroclastic rocks are found in the basalt as well as

intercalations of clastic sediments laterally though the rock mass (Baker, 1979; cited in Barker et al. 2006). The Sibasa basalts are described as dark green and massive with zones of white amygdales, the rock usually is epidotised. According to Baker (1979; cited in Baker et al. 2006) clinopyroxene and plagioclase are visible between the epidote, chlorite and quartz matrix in less altered rocks. The Sibasa basalts are predominantly volcanic rocks that reaches an estimated thickness of 3 000m, numerous lenticular laterally persistent clastic sediment intercalations are also present. These clastic sediments are mostly quartzite, shale and some conglomerate beds that reaches thicknesses of 400m (Barker et al., 2006).

Further intercalated epidotized basalt layers between the sedimentary layers are present in the overlying Fundudzi and Musekwa Formations of the Soutpansberg Group. The Fundudzi Formation has an approximate 50m thick basalt layer and the Musekwa Formation a 400m thick layer which are very similar to the Sibasa Formation although it has individual layers that show a coarse gabbroic texture. These former two Formations are only present and visible in the central and eastern Soutpansberg area (Barker et al., 2006).

Approximately 190Ma ago the Karoo sedimentation was terminated due to ruptures in the Earth's crust when compression of the crust during the Karoo sedimentation relaxed. This led to a large amount of basalt pouring out onto the Clarens Formation that resulted in the Karoo Flood Basalt Province. The Karoo basalts are mostly distinguished as the Drakensburg Group, although a second eruption event to the east along the Mozambique border resulted in the Lebombo Group basalts (McCarthy and Rubidge, 2005). The Drakensberg and Lebombo Groups constitute the uppermost units of the Karoo Supergroup (McCarthy and Rubidge, 2005). The eruptions of the lava mainly occurred from long fissures in the earth's crust and flowed as massive sheets typically between 10 to 20m thick. A large portion of the lava from the Lebombo Group also consists of a felsic melt forming rhyolitic rock. Although the majority of the Lebombo Group contain silica rich rocks there are still formations that are basaltic in origin such as the Letaba, Sabie River and Movene Formations (from oldest to youngest).

The Drakensberg Group which constitute the main body of flood basalts covering the Karoo sediments is made up of the Barkley East and Lesotho Formations (Duncan

and Marsh, 2006). The total thickness of the Drakensberg Group is approximately 1 400m, created by several rapid and successive low viscosity lava flows.

Olivine basalt is the dominant basalt type with different degrees of amygdale content of non-amygdaloidal, moderately amygdaloidal (less than 10% amygdales) and highly amygdaloidal types (Bell and Haskins, 1997). The individual lava flows are mostly characterized by three zones, the basal, central and upper zone. The basal zone is characterized with moderate to high amygdale content with distinctive pipe amygdales. This formed as trapped gas in the lava progressed upwards due to the rapid cooling of the basalt, when it made contact with the floor rocks on which it extruded, this formed fine grained basalt. The central zone contains no or very few amygdales compared to the basal and upper zones. This zone also has more time to cool which resulted in medium to coarse grained basalt. The upper zone is again fine grained with the highest occurrence of amygdales as well as volcanic glass due to rapid cooling on exposure to the atmosphere. The flow contacts show very little weathering due to the rapid extrusion of the various basalt flows following on one another (Bell and Haskins, 1997).

The Letaba Formation is described as picritic (olivine-rich) basalt, forming the main mafic unit in the northern Lebombo area that thins out towards the 25° S line. The Sabie River Formation overlies the Letaba formation from here with olivine-poor tholeiitic basalt which extends southwards to the end of the Lebombo mountain range west of Richards Bay, KwaZulu-Natal. Following these two dominant basalt units are two silicic sequences of the Jozini and Mbuluzi Formations ending in the Movene basalt Formation that has interbedded rhyolitic flows. The Movene Formation is confined to Mozambique with a small portion present in northern Kwazulu-Natal just south of Mozambique (Duncan and Marsh, 2006).

The inter-continental volcanic eruptions which created the Drakensberg and Lebombo basalts and terminated the Karoo sedimentation only lasted approximately two million years. Following this volcanic event most of South Africa experienced uplift in conjunction with intense erosion, this removed large parts of the previously extensive lava sheets. Although uplift dominated most of South Africa, a region in the central Bushveld experienced subsidence which led to the preservation of the Karoo sedimentation and volcanics, now known as the Springbok Flats Basin (McCarthy and Rubidge, 2005).

The Springbok Flats Basin is an extremely flat-lying section of the African erosion surface which extends from Modimole (Nylstroom) to Mokopane (Potgietersrus) (McCarthy and Rubidge, 2005). Outcrops are virtually absent in the exceedingly flat area of the Springbok Flats Basin, therefore information on the stratigraphy of the basin was mostly acquired from borehole data conducted by the Geological Survey (Johnson et al., 2006). This borehole data indicates that the preserved Karoo basalts in the basin has a maximum thickness of 460m in the north-eastern basin section and more than 750m in the south-western basin section (Marsh, 1984).

The basalts of the Springbok Flats, according to SACS (1980; cited in Marsh, 1984), was originally correlated to the Letaba Formation of the Lebombo Group. This name was collectively given to all basalts that were located below the rhyolites in Lebombo. After additional investigations it was however found that the basalts of the Springbok Flats were chemically and petrographically different to the Letaba Formation basalts. From additional data presented by Marsh (1984) the Springbok Flats basalts more closely associates to the Sabie River Formation and Lesotho Formation (the Drakensberg's Formation equivalent in Lesotho), although having a stronger supporting correlation to the former.

2.3 Weathering of Basalt

The engineering properties of any rock or residual soil is dependent on the degree and/or type of weathering the rock has undergone. Basalt is a basic crystalline rock, consequently the rock can undergo chemical and physical weathering (decomposition and disintegration) depending on the climate. Physical weathering is the process by which a rock mass is broken down mechanically into smaller fractions of the original rock material and eventually individual mineral grains. Through physical weathering the fresh rock surface is exposed to the atmosphere to be influenced by chemical weathering (Bih Che, 2012), if present in a climate which would induce chemical weathering. When chemical weathering is dominant the mineralogy and chemistry of the rock material are affected, creating mineralogical and geochemical changes, witnessed through textural changes to the rock.

These mineral and geochemical changes are achieved through a range of different processes such as hydration, hydrolysis, oxidation, reduction, carbonation, dissolution, leaching, precipitation and enrichment which leads to the formation of secondary minerals which in turn reduces the strength of the rock. This is based on the principal that minerals in an igneous rock that crystalized under high temperatures and pressures are intrinsically unstable at the current atmospheric conditions. These minerals react readily to change to more stable minerals such as clay minerals (Bih Che, 2012 and Paige-Green, 2007).

The chemical, mineralogical and physical properties of rocks change when weathered, creating weaker material that is difficult to use as engineering material or to engineer structures on (Moon and Jayawardane, 2004). This was observed with variation in performance of weathered dolerite and basalt in road construction, due to the varying degrees of weathering the rocks have undergone, as a result of different climatic conditions (Weinert, 1980). Non-uniform weathering and redistribution of elements result in the creation and accumulation of secondary (clay) minerals which create heterogeneity in a rock mass or soil (Bih Che, 2012).

The different climatic environments and influences on the weathering of rock and residual soil development is best represented by Weinert's climatic N-value. This is calculated from the total annual precipitation and maximum evaporation month in the year (which usually is January in South Africa) times a factor of 12 to represent the year. The N-value is calculated according to the equation below (Weinert, 1980):

$$N = \frac{12.Ej}{Pa} \qquad \text{Equation 1}$$

Where E_j = evaporation during January

P_a = annual precipitation

The most significant integers to regard for the N-value from this calculation is N=1, N=2, N=5 and N=10. Where N>5 represents more arid areas with rainfall of approximately less than 550mm per annum. More humid areas are represented by N<5 that has higher rainfall of approximately more than 800mm per annum (Weinert, 1980 and AFCAP, 2012).

In very high humidity areas where Weinert's climatic N value is less than 2, deep residual soils would develop with a strong development of secondary minerals such as smectite, notably montmorillonite, due to decomposition as the dominant mechanism. Similar conditions are found in sub-humid areas where N is between 2 and 5 with a decreased residual soil thickness compared to N<2 areas. Disintegration becomes more influential as N approaches 5, with smectite minerals developing only after extended weathering. In climatic areas where N>5 and approaching N=10 disintegration would be dominant resulting in a thin residual soil cover, where decomposition of crystalline rock would be insignificant, only a few secondary minerals would develop (Brink, 1979 and Weinert, 1980).

Generalizing Weinert's N-value, areas of N<5 tend to have higher concentrations of iron and aluminium oxides, where areas of N>5 or approaching 5 have a higher concentration of soil carbonates (Brink, 1979). As indicated above, rainfall is not the only deterministic factor for the calculation of Weinert's climatic N value, evaporation in the area also plays a significant role.

Small areas exist, due to topography such as mountainous areas, with different rainfall and evaporation conditions creating localized contrasting N values (Brink, 1979 and 1983 and Weinert, 1980). An area with a high rainfall and high evaporation will have similar N-values to an area that has lower rainfall and low evaporation. **Figure 3** indicates the N=5 line in southern Africa with specific climatic N-values indicated.

The Drakensberg and Lebombo Group basalts in South Africa are located in areas where the N-value is between 2 and 5 which implies that decomposition with a degree of disintegration is present. As a result of the mountainous conditions of the Drakensberg, intensive erosion is present preventing deep residual profiles to form but rather created large exposures of fresh basalt, even though the climatic setting is favourable to chemical weathering (Sumner et al., 2009). The annual precipitation is around 1000mm (Bell and Haskins, 1997) indicating very low N-values. In lower relief and flat lying areas decomposition creates deep soil profiles such as on the Springbok Flats with highly active soils, this also occurs to a degree in the Lebombo Group basalts in the Kruger National Park (Brink, 1983).

When basalt is exposed to the atmosphere in environments closer to N=5 the rock preferentially disintegrates to coarse-grained material and is associated with strong development of calcretes (Brink, 1983).

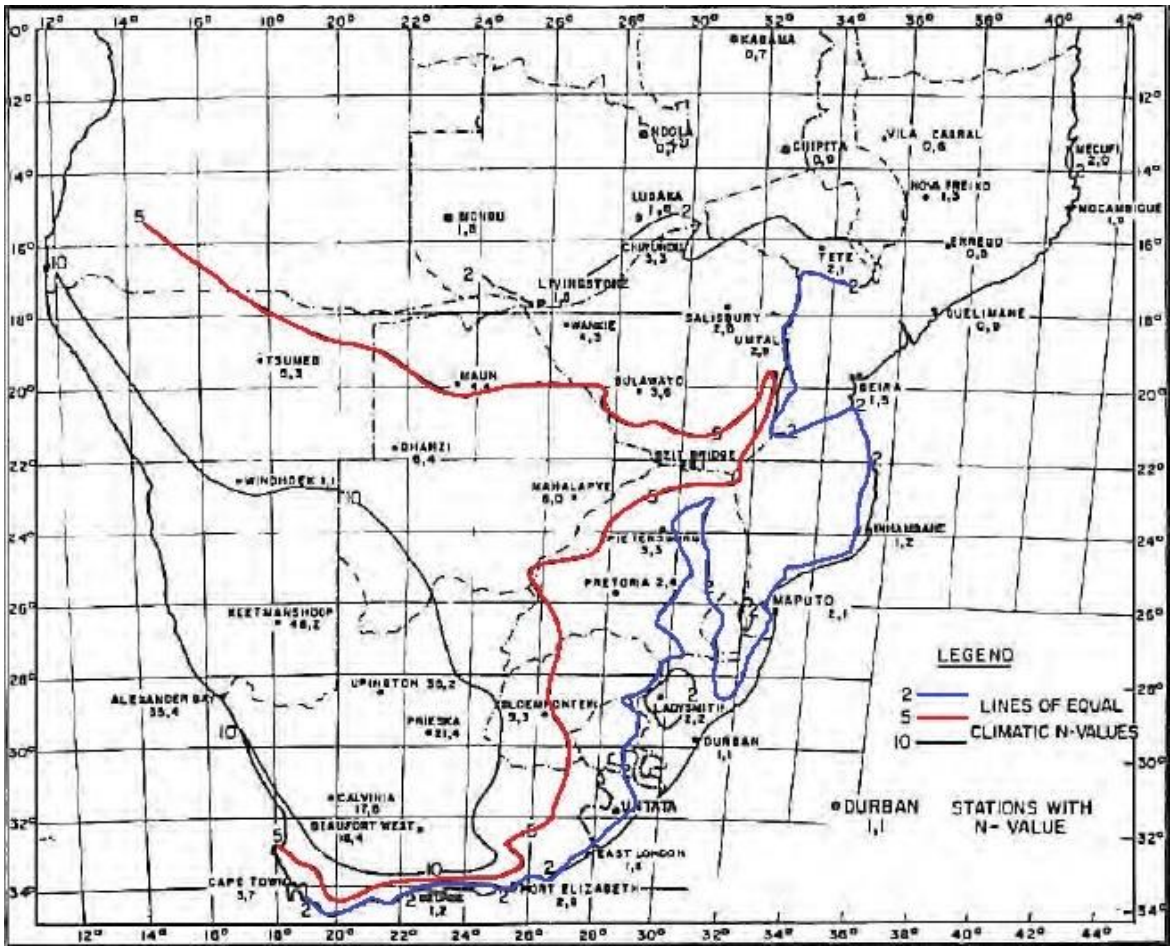

Figure 3: Weinert's climatic N-value, with N=2, N=5 and N=10 contour lines (adapted from Weinert, 1980).

With the decomposition of a basic crystalline rock, such as basalt, the breakdown and alteration of minerals will occur in conjunction with element exchange from the fresh basalt rock to a residual soil throughout the profile. Houston and Smith (1997) determined the degree of alteration of basalt by comparing a primary mineral in basalt to a weathered product or secondary mineral in basalt from New South Wales Australia. In their case using plagioclase feldspar (primary mineral) altering through decomposition to smectite clay (secondary mineral). Moon and Jayawardane (2004) investigated the Karamu basalts in New Zealand, and Hill et al. (2013) the basalts in northeast Ireland.

The abovementioned found that after initial weathering, Fe-rich smectites are the replacement product of weathered olivine and augite, and Al-rich smectites the replacement product of weathered plagioclase. The study of Bih Chi et al. (2012) on basaltic soils in humid tropic climates in south-western Cameroon, concentrated on the weathering of olivine, pyroxene, amphibole and calcic plagioclase as the principal minerals weathering from fresh rock to soil. These minerals forms first in the crystallization process and therefore the most unstable minerals that readily reacts to change compared to more stable minerals (Sumner et al., 2009). Bih Che et al. (2012) portrayed the variable weathering trends of major elements in basaltic material in humid climatic conditions, especially the alkali and alkali earth metals.

X-ray diffraction (XRD) is generally used to determine the secondary minerals as it is a fast, accurate and cost-effective way of determining alteration minerals. XRD spectra; a rapid semi-quantitative evaluation was used in the study of Houston and Smith (1997). XRD is a widely used analytical technique to determine the type, amount and textural distribution of altered or secondary minerals, such as plagioclase, olivine and augite altering to smectite clay minerals. This is used in order to predict the engineering quality of aggregates for use in road construction (Houston and Smith, 1997). The higher the percentage of smectite present in basalt the less usable it will be as a building and road aggregate, and residual soil will be less useful with an increase in plastic fines content from the presence of smectite.

It is generally accepted and researched that the expansion of these Smectite Group clays during the absorption of water is the main driving factor that deteriorates basic crystalline material such as basalt (Paige-Green, 2007). In the basalts of the Karoo Supergroup these clays or clay spots form as a result of deuteric alteration during the cooling and crystallization of the melt. Deuteric alteration occurs where volatiles and vapours from the magma are trapped immediately after or at the time of solidification in the cooling rock mass. This results in the formation of volcanic glass and initiates the alteration of the unstable primary minerals to change to secondary minerals. This is especially relevant to active swelling clays and secondary minerals such as; zeolites, chlorite, metallic oxides, montmorillonite and smectite clays (Bell and Haskins, 1997 and Paige-Green, 2007).

The volcanic glass, after formation, also start altering at an early stage to the minerals listed above (Bell and Haskins, 1997, Paige-Green, 2007 and Sumner et al., 2009). These secondary and clay minerals, specifically zeolite and metallic oxides, are present in the Termaber basalt in Central Ethiopia. This was discovered during the assessment of the rock mass for use as crushed aggregate and building stone (Engidasew and Barbieri, 2014). With olivine and plagioclase feldspar as the first formed minerals and therefore the most unstable minerals, they tend to be the minerals which alter first to these secondary and clay minerals. Olivine in basalt tend to be limited due to this high alteration to secondary minerals (Sumner et al., 2009). Engidasew and Barbieri (2014) notes that an olivine basalt will be more altered than an olivine free basalt due to olivine being more susceptible to alteration than augite. This can be attributed to olivine as a high temperature mineral.

This early on alteration of the primary minerals to secondary and active clay minerals is known as primary deuteric alteration. Secondary deuteric alteration occurs much later when mineralizing fluids percolate through the solid rock and then deuterically alter the remaining volcanic glass and primary minerals. This secondary deuteric alteration can be witnessed and occurs at vesicular cavities and amygdales that alters to these clay minerals (Bell and Haskins, 1997 and Sumner et al., 2009). These weathered amygdales and altered glass patches in the rock create clay spots in the rock mass which predominantly consist of montmorillonite (Bell and Haskins, 1997). Studies conducted on the Karoo basalts during the Lesotho Highlands Water Project found that montmorillonite is also the dominant replacing clay of olivine and plagioclase feldspar. The latter appearing fresh although still contain alteration zones on the mineral grain edges and cleavage plains in the form of montmorillonite (Sumner et al., 2009).

This all led to the now widely accepted fact that the main driving force that causes basalt deterioration, is the volume changes associated with dehydration and hydration of swelling clays and some zeolites present in the rock mass. This decreases the durability of basalt for use as aggregate, building material and pavement construction (Bell and Haskins, 1997).

Apart from mineralogical alterations such as the percentage of secondary minerals/clay content in a rock or residual soil, slight differences in terms of element exchange or movement can indicate that weathering or alteration is taking place. An indicator for slight weathering can be determined by the cation loss of a rock or soil (Eggleton, 2001 cited in Moon and Jayawardane, 2004). In the early stages of basaltic rock weathering the loss of Ca, Mg and Fe does not influence the change of mineralogy, but rather changes the structure of the crystal lattice which will lead and result in mineralogical changes (Moon and Jayawardane, 2004). The study conducted by Moon and Jayawardane (2004) focused on stages of weathered basaltic rock.

During the common weathering trend, basalt experiences a loss of mobile elements such as Mg^{2+}, Ca^{2+}, Na^{2+} and Fe^{2+} when transitioning from fresh basalt to a weathered state as well as an Fe^{3+} increase (Moon and Jayawardane, 2004). This indicates that in the initial processes of weathering iron oxidizes and basalt experiences a loss of cations. Two stages of element exchange were noted by Moon and Jayawardane (2004) *viz.* at the fresh to moderately weathered stage a rapid decrease in oxide concentrations (CaO, MgO, FeO) occur followed by smaller changes from moderately weathered onwards. Bih Che et al. (2012) displayed intense to complete decomposition of plagioclase from signs of strong depletion of K_2O, Na_2O and CaO, the alkali and alkali earth metals.

Liu et al. (1996, cited in Bih Che et al., 2012) as well as Bih Che et al. (2012) noticed higher concentrations of Fe family elements (Ti, V, Co, Cr and Ni) in basalt derived soils than the felsic counter parts. Bih Che et al. (2012) indicated that a greater emphasis should be placed on using density measurements for mass balance equations. This is to determine enrichment or depletion of an element, opposed to only relying on relationships of element concentration between parent rock and soil. This was observed by Bih Che et al. (2012) of elements that originally showed enrichment based on element concentration relationships, where after the density of the soil and parent rock was considered showed depletion of said element. This is due to a decrease in density from parent rock to highly weathered rock to soil, as a result of altered minerals that changed into secondary minerals. This leads to a progressive increase in porosity due to element loss/transfer (Bih Che et al., 2012).

As a result of utilizing the densities in the mass balance calculations, Fe and Al are shown to be leached in certain horizons and not experience enrichment as most humid tropic profile studies indicate. During the early phases of weathering, secondary minerals such as non-swelling clays, hydroxides and goethite that can host Al_2O_3, Fe_2O_3 and TiO_2 shows slight enrichment of these elements (Bih Che et al., 2012).

The study of Ameyan (1986) in northern Nigeria to determine the quality of land facet mapping, used the coefficient of variance (CV) of their data (soil texture and cation exchange capacity) in order to determine differences within a land facet and between different land facets. Ameyan (1986) stated that there should exist a smaller variance of the data within a land facet than between land facets in order to be grouped together or indicate change in a dataset. Ameyan (1986) regarded a land facet or similar dataset group as where the CV of a particular property is less than 33%. Whereby if it is greater than 33% it would indicate a high enough variance and result to grouping the particular property into a new land facet. The ranges of acceptable variance to land facets and further soil classification and mapping are subjective and freely chosen. Although, the effectivity of soil mapping or determination of the extent of change or variance of a dataset is determined by the goals and objectives set out on what needs to be determined and achieved (Ameyan, 1986).

Moon and Jayawardane (2004) determined an increase in trace element concentrations in the initial weathering stages from fresh to moderately weathered basalt. This could only be an apparent concentration increase that reflects the loss of Ca, Mg and Fe instead of an inflow of trace elements into the system. The loss of the major elements Ca, Mg and Fe are accompanied by the trace elements Rb and Sr, especially with Ca due to similar ionic radii, therefore it is lost out of the system in similar manners. Bih Che et al. (2012) also experienced Sr as the most mobile trace element in their study, relating it to the decomposition of plagioclase. Sato et al. (1990, cited in Bih Che et al., 2012) as well as Bih Che et al. (2012) noticed that the Fe_2O_3/MgO concentration decreased in the rocks from Mt. Cameroon as the Ni and Cr concentrations increased, from fractional crystallization model estimates. They also indicated that with an increase in weathering the iron group elements would be enriched as silica, alkali and alkali earth metals get depleted.

It has been assumed that Yittrium (Y) is an immobile trace element in the alteration and weathering of crystalline basalt. Although under extreme weathering conditions with the formation of basalt derived laterites it is found that yittrium is leached out and is mobile (Hill et al. 2013). In contrast to this Bih Che et al. (2012) noticed in their study that with increased weathering intensity, Y progressively increased. Similarly, they noticed that as weathering progresses most trace elements (Ba, Y, Zr, V, Ni, Co and Ce) showed a relative enrichment, the most weathered sections having the highest concentrations. Hill et al. (2013) noticed in their study that the Titanium (Ti) content increases from fresh basalt to laterite formation, whereby it was previously considered immobile during weathering. Zirconium (Zr) also follows a similar trend of increase (assumed to be immobile) whereas Y concentrations decreases from fresh basalt to weathered products. Similar to this, the study conducted by Bih Che et al. (2012) also found mobilization of Ti and Zr from parent rock to residual soil, indicating that these elements are not immobile.

2.4 Pedogenesis

Pedocrete formation is a prominent product from the continuous exchange of elements and mineral alterations, through different weathering processes such as disintegration, decomposition, hydrothermal alteration, diffusion etc. Taking place together with continuous climate influences such as water table fluctuations, shallow seepage water, rainfall intensity and evaporation rates. Pedocretes are a combination of the in situ parent material and the different authigenic cement acquired through leaching and then relatively concentrated (Brink, 1985). The authigenic cement for pedocretes such as calcrete and ferricrete are formed when calcium carbonate ($CaCO_3$) and iron oxide (FeO) respectively are introduced into an existing soil, cementing or replacing the in situ material. This is done by deposition through groundwater or from the soil (AFCAP, 2012). Other pedocretes also include silcrete from silica, manganocrete from magnesium, phoscrete from phosphate and gypcrete from gypsum deposition (Brink, 1985). Collectively ferricrete, calcrete and silcrete are known as duricrusts, pedocretes or pedoderms are an important natural gravel group for the purpose of making roads (McNally, 2003). The terms ferricrete, calcrete and laterite should predominantly only be used if more than 50% of the pedocrete forming material is present (Brink, 1985).

The iron rich fluid and deposited material that forms ferricrete and laterite is focused around an Fe and Al sesquioxide-rich (Fe_2O_3+Al_2O_3) solution (McNally, 2003). Ferricrete or ferruginous pedocretes are formed through two main processes *viz.* absolute accumulation and relative accumulation, this also governs the formation of other pedocretes. Absolute accumulation is focused around the addition of the sesquioxides to the parent material. Whereas relative accumulation occurs when the soluble constituents in the parent material are removed by intense weathering and free draining that results in the sesquioxides to be concentrated. Even though these two processes usually occur together at some degree one process is usually dominant (Brink, 1985). Indurated ferricrete is predominantly formed through absolute accumulation from the upward, downward or lateral transportation of iron (Brink, 1985).

Laterite is an iron rich horizon created by the in-situ breakdown and dissolution of primary minerals with the removal of bases and silica, that got deposited in the horizons above the breakdown. This term is usually given to tropical soils that underwent advanced weathering (Brink, 1985 and Widdowson, 2003). Ferricrete differently to laterites are dependent on the transportation of the material from another source. In this study the term ferricrete will be collectively used for ferricrete and laterite, due to the difficult determination of the constituent material origin, as a consequence of the flat topography of the study sites (Widdowson, 2003).

Calcretes in South Africa are labeled by two processes *viz.* groundwater calcrete, where carbonate is deposited above a fluctuating shallow perched or permanent water table or lateral seepage of groundwater. The second process is pedogenic calcrete where carbonate is leached by infiltrating rainwater through the upper horizons (AFCAP, 2012 and Brink, 1985). Although, most to all calcretes are part of the absolute accumulation process (Brink, 1985). The geology or solid rock also determines if calcrete would form, if the residual and/or transported soil is thin enough. If such a condition is present, formation then most likely would occur above calcareous rocks such as limestone, dolomite, calcareous shales and mudstones where calcium carbonate is leached out. Calcrete formation is also possible with the release of calcium and magnesium above basic rocks such as dolerite and basalt (AFCAP, 2012).

A generalization made on Weinert's climatic N-value to pedocrete formation is that pedocretes in more arid, N=5 to N=10 climates in South-Africa, the western part of the subcontinent, are more likely to be calcretes. Pedocretes in more sub-humid (N<5, N=2) climates, the eastern and northern parts of the subcontinent, are more likely to form ferricretes (Brink, 1979). This is due to the fact that reducing conditions mobilises iron more readily, such as a wet season or high rainfall areas. The iron gets precipitated when oxidizing conditions then occur e.g., when a dry season follows the wet season or high evaporation occurs after heavy rainfall. At this point the calcium in the material would already have been leached out and transported with this high degree of "wetness", as calcium is a readily mobile element (Brink, 1985). This can be interpreted that calcretes tend to form more readily in low rainfall and high evaporation areas and ferricretes in higher rainfall and lower evaporation areas. Netterberg (1969 and 1971 cited in Brink, 1985) stated that calcretes would predominantly form in areas with a rainfall less than 550mm. A good correlation for this statement would be the Weinert's N=5 line for calcrete formation representing arid conditions. A sub-humid climate N<5 would be more favourable for ferricrete formation as stated above (Brink, 1985).

2.4 Engineering Geology

Basaltic rock is generally used as aggregate in concrete for building material and road construction purposes. Certain calcretes that form in residual basalt above basaltic rock are also used as road surfacing (Brink, 1983 and AFCAP, 2012). The durability of basaltic rock as an aggregate is drastically affected by the decomposition a basic crystalline rock usually undergoes. The integrity of material for use as a road aggregate depends on the presence of certain alteration products in a weathered rock, such as the increase of clay minerals with a high plasticity index (Houston and Smith, 1997 and Brink, 1983). As described above the main driving force to secondary clay mineral formation is a result of deuteric alteration. The durability of basalt is significantly affected by the minerals created through deuteric action, which already occurs during the solidification of a basic crystalline rock (Bell and Haskins, 1997). These clay minerals are sensitive to water and have low shear strengths and reduces a pavement structure's durability.

The construction of the Lesotho Highlands Water Project led to confirming the presence of this deuteric alteration in the Drakensberg basalts and the influence it had on the construction of the Katse Dam and transfer tunnel. Due to the presence of these swelling clays on the mineral structure and clay spots in the rock mass, volume changes occur when these clays are exposed to a change in moisture conditions. This results in micro-fissuring, fissuring, jointing, fracturing and crazing to occur which increases the porosity of the rock mass. The rate of disintegration is determined by the degree of porosity created, strength of the rock and the distribution of active clay minerals (Sumner et al., 2009).

Although, this process is self-perpetuating, as a result of the already formed fractures/fissures in the rock mass which allows an increase in moisture to enter the rock mass and reach the expanding clays. This in turn increases the fracture density and opens new clay spot areas to an increase in moisture content which accelerates the rate of rock disintegration (Bell and Haskins, 1997). This led to the transfer tunnel of the Katse Dam to be completely lined by concrete instead of only partially, as well as the foundation depth for the dam wall to be increased several meters due to the presence of extended fractures (Bell and Haskins, 1997). This action of the active minerals is also dependent on the texture of the parent rock. If the rock has a low permeability due to the rock texture the active minerals won't have such drastic effect on the strength and durability of the rock. Whereby the mineralogy will not exclusively be sufficient enough to cause deterioration of the rock for the design life of an engineering structure (Sumner et al., 2009).

Van Rooy (1994, cited in Paige-Green, 2007) indicated that basalt material can be considered suitable for concrete, road aggregate and rip-rap if less than 20% smectite and 10% amygdales are present in the rock mass. Although, a more recent study conducted by Paige-Green (2007) on durability testing for basic crystalline rocks to use as road base aggregate had opposing results. Paige-Green (2007) noticed that the majority of samples containing less than 20% smectite proved to be unsuitable for use as aggregate based on additional testing such as, aggregate crushing value, durability mill index and ethylene glycol testing. Paige-Green (2007) also noted that no deterioration occurred in the samples containing amygdales during the ethylene glycol soaking test; which accelerates the swell of the clay lattice. This indicated that more factors than just the

mineralogy present in the rock mass affects the durability of the rock, such as the ease of access available water has to the clay minerals.

This led to the notion that existing limit recommendations based on secondary mineralogy which determines material durability is not completely refined. This approach can't exclusively be used to discriminate between minerals aiding in degradation or aiding in performance (Paige-Green, 2007). The use of secondary minerals in determining material durability for use as aggregate was refined by Paige-Green (2007), it is indicated that materials can likely be durable for use as aggregate if smectite content is less than 10%. Material would possibly be non-durable with smectite greater than 10% if complemented with additional tests and compared to recommended limits determined by Paige-Green (2007). These additional tests to be conducted when the smectite content exceeds 10% are: Durability Mill Index, 10% Fines Aggregate Crushing Value/Aggregate Crushing Value, Aggregate Impact Value and Ethylene Glycol soaking test.

Due to the fine grained mineral structure of basalt it experiences a polishing effect under traffic when used as a surfacing aggregate, it then does not adhere to bituminous binders (Brink, 1983). Basaltic rock aggregate poses the risk of crumbling if it contains nepheline which changes to analcime when exposed to the atmosphere, this mineralogical change creates the crumbling of the aggregate (Brink, 1983).

Residual soils of basalt forming in areas where Weinert's N-value is less than 5 contain active clays, especially in flat lying areas such as the Springbok Flats where highly expansive decomposed basalt profiles occur (Brink, 1983). It is this expansive component of the soils which creates problematic founding conditions.

Many pedocretes have a gap-graded material grain distribution as a result of recemented, reworked and redepositional actions by alluvial, colluvial and groundwater processes, creating an absence of coarse sand (McNally, 2003). Due to cavities created after the processes of solution, redeposition and cementation, the particles of certain pedocretes tend to have a porous structure.

High liquid limits and plasticity indices in these materials are the result of microporosity in the fines instead of excess clay minerals (McNally, 2003). It is due to this porosity that unrippable indurated layers pose problems when blasted due to the depressurization of the explosive gases through connected porosity (McNally, 2003).

Due to the high specific gravity of the hematite concretions created in a ferricrete layer it can be compacted to a high density. As a result of this gravel content, surface rutting can be counterattacked when unsealed. Most duricrust/pedocrete sheets and boulders that are well-cemented are crushed and produce densely-graded road bases and aggregate. Although, the dependability of the material can be suspect as well as the yield of the coarse chips can be low (McNally, 2003). Base course crushed from calcrete can pose problems of bitumen seal debonding as a result of salt presence or dust particles that are incompatibly charged (McNally, 2003).

The properties of calcrete and specifically the range of engineering properties calcrete can contain differ on the extent of cementation, which depends on varying quantities of $CaCO_3$. Calcrete can be a very hard material similar to limestone having high cementation or have low cementation where the calcification is a soft powder in the host material. In short summary, the calcrete types with increasing cementation are; calcified soil, powder calcrete, nodular calcrete, honeycomb calcrete, boulder calcrete and hardpan calcrete (AFCAP, 2012).

The geotechnical properties are significantly different for each calcrete category due to different weathering properties, degree of cementation and the nature of the host material (AFCAP, 2012). The degree of calcrete cementation is determined by factors such as the environment and parent material present. In drier areas where Weinert's N-value is greater than 5, well developed calcretes that are useable in road construction will be present, whereas in wet areas of $N<2$ calcretes would generally be absent (Brink, 1983). In sub-humid areas a range of calcretes would be able to form, although the calcrete horizon would be too thin to excavate for road construction use (AFCAP, 2012). The clay minerals that are most common in calcretes are palygorskite, montmorillonite and seopilite. The most abundant clay mineral palyforskite has some unusual although beneficial properties.

It has a similar plasticity index to certain smectites but has a non-expansive lattice and needle like shape instead of the typical flaky shape (AFCAP, 2012 and Brink, 1985). Calcretes are useful as road construction material due to palygorskite having higher shear strengths at similar moisture contents of other clays, a well as the low linear shrinkage and dry densities (AFCAP, 2012). Calcretes have a range of engineering properties which make it very useful in road construction such as having relatively low swell in respect to high Atterberg Limits. This relates to having higher liquid limits and linear shrinkage in relation to their Plasticity Index. Most calcretes have rather good CBR compaction and low CBR swell despite having poor gradings and Atterberg Limits (AFCAP, 2012).

Brink (1983) provides tables of expected values for residual basalt of the Drakensberg Formation in Lesotho (valley and mountainous settings) and the Letaba Formation of the Lebombo Group in Komatipoort, from previous investigations. Typical values for the residual basalt for the Sibasa basalt Formation from the Nzhelele dam in Venda is provided in Brink (1981). Averages of these formations and settings area summarised in **Table 1**. A valley setting in Lesotho is considered below 2 500m and a mountainous setting above 2 500m:

Table 1: Expected Average values of Residual Basalt for Drakensberg, Sibasa and Letaba Formations, Brink (1981 and 1983).

Formation	Setting / Location	Percentage passing 0.075mm	Atterberg Limits			Mod ASSHTO		CBR VALUES at% Mod. AASHTO		
			Plasticity Index (PI)	Liquid Limit (LL)	Linear Shrinkage (LS)	MDD (kg/m3)	OMC (%)	90%	93%	95%
Drakensberg	Valley	9.7	13	38.8	7.7	2060	10.3	18	24.9	29.3
	Mountainous	14.2	11.4	37.5	5.7	967.6	13.3	11.9	18.5	24.3
*Sibasa	Nzhelele Dam	16	14.5	50.5	6	-	-	-	-	-
Letaba	Komatipoort	40	18	40	9.5	1996	12.5	-	-	45

MDD – Maximum Dry Density; OMC – Optimum Moisture Content, PI – Plasticity Index

*Brink (1981) indicates the values are similar to the Sibase area but somewhat drier.

The valley and mountain settings display similar values in all aspects from the Atterberg Limits to the compaction characteristic.

3. CASE STUDY

This research study focuses on 5 sites chosen based on data availability, locality and opportunity. These sites are: the northern basalt (Mooiplaas) and southern basalt (Nhlowa) supersites in the Kruger National Park (KNP) where an opportunity existed to investigate undeveloped and undisturbed landscape. This also provided the prospect to be part of the well-established and growing research community of the KNP in contributing to a collective data set for different disciplines. It also provided a large study area, these two sites forming the main focus of the research. The remaining sites are at Siloam (Soutpansberg) and Roedtan (Springbok Flats) which are smaller and more concentrated in respect to size and data points. These two sites were available from previous personal shallow soil site investigations. The Codrington site was investigated as another frame of reference for the Springbok Flats basalts and to extrapolate the data from the Roedtan site. A more specific description on the individual site's climate and geology follows.

3.1 KNP Supersites

3.1.1 Supersite background

The selection of the supersites in the KNP was done by a group of SANpark scientists as well as research collaborators from outside the park. The general selection of the sites was based on catchment boundaries so that arbitrary boundary shapes could be avoided. This was also decided since the availability of water spatially and temporally constrains ecological processes (Smith et al., 2013). Many of these ecological processes play out on a template created by patterns of geology, climate, morphology, soils and vegetation which would control water fluxes. These patterns are mostly tied together in semi-arid climates found in the KNP (Smith et al., 2013).

An example of this is that at certain hillslope positions, catenas of soil and associated vegetation are found, which creates sequences that reflects patterns of water availability within a sub-catchment (Smith et al., 2013). Areas with similar climate, geology and morphology create repeated sequences of these catenas which produces physiographic zones or land systems (Venter, 1990 cited in Smith et al., 2013). Catchment/sub-catchment boundaries and catenal elements were used to delineate research and monitoring sites within distinct physiographic zones (land systems),

The aforementioned, allowed sites to be placed within an eco-hydrological context that controls many ecological processes. The more specific criteria for selecting the supersites were based on the following as stipulated in Smith et al. (2013):

1. That the sites should cover the two main abiotic variables that create the large scale differences in the park *viz.* the geology which would be granite and basalt as well as rainfall intensity with higher rainfall in the south and lower in the north.
2. Furthermore, the sites should be large enough so that at least one 3rd order catchment/river occur solely on a single geology type. This allows studies to take place at three different scales *viz.* primary, secondary and tertiary streams.
3. The sites should also include the soil patterns (catenal sequences) and hillslope vegetation that normally occurs in the local land system.
4. The sites should be easily accessible from as many sides as possible
5. They should be located near research camps and facilities.
6. Be outside areas demarcated as “Wilderness” or “Remote” in the KNP zoning plan, in order to allow installation of instrumentation.

Based on criteria 4 – 6 the main boundaries of the supersites are formed mostly by roads, and that a single order catchment may be too small or difficult to access for certain study types. Therefore, the sites were outlined larger than the catchment itself, where the sub-catchment should become the focal point of research (Smith et al., 2013).

The KNP was divided by Venter (1990), into 11 land systems based on the similarities in landforms and hillslope sequences of soils, and dominant woody and herbaceous vegetation on a 1:1 000 000 scale. These land systems were further sectioned into 56 land types at a 1:250 000 scale; see **Figure 4** for representation. The two southern supersites chosen, occur within two of the four largest land systems which make up 40% of the total park area. As indicated by **Figure 4**: the southern granite supersite is part of the Skukuza land system and Renosterkoppies land type with the southern basalt supersite part of the Satara land system and Satara land type, both receives relatively high rainfall. The northern supersites receive less rainfall than the southern supersites (Venter 1990, cited in Smith et al., 2013). The northern granite supersite is part of the Phalaborwa land system and Shivhulani land type and the northern basalt supersite is part of the Letaba land system and Mooiplaas land type (Venter 1990, cited in Smith et al., 2013).

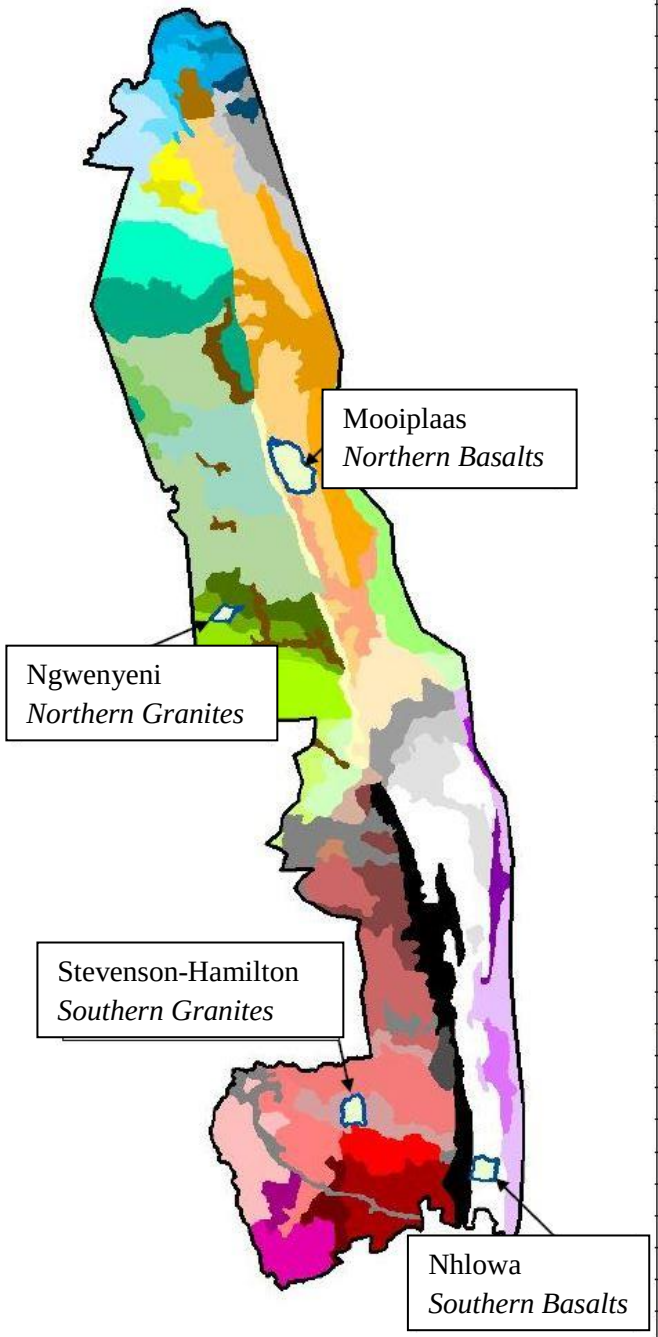

Classification	Landtype	Landsystem
BU01	Bulweni	BULWENI
BU02	Marithenga	
BU03	Tsotsi	
KL01	Gorge	KLIPKOPPIES
KL02	Klipkoppies	
LE01	Olifants	LETABA
LE02	Letaba	
LE03	Mooiplaas	
LE04	Manyeleti	
LE05	Shingwedzi	
LE06	Mashikiri	
LE07	Shilawuri	
MA01	Malelane	MALELANE
MA02	Stolsnek	
NW01	Nwambiya	NWAMBIYA
NW02	Masokosa	
PA01	Punda	PAFURI
PA02	Madzaringwe	
PA03	Lanner Gorge	
PA04	Baobab Hill	
PA05	Pafuri	
PA06	Malonga	
PH01	Houtboschrand	PHALABORWA
PH02	Shidyanamani	
PH03	Tsheri	
PH04	Phalaborwa	
PH05	Shivhulani	
PH06	Malopeni	
PH07	Mahlangeni	
PH08	Tsende	
PH09	Nalatsi	
PH10	Bububu	
PH11	Mphongolo	
PH12	Dothole	
SA01	Satara	SATARA
SA02	Mavumbye	
SA03	Bangu	
SA04	Balule	
SA05	Orpen	
SA06	Salitje	
SK01	Pretoriuskop	SKUKUZA
SK02	Napi	
SK03	Randspruit	
SK04	Lwakahle	
SK05	Makhuthwanini	
SK06	Renosterkoppies	
SK07	Skukuza	
SK08	Nhlanguleni	
SK09	Muzandzeni	
SK10	Rabelais	
SK11	Timbavati	
SP01	Sabiepoort	SABIEPOORT
SP02	Rietpan	
SP03	Pumbe	
SP04	Nwanetsi	
VU01	Vutome	VUTOME

Figure 4: Supersites, Land Types and Land Systems of the Kruger National Park (Smith et al., 2013, originally adapted from Venter, 1990).

3.1.2 Geology — Mooiplaas and Nhlowa

The northern basalt (Mooiplaas) and southern basalt (Nhlowa) Supersites are respectively underlain by basaltic bedrock of the Letaba Formation and Sabie River Formation of the Lebombo Group (Duncan and Marsh, 2006), **Figure 7**. The western portion of the Nhlowa site is underlain by a narrow slice of sandstone from the Clarens Formation, Karoo Supergroup (Barberton, 1986). This portion is approximately 962ha (26.92%) of the site and is portrayed in **Figure 5** below. The north-western corner of the Mooiplaas site is underlain by the Goudplaats biotite gneiss, Timbavati olivine gabbro and sandstone, which constitutes 1 574ha (13.85%) of the total surface area of the site and is portrayed in **Figure 6** below (Tzaneen, 1985).

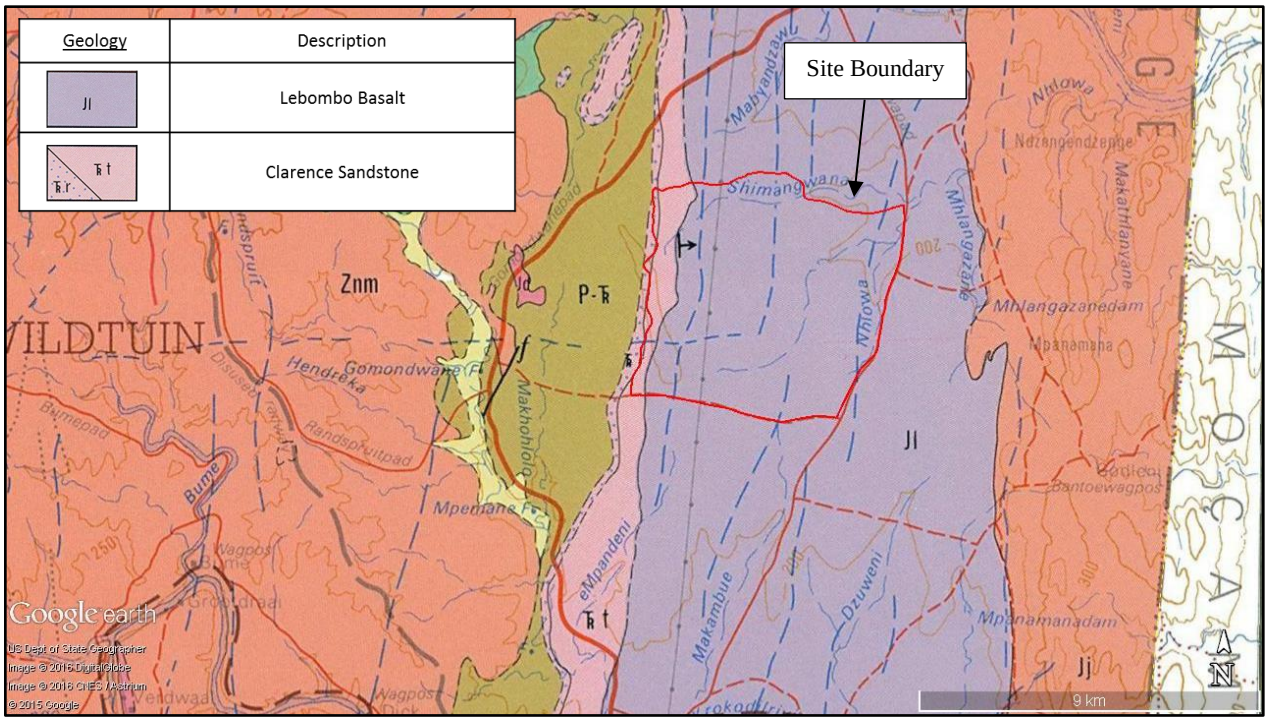

Figure 5: Geological map overlay of the Nhlowa research supersite (©Google Earth, 2015 and Barberton, 1986).

The Lebombo basalts are collectively labelled as the Letaba Formation basalt according to the published 1:250 000 Geological map, sheets 2530 Barberton, and described as green, fine grained mafic lava, locally porphyritic, amygdaloidal in places and interlayered with rhyolite near the top.

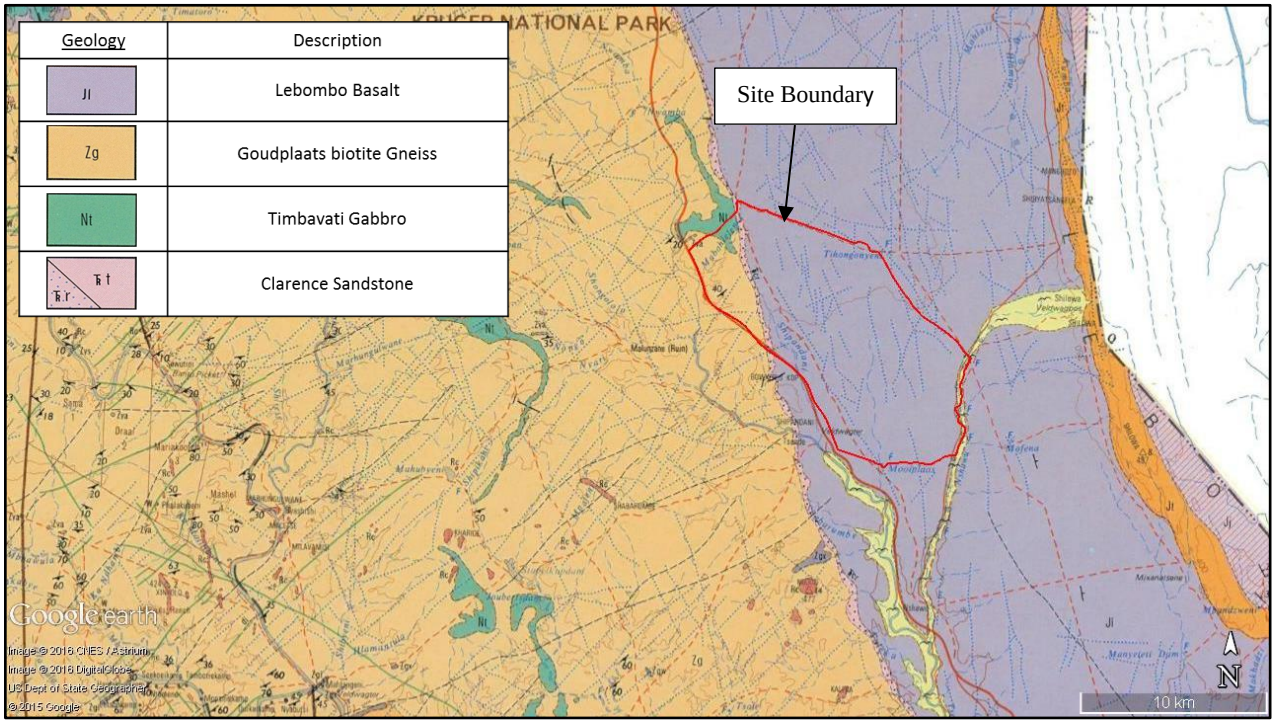

Figure 6: Geological map overlay of the Mooiplaas research supersite (©Google Earth, 2015 and Tzaneen, 1985).

Both the northern and southern basalt landscapes are topographically characterized by flat to moderately undulating plains. This is a result of the near horizontal lava flow sheets as well as the ease with which the mafic lavas decompose (Venter, 1990). As a result, the soil profiles across a site do not differ as extensively as for example on the granite sites that contain more pronounced land forms such as hills and valleys.

3.1.3 Southern Basalt Research Supersite (Nhlowa)

The Nhlowa site is situated approximately 10km south of the Lower Sabie rest camp. The site is bounded by three public dirt roads for the eastern, northern and western boundaries, and one private dirt road as the southern boundary, depicted in **Figure 8**. The site is approximately 3 573ha in size. The 1:50 000 Topographical map, sheets 2531 BA and BB Mpumalanga, indicate that the site contain three river systems flowing through the site to the north-east. Along the northern boundary is the Shimangwana River, through the middle of the site is the Nhlowa River. Along the eastern boundary flowing north is the Nhlanganzwane River, all three rivers are ephemeral/non-perennial streams.

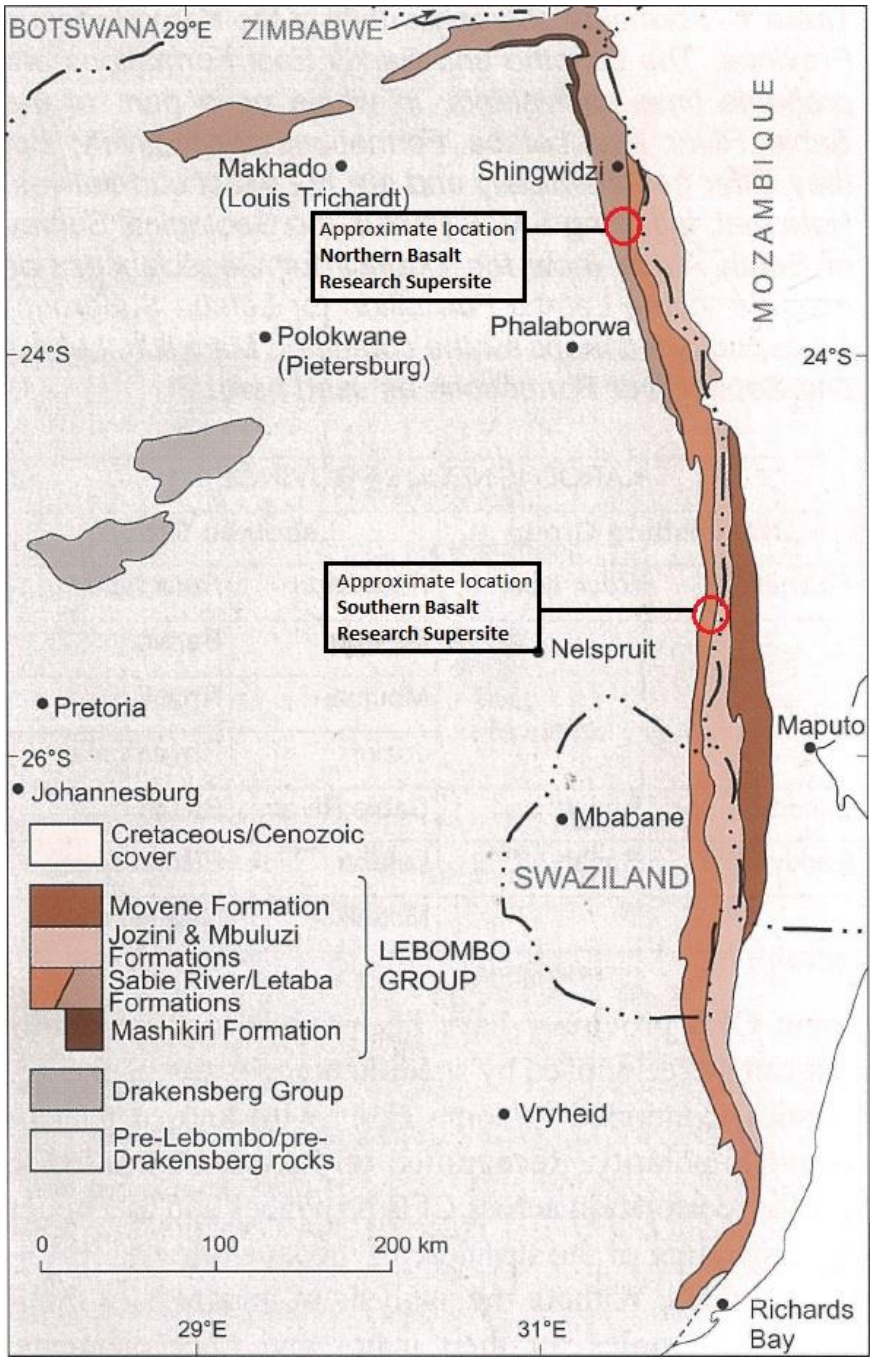

Figure 7: Lebombo Group distribution and supersite localities (Duncan and Marsh, 2006).

Figure 9 below shows a graphical representation of the stream orders and boundaries of the Nhlowa site that occurs in the Satara land type. This area is characterized by shallow to moderately deep red olivine-poor clays according to Smith et al. (2013) and is found to be very flat with open tree savannah. The flat to moderately undulating plains being a result of the mafic lavas weathering easily (Venter, 1990).

The Nhlowa site has a maximum gradient of 0.39 degrees from the south western corner to the north eastern corner (© 2015 GoogleEarth), representing a change in elevation of approximately 60m over 8 666 m.

The southern supersites receive more rainfall than the northern supersites according to Smith et al. (2013), the average rainfall for the Nhlowa site is 610mm/annum. This was measured through long term rainfall at Crocodile Bridge approximately 13km from the Nhlowa site center between 1940-1941 and 2010-2011. **Figure 18** indicates that the Nhlowa site is located in an area with a mean annual evaporation of between 1600-1700mm (Middleton and Bailey, 2008, based on the WR2005 map). The conceivable calculated Weinert's climatic N-values, based on the range of rainfall and evaporations, according to Equation 1 in Chapter 2.3 are:

With 1600mm mean annual evaporation:

N-value = 2.62

With 1700mm mean annual evaporation:

N-value = 2.78

From these calculated N-value the Nhlowa site is located in the N-value range of between 2 and 5, classified as a sub-humid area (Brink, 1979).

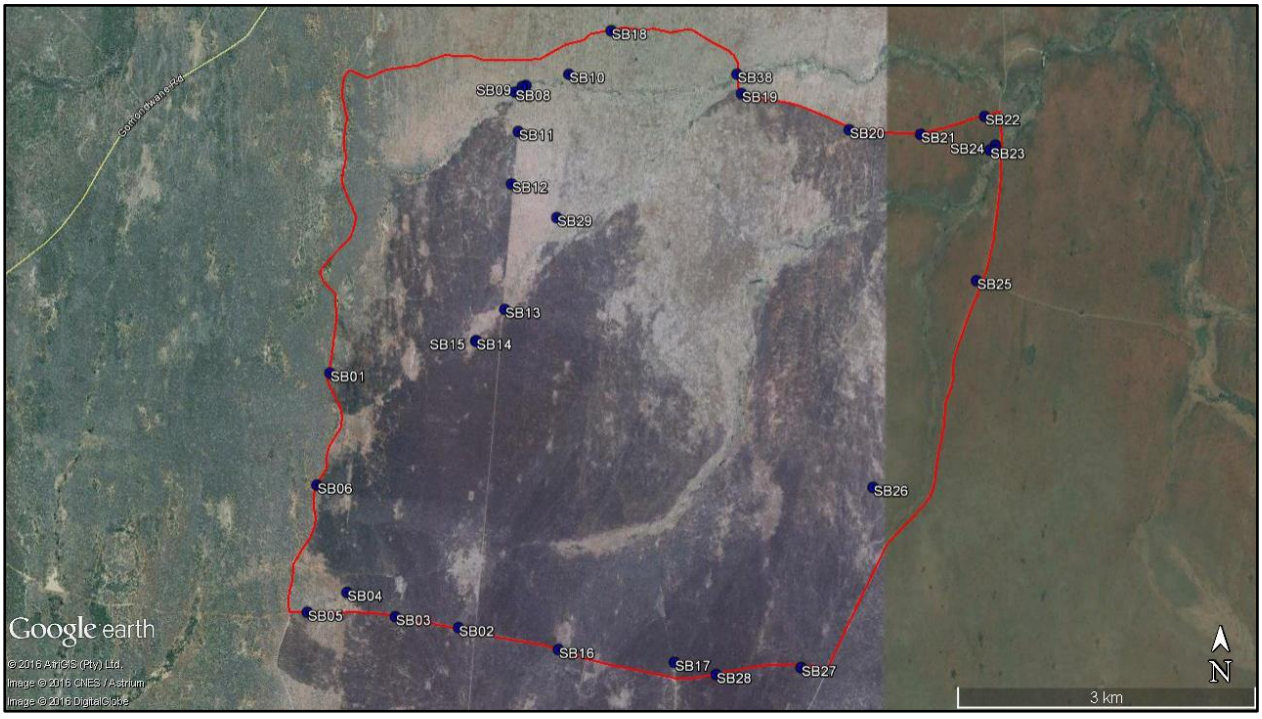

Figure 8: Site boundary and auger hole positions: Nhlowa research supersite on the Southern Basalts (©Google Earth, 2015).

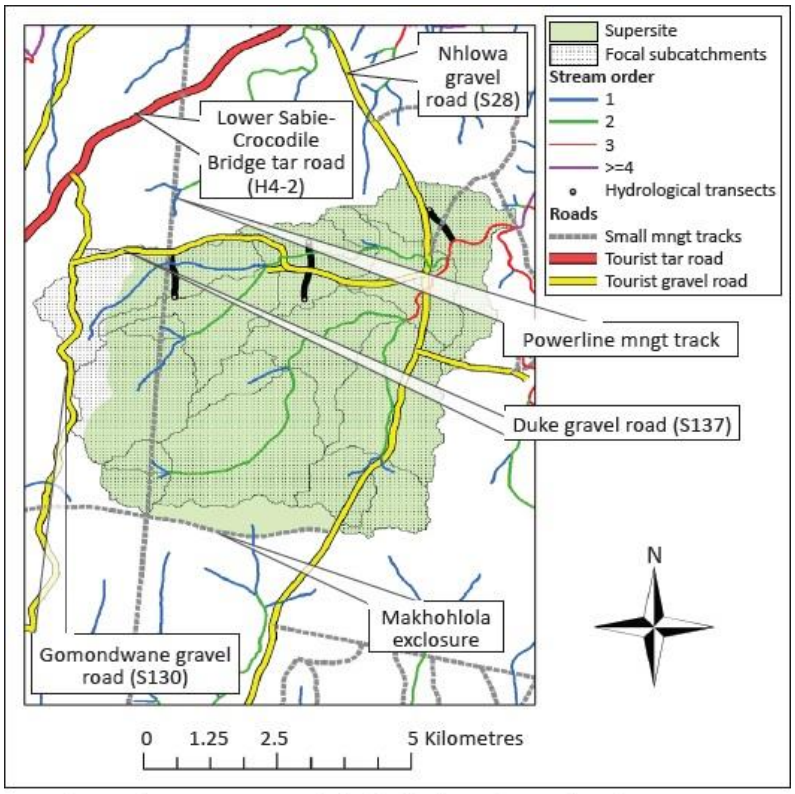

Note: The small western section of the focal sub-catchment along the S130 occurs on sandstone – most studies should therefore focus on the area indicated in green within the sub-catchment, but catchment-scale hydrological studies may be interested in the entire catchment – this setup is because no third-order catchments in the south of the park were fully contained on basalts and so this catchment, where a small proportion occurs on the sandstone, was the best available option.
mngt, management.

Figure 9: Stream orders: Nhlowa research supersite on the Southern Basalts (as depicted in Smit et al., 2013).

3.1.4 Northern Basalt Research Supersite (Mooiplaas)

The Mooiplaas site is located approximately 1.40km north-east of the Mopani Rest Camp from the site's western boundary. The Mooiplaas site, at 11 368ha, is much larger than the Nhlowa site. The boundaries of the site are also formed by public dirt roads along the northern, southern and western boundary with the H1-6 Mopani-Shingwedzi tar road as the western boundary, depicted in **Figure 10** below.

As mentioned above the Mooiplaas supersite is situated within the Mooiplaas land type and according to Smith et al. (2013) is characterized by dark olivine-rich soils. The site has very low stream density as well as very flat topography. The Mooiplaas site has a maximum gradient of 0.20 degrees from the north western corner to the south eastern corner, representing a drop in elevation of approximately 60m over 17 000m.

The Mooiplaas site has the Mabohlelene river system (a 2nd order river) in the north-western corner of the site flowing south-west, eventually flowing into the Tsende River. The Shipandani 1st order stream on the western boundary of the site flows south south-east, with the Mooiplaas 1st order stream in the middle of the site flowing south which also flows into the Tsende River. The Tsende River flows south-east and eventually south outside the site boundary. Here the Tsende River joins with the Nshawu River on the eastern border of the site flowing south as well. **Figure 11** portrays the rivers in and around the site (1:50 000 Topographical sheet 2331 AD and CB).

The northern supersites receive less rainfall than the southern supersites according to Smith et al. (2013), the average rainfall for the Mooiplaas site is 480mm/annum. This average was determined through long term rainfall measurements approximately 5km from the Mooiplaas site center between 1940-1941 and 2010-2011. **Figure 18** indicates that the Mooiplaas site is possibly located across two areas with different evaporation rates divided along north-east south-west. The mean annual evaporations of these areas are 1700-1800mm and 1800-1900mm (Middleton and Bailey, 2008, based on the WR2005 map).

The conceivable calculated Weinert's climatic N-values, based on the range of rainfall and evaporations, according to Equation 1 in Chapter 2.3 are:

With 1700mm mean annual evaporation:
N-value = 3.54
With 1800mm mean annual evaporation:
N-value = 3.75
With 1900mm mean annual evaporation:
N-value = 3.95

The large evaporation range indicated no significant difference to the calculated N-value. According to the calculated climatic N-values, the Mooiplaas site is located in the N-value range of 3.54 to 3.95 which would be classified as a sub-humid to slightly arid areas with N<5. These values indicate that the Mooiplaas site is a drier area than the Nhlowa site with higher evaporation and lower rainfall.

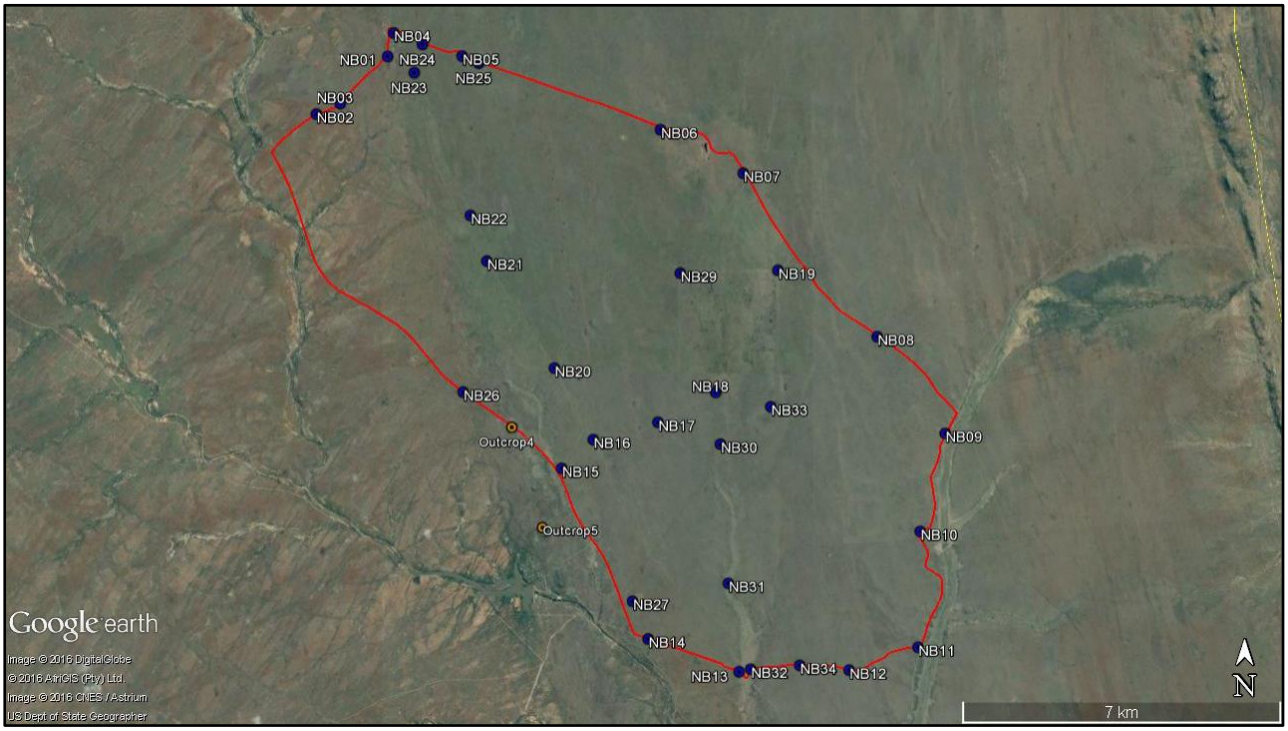

Figure 10: Site boundary and auger hole positions: Mooiplaas research supersite on Northern Basalts (©Google Earth, 2015).

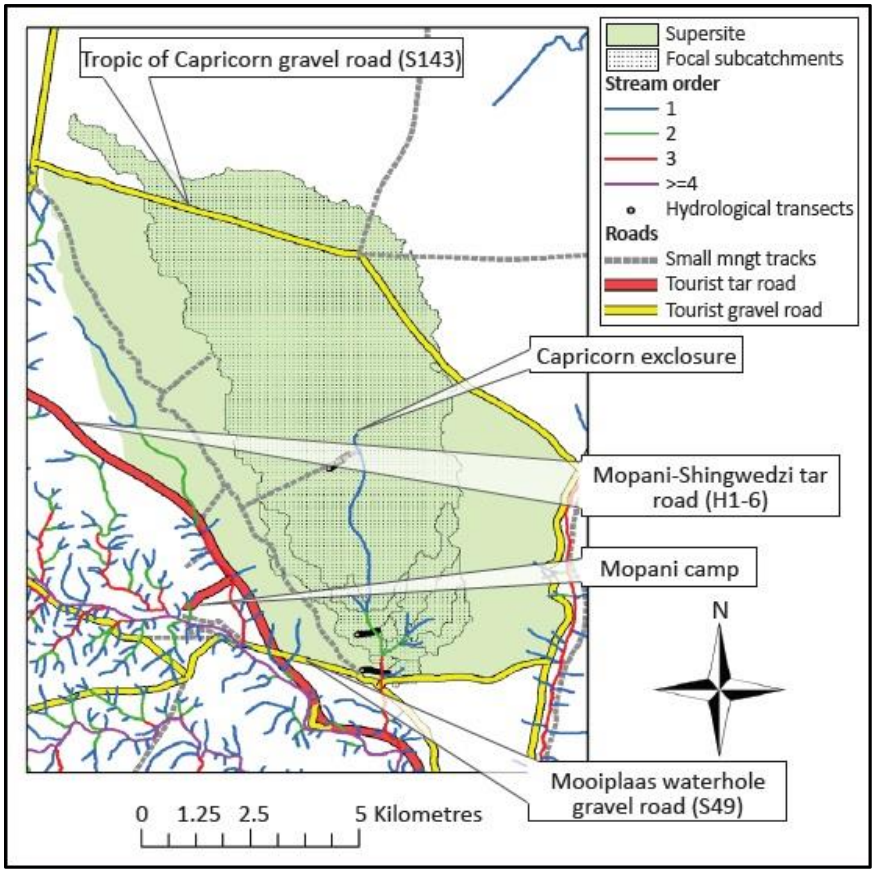

Figure 11: Stream orders: Mooiplaas research supersite on Northern Basalts (as depicted in Smit et al., 2013).

3.2 Siloam site

3.2.1 Site description

The original investigation at Siloam on the Sibasa basalts was to conduct a shallow soil engineering geological investigation for the proposed new residential extensions and road construction at the Siloam hospital. The site is situated in the Siloam area south of the R523 (Musina road), it is located approximately 30km from the N1 highway on the R523 towards Thohoyandou, see **Figure 12** for view of site.

The site is mainly covered with natural grass and small to medium size shrubs and larger trees and has a size of 9.17ha (91 691m^2). The general slope direction is towards the south to south-east with an elevation difference of 832mamsl (meters above mean sea level) to 815mamsl. This represents a drop in elevation of 17m over approximately 400m which gives an average slope of 5% to 6% or approximately 3° (© 2015 GoogleEarth). A branch of the Mutangwi river system is located approximately 60m south-east from the site. This river flows south-west into the Nzhelele River system approximately 820m south of the site which in turn flows west North-west.

A small drainage channel from the mountain is also present approximately 260m west of the site flowing into the Nzhelele River (1:50 000 Topographical sheet, 2330 CC). Numerous valleys formed in the Soutpansberg due to the headwaters of the Nzhelele and Pafuri rivers cutting through the quartzites. Two of these valleys that have formed divide the Soutpansberg into three mountain ranges and valleys where Siloam falls within the first valley between the first two mountain ranges (SoER, 2004).

3.2.2 Rainfall and evaporation

High rainfall of more than 2 000mm occur in the eastern areas of the Soutpansberg between Louis Trichardt and the Kruger National Park. The northern and western areas receive much less rainfall of between 200mm and 300mm. The site on the Sibasa basalts are located north of the R523 in the town Siloam which places the site in the high rainfall section of the Soutpansberg. As a result of such high rainfall these basalts have varying weathering depths which can extend from approximately 2m to 3m to 20m with fresh rock and core-stones present from shallower depths (Brink, 1981).

Figure 12: Site boundary and test pit positions: Siloam site on Sibasa Basalts (©Google Earth, 2015).

Thohoyandou is approximately 30km from Siloam and the closest town that has research and measured data pertaining to the Soutpansberg climate. This would therefore be the closest representation to the climate at Siloam. **Figure 17** below shows that Siloam and Thohoyandou fall approximately in similar mean annual precipitation ranges, with Thohoyandou in the 800-1000mm/annum and Siloam between the 600-800mm/annum and 800-1000mm/annum range. According to the data gathered for the Limpopo State of the Environment Report (SoER, 2004), the average rainfall in Thohoyandou for the period of 1982-1990 was 679mm and for the period of 1997-2003 was 810.63mm, portrayed in **Table 2** below (SoER, 2004).

Figure 18 indicates that the Siloam site is also on the border of two areas with different evaporation rates. The mean annual evaporations of these areas are 1300-1400mm and 1400-1500mm (Middleton and Bailey, 2008, based on the WR2005 map).

The conceivable calculated Weinert's climatic N-values, based on the range of rainfall and evaporations, according to Equation 1 in Chapter 2.3 are:

With 1300mm mean annual evaporation and 679mm rainfall:

N-value = 1.91

With 1300mm mean annual evaporation and 810mm rainfall:

N-value = 1.60

With 1400mm mean annual evaporation and 679mm rainfall:

N-value = 2.06

With 1400mm mean annual evaporation and 810mm rainfall:

N-value = 1.73

With 1500mm mean annual evaporation and 679mm rainfall:

N-value = 2.21

With 1500mm mean annual evaporation and 810mm rainfall:

N-value = 1.85

The Siloam site falls in the N-value range of 1.60 to 2.21 which would be classified as a sub humid area N<5 to humid area N<2 (Brink, 1979).

3.2.3 Geology

The Sibasa basalt Formation at Siloam forms part of the Soutpansberg Group which erupted approximately 1769 ± 34 Ma ago with repetitive and cyclical eruptions, slightly exposed to air (Baker, 1979 cited in Barker et al. 2006). Therefore, zones of lenticular pyroclastic rocks are found in the basalt as well as intercalations of clastic sediments laterally through the rock mass (Baker, 1979 cited in Barker et al. 2006). The Sibasa basalts are described as dark green and massive with zones of white amygdales where the rock is usually epidotised. According to Baker, 1979 cited in Baker et al. 2006, clinopyroxene and plagioclase are visible between the epidote, chlorite and quartz matrix in less altered rocks.

The Sibasa basalts are dominantly volcanic rock and reaches an estimated thickness of approximately 3000m. Although numerous lenticular laterally persistent clastic sediment intercalations are also present. These clastic sediments are mostly quartzite, shale and some conglomerate reaching thicknesses of 400m (Barker, 2006).

According to the published 1:250 000 Geological map, sheet 2230 Messina, the Sibasa basalt deposit is described as; basalt with minor tuff, sandstone, quartzite and shale; see **Figure 13** for geological map.

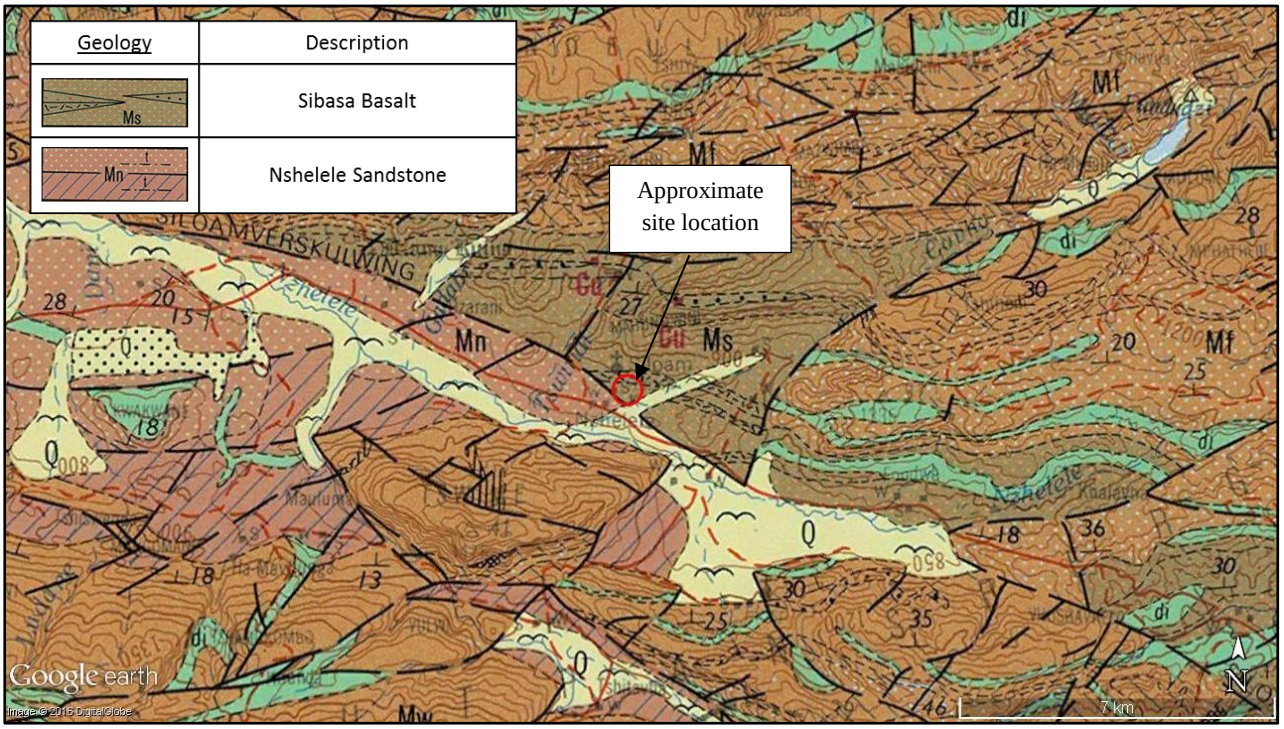

Figure 13: Geological map overlay of the Siloam site (©Google Earth, 2015 and Messina, 1981).

3.3 Roedtan and Codrington

3.3.1 Site description

The investigation that was conducted at Roedtan was for a shallow soil engineering geological assessment for the construction of a proposed Police Station. The site is located on the eastern side of the N11 highway 400m south of Roedtan, see **Figure 14**.

The site is covered in long natural grass with minor shrubs and small to medium sized trees across the site. The site is fairly flat with an elevation difference of 975mamsl to 972mamsl across the 3.57ha (35 717 m^2) site (© 2015 GoogleEarth). The site is located in a low relief area with no large prominent hills or mountains in a radius of approximately 26km. The nearest pronounced drainage feature or river is the Olifants River approximately 40km east from the site.

The only visible drainage feature near the site is a small stream approximately 1.80km north of the site flowing south east (Topographical map, sheet 2429 CA and CB).

Figure 14: Site boundary and test pit positions: Roedtan site on Springbok Flats Basalts (©Google Earth, 2015).

The data at the Codrington site was taken from an open quarry located on the R576 road to the R101 road to Codrington. The quarry is approximately 2km from the N1 on-ramp to Codrington along the R576 west and 400m east of the R101.

The site is fairly flat with no prominent hills or mountains in a radius of approximately 20km. The Langkuilspruit is located approximately 2.70km north-west of the site flowing in a western direction. Larger rivers such as the Platrivier (Utsane) is located approximately 9km west of the site flowing south South-east and the Pienaarsrivier approximately 16km south from the site flowing west. The Codrington site in contrast to the Roedtan site has much more small streams and dams located around it in an roughly a 4km radius (Topographical map, sheets 2528 AB and AA).

Figure 15: Codrington site on Springbok Flats Basalts, approximate area of investigated quarry (©Google Earth, 2015).

3.3.2 Rainfall and evaporation

Mokopane (Potgietersrus) is situated approximately 50km north along the N11 from Roedtan and is the closest town with research data to represent the environment and climate in the area (the Limpopo State of the Environment Report, 2004). **Figure 17** below shows that Roedtan, Mokopane as well as Polokwane falls roughly in the same mean annual precipitation range of 400-600mm/annum. Mokopane possibly also falls within the 600-800mm/annum range. **Table 2** below indicates Mokopane had an average rainfall of 344.18mm for the period of 1996-2003.

Polokwane had an average rainfall of 472.86mm for the period of 1993-2003 and 478mm for the period of 1961-1990 (SoER, 2004). The website SAexplorer indicates that Roedtan receives roughly 443mm per year the highest rainfall occurring in December with 93mm (SAexplorer, 2000-2014). **Figure 18** indicates that the Roedtan site is located in an area with a mean annual evaporation of between 1800-2000mm (Middleton and Bailey, 2008, based on the WR2005 map).

The conceivable calculated Weinert's climatic N-values, based on the range of rainfall and evaporations, according to Equation 1 in Chapter 2.3 are:

With 1800mm mean annual evaporation and 400mm rainfall:
N-value = 4.5
With 1800mm mean annual evaporation and 600mm rainfall:
N-value = 3.00
With 2000mm mean annual evaporation and 400mm rainfall:
N-value = 5
With 2000mm mean annual evaporation and 600mm rainfall:
N-value = 3.33

The Roedtan site falls in the N-value range of 3.00 to 5.00 which would classify as a sub humid to slightly arid area (N<5). With the highest calculated value of N=5, the site would be considered to tend more to an arid climate area (Brink, 1979). According to Figure 3 Roedtan is located between the N=5 and N=2 lines displaying the accuracy of the calculated values.

Bela-Bela (Warmbaths) is approximately 18km north from Codrington which is the closest town with measured rainfall data in the Limpopo State of the Environment Report (2004). According to SoER (2004) the average annual rainfall in Bela-Bela for the period of 1961-1990 was measured at 634mm. According to **Figure 17** Bela-Bela is located in the mean annual precipitation range of 600-800mm which supports the measurements. Although Codrington is located more in the 400-600mm mean annual precipitation range it is close to the 600-800mm range.

The mean annual precipitation measurement of 634mm is then interpreted as a maximum possible value for Codrington and 400mm the minimum. **Figure 18** indicates that the Codrington site is located in an area with a mean annual evaporation of between 1700-1800mm (Middleton and Bailey, 2008, based on the WR2005 map).

The conceivable calculated Weinert's climatic N-values, based on the range of rainfall and evaporations, according to Equation 1 in Chapter 2.3 are:

With 1700mm mean annual evaporation and 400mm rainfall:

N-value = 4.24

With 1700mm mean annual evaporation and 634mm rainfall:

N-value = 2.68

With 1800mm mean annual evaporation and 400mm rainfall:

N-value = 4.50

With 1800mm mean annual evaporation and 634mm rainfall:

N-value =2.84

The area of Codrington falls in the calculated N-value range of 2.68 to 4.50, which would classify as a sub humid to slightly arid area (N<5) (Brink, 1979). According to Figure 3, Codrington is located between the N=5 and N=2 lines, closer to the N=5 line, which would indicate the values of N=4.5 to 4.24 more likely values.

3.3.3 Geology

The inter-continent volcanic eruptions which formed the Drakensberg and Lebombo basalts and stopped the Karoo sedimentation only lasted approximately two million years. Following this volcanic event most of South Africa experienced uplift in conjunction with intense erosion removing large parts of the previously extensive lava sheets. Although uplift dominated most of South Africa, a region in the bushveld experienced subsidence which led to the preservation of the Karoo sedimentation and volcanics, now known as the Springbok Flats basin (McCarthy and Rubidge, 2005).

The Springbok Flats Basin is an extremely flat section of the African erosion surface which extends from Modimolle/Nylstroom to Mokopane/Potgietersrus (McCarthy and Rubidge, 2005). Outcrops are extremely scarce in the exceedingly flat area, therefore information on the stratigraphy of the basin was mostly acquired from borehole drilling conducted by the Geological Survey (Johnson et al., 2006). These borehole data indicate that the preserved Karoo basalts in the basin has a maximum thickness of 460m in the north-eastern section and more than 750m in the south-western section (Marsh, 1984).

The basalts of the Springbok Flats according to SACS, (1980 cited in Marsh, 1984), was originally correlated to the Letaba formation of the Lebombo Group. This name was collectively given to all basalts that were located below the rhyolites in Lebombo. Although after additional investigations it was found that the Springbok Flats were chemically and petrographically different to the Letaba Formation basalts.

Additional data presented by Marsh (1984) indicate the Springbok Flats are more closely associated to the Sabie River Formation and Lesotho Formation, although having a stronger supporting correlation to the former. See **Figure 16** below for geological map representation.

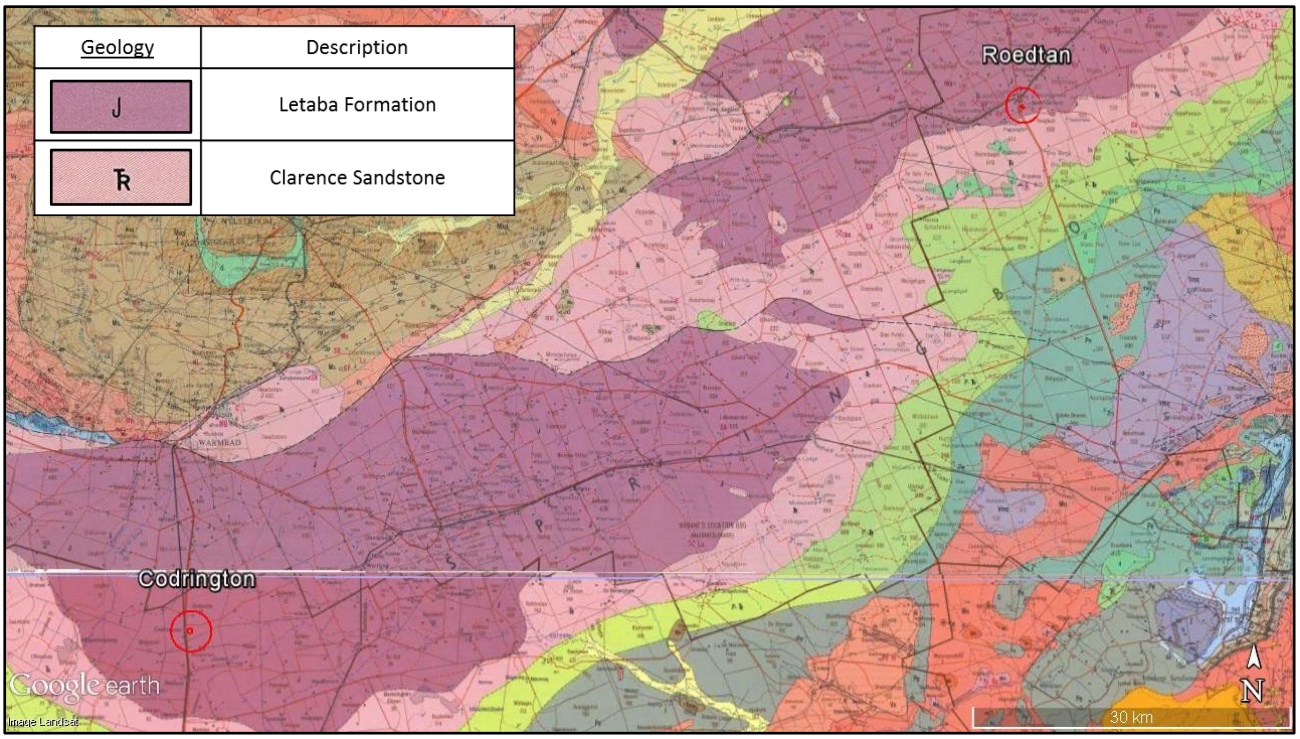

Figure 16: Geological map overlay of the Roedtan and Codrington site on the Springbok Flats, (©Google Earth, 2015, Nylstroom, 1978 and Pretoria, 1980).

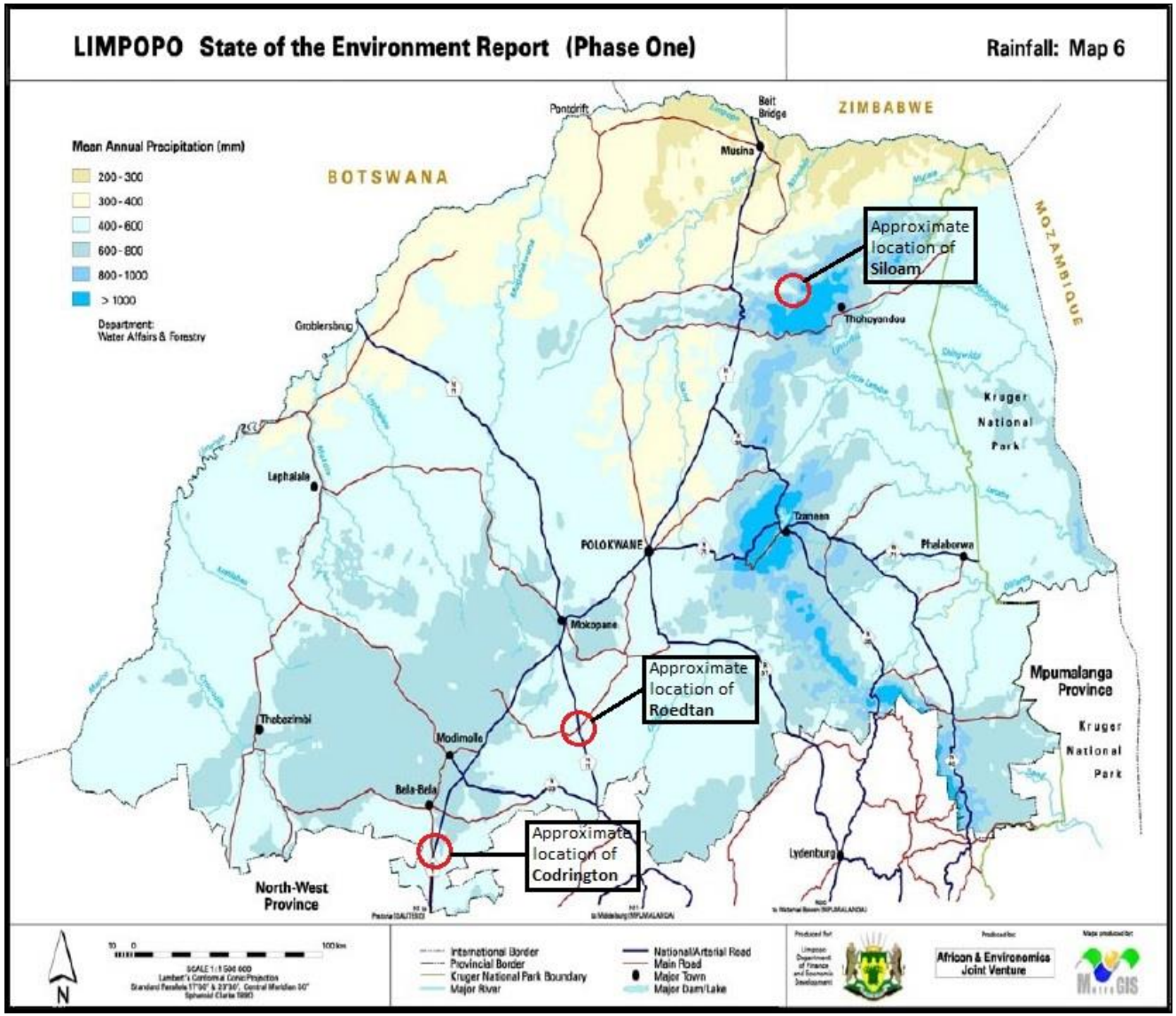

Figure 17: Mean annual precipitation across Limpopo Province (SoER, 2004).

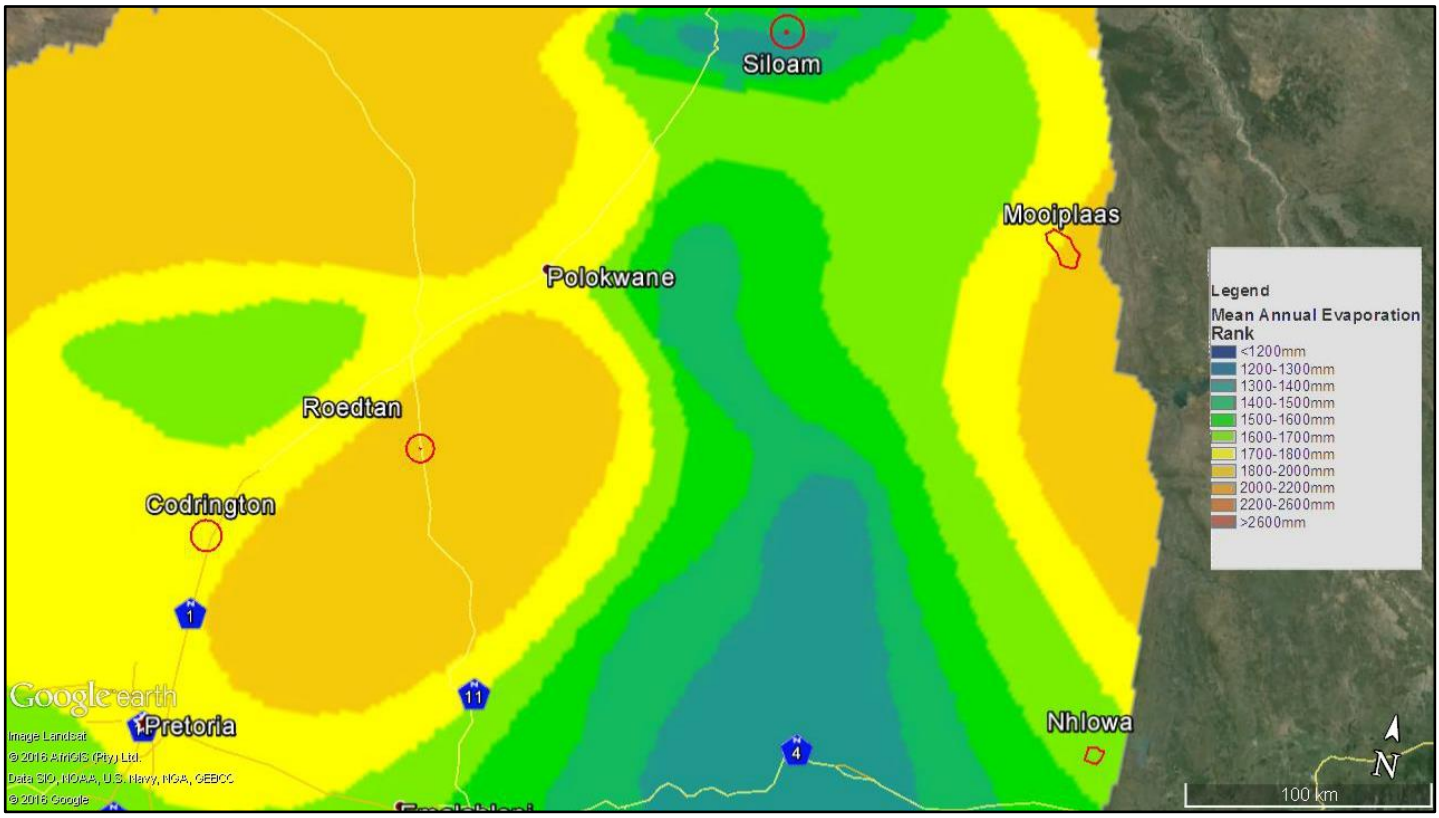

Figure 18: Mean Annual evaporation of reasearch sites (WR2005 map overlay to ©Google Earth, 2015).

Table 2: Total Annual Rainfall data for selected towns in Limpopo.

Year	Mokopane in (mm/annum)	Polokwane in (mm/annum)	Thohoyandou in (mm/annum)
1993	*	356.30	*
1994	*	381.60	*
1995	*	678.00	*
1996	797.60	869.40	*
1997	470.40	584.80	415.40
1998	366.00	438.20	722.80
1999	379.20	368.80	872.00
2000	456.60	637.40	1968.20
2001	98.80	480.60	1004.20
2002	132.00	254.60	362.40
2003	52.80	151.80	329.40
Average (mm)	344.18	472.86	810.63
Avr. 1962-1990 (mm rainfall)	*	478.00	(1982-1990) 679.00

*Data not available/measured

(Table adapted from Limpopo State of the Environment, 2004)

4. METHODOLOGY

4.1 Desk study procedure

The basic site investigation procedures as outlined in SANS 634 2012: Geotechnical Investigations for Township Development was followed in the investigation of the sites. This procedure was followed in order to cover all relevant aspects of the site and have a structure to the investigation that is tested and proven to work. The Mooiplaas and Nhlowa sites in the KNP had 1:10 000 orthographic photographs available that were studied, along with the 1:50 000 topographical maps of sheets 2331 AB, CB and sheets 2531 BB, BD respectively. The 1:250 000 published geological maps, sheet 2330 Tzaneen were used for the Mooiplaas site and sheet 2530 Barberton was used for the Nhlowa site. These were used in conjunction with the other maps in order to determine all possible structures on the sites before the field work was conducted.

This allowed for more precise planning on auger hole excavation, focusing on different land facets. Due to the size of the KNP sites the land facets that were focused on were hill crests, hill midslopes and footslopes. Although as a result of the extremely flat slopes on site (due to the nature of how the basalts were deposited and weathered) differences in these land facets was problematic to determine on the topographical map and the naked eye on site. The contour lines on the topographical map were spaced so far apart that distinct hill- crests, -midslopes and -footslopes could not be effectively identified and merge together. This was also noticed on site trying to distinguish the slight rise and fall of the slopes with the naked eye. This resulted in a large decrease in accuracy to the land facet system. As a result of this, the system became ineffective and primary use of the system had to be abandoned. The land facet system still provided guidance together with the information on stream flow in the area and professional judgement to determine auger positions.

The same desk study investigative structure described above was used with the Sibasa basalts at Siloam and the Springbok flats basalts at Roetan and Codrington. For the Sibasa basalts the 1:50 000 Topographical map, sheet 2230 CC, together with the 1:250 000 published Geological map, sheet 2230 Messina, was used to analyse the possible geomorphological environment.

For the Springbok flats basalt at Roetan the 1:50 000 Topographical map, sheet 2429 CA and 1:250 000, sheet 2428 Nylstroom was used. For Codrington the 2528 AB sheet of the 1:50 000 Topographical map and the 2528 Pretoria sheet of the 1:250 000 Geological map was used. Only one data point at the quarry at Codrington was gathered in order to provide extrapolative data for Roetan. Due to the smaller sizes of these sites focus was not placed on land facets and major structures across site. Emphasis was on investigating as much of the site as possible and not to overlook important soil development characteristics of the basaltic site. The difficulties and problems experienced with the KNP sites would only increase with the decrease in size of the sites. Where the contour lines on the topographical map were spaced so far apart that the distinct hill- crests, -midslope and –footslope land facets were not found together on the small sites.

4.2 Field work procedure

Due to the pristine conditions of the supersites in KNP, large machines such as a tractor loader backhoe (TLB) could not be utilized to excavate test pits for soil profile descriptions or sampling. The investigations at the Mooiplaas and Nhlowa sites were therefore conducted using a hand auger to excavate, sample and describe the soil profile. The effective description of the soil profile with the use of a hand auger was concerning at first. Although Botha and Porat (2007) portrays the successful use of a hand auger down to 6m for the description of soil profiles in dunes on the southeast African coastal plains in Maputaland, South Africa. Similarly, more recently, Connallon and Schaetzel (2017) successfully sampled and described the Chippewa river delta of Glacial Lake Saginaw in central lower Michigan, USA, with the excavation of 180 auger holes with a 2m long auger.

Therefore, a hand auger with a 1 m long shaft and bucket dimensions of 12 cm in diameter and 22 cm long was used. The depth of the auger holes was limited to the type and extractability of the material encountered. At the research supersites in KNP the hand auger could not excavate through the highly weathered basalt horizon and mostly refused in this horizon. This shallow refusal was not a critical problem as information down to the highly weathered basalt was sufficient for the study.

As a result of this fact the use of a hand auger became beneficial, as it was much more cost effective compared to the hire of a TLB. Masoud et al. (2013) indicates the cost effectiveness of using a hand auger for investigations. At the shallow excavation depths encountered, the speed of excitability and in turn data point collection further supported the beneficial use of a hand auger, especially for the large research supersites.

A total of 21 soil profiles were described in the Nhlowa site and 36 profiles in the Mooiplaas site. Due to the limited amount of soil excavated with a hand auger as well as soil weight restrictions that are allowed to be taken out of the KNP only sample sizes for foundation indicator, X-Ray Diffraction (XRD) and X-Ray Fluorescence (XRF) tests were retrieved from representative selected horizons.

The smaller site investigations provided the opportunity of utilizing a TLB for excavation of deeper basalt profiles to be inspected, not limited by pristine conditions such as in the KNP or sample weight limits. This provided the opportunity of sampling large amounts of soil for compaction testing as well as samples for foundation indicator, XRF and XRD analysis. Eight test pits where excavated at the Siloam site spaced approximately 80m to 120m apart. The Roedtan site was investigated with the excavation of seven test pits across the site also spaced approximately 80m to 120m apart. No XRF and XRD analyses were done at Roedton, as the investigation occurred before the commencement of this study. At the Codrington site, only one open profile from a quarry wall was profiled and sampled in each horizon for foundation indicator, XRF and XRD analysis, to provide some extrapolative data for Roedtan not having XRD and XRF information.

The soil profiles were recorded using the standard procedures as per the guidelines from AEG/SAIEG/SAICE (2002). The use of a hand auger in the KNP supersites precluded the description of certain attributes of the soil profiles, such as soil consistency and soil structure. These characteristics if described were based on experience and professional opinion. For example, with consistency the interpretation was based on the difficulty of augering as well as the strength and hardness of soil lumps that were excavated. These intact soil lumps also provided some visual assessment on the soil structure, be it open structure or slickensided etc.

The presence of joints and fractures in the weathered basalt excavated by the auger were determined also by ease or difficulty of augering and size and shape of weathered basalt gravel retrieved from the auger hole.

4.3 Tests conducted

Disturbed soil samples were selectively retrieved for mineralogical and geochemical analyses (X-Ray Diffraction (XRD) and X-Ray Fluorescence (XRF)) as well as soil mechanical (foundation indicator, Mod. AASHTO and CBR tests). XRD analyses were assessed in order to determine both the primary and secondary/alteration mineralogy of the parent basaltic rock and the weathered residual soil horizons. The XRF analyses were conducted to assess the element transfer, gain or loss, which occurs with the weathering process from rock to residual material. Together the XRD and XRF data were used to determine the mineralogical and chemical compositions of the different soil horizons, as well as the degree of weathering the soil and rock has undergone.

The foundation indicator tests were conducted in order to determine the percentage particle size distribution and provide the Atterberg limits of the soil. The additional Mod. AASHTO (Modified American Association of State Highway and Transportation Officials) and CBR (California Bearing Ratio) tests that were conducted at Roetan and Siloam (only available at these sites), provided additional insight in the compaction characteristics of the residual and highly weathered basalt material. The CBR value is a relative strength measurement for the subgrade soil or base/subbase aggregate.

The Mod. AASHTO is a standard test procedure used in acquiring the CBR value and additional information. This includes the maximum dry density and optimum moisture content of the soil under different compaction efforts. This is determined by establishing the moisture-density relationship of the material when prepared and compacted at different Mod. AASHTO compaction efforts and at different moisture contents (Brink, 1983). The CBR values are also determined, these values are used to evaluate the mechanical strength of the material for different road layer construction.

5. RESULTS AND ANALYSIS

This chapter contain the results of the tests conducted on the five different low relief basalt sites. The chapter will start with an overview of the different profile types encountered at each site. The focus will be on the profile description, depth and thickness of horizons, presence of pedogenic material and the sieve analysis for horizons tested. The chapter will continue onto the chemical and mineralogical results for the parent rock and soil samples from the XRF and XRD testing for each site. The chapter will end with the presentation of engineering data on sites that have been tested. This chapter will be a combination of presented results as well as immediate analysis and comparison where possible. This was done due to the large size of data and quantity of sites in the study. This approach was taken so that a coherent flow to the results, discussions and comparisons between sites can be viewed together to make more sense and create a better picture of the data. Chapter 6 will summarize important aspects of the discussions.

5.1 Profiles

The emphasis during the soil profile description was placed on the vertical succession of the different soil horizons. The rather flat-lying nature of the sites creates very similar profiles with only subtle differences. The separation between the various vertical soil horizons are based on differences in colour, soil texture, presence and extent of rock formation and/or pedogenesis in the soil horizons. Descriptions in brackets [ ] indicate occasional occurrence of the component in the horizon or the horizon itself, as well as interpreted parameters not easily determined during hand augering, the latter for the KNP supersites.

It is important to note that minimum thickness does not always represent the thinnest horizon encountered as certain auger holes/test pits were terminated in a horizon due to auger refusal and/or inability to extract material. This is also true for maximum values that does not represent the complete maximum especially for termination of excavation in a horizon, termination occurred mostly due to the extent of auger/TLB, refusal of auger and inability to extract material from auger hole.

5.1.1 Nhlowa Profiles — Lebombo Basalt

SBProfile 1: Colluvium - residual basalt - highly weathered basalt

Seven similar profiles with the sequence of colluvium, residual basalt then highly weathered basalt were encountered and described, represented by profiles SB02, SB03, SB10, SB16, SB17, SB22 and SB23. Summarised below in **Table 3**.

Table 3: Profile description summary for SBProfile 1 - Nhlowa site.

Horizon	**Horizon Description**	**Base of horizon below ground level (m)**	**Horizon Thickness (m)**	**Additional Information**
Colluvium	• Slightly moist, • Dark brown, • [Shattered], • Slightly gravelly silty SAND / clayey sand [sandy clay].	0.06{0.28}0.60 *0.19	0.06{0.27}0.60 *0.19 n=7	No pedogenic material encountered.
Residual basalt	• Slightly moist, • Light brown to yellow brown [medium and red brown], • [Shattered], • Silty sand/clayey sand [sandy clay/silt].	0.53{0.72}1.05 *0.20	0.27{0.43}0.50 *0.06 n=6	Ferricrete nodules as gravel present, can then be described as sandy gravel as well. SB17 contained calcrete, the only auger hole to contain calcrete.
Highly weathered basalt	• Slightly moist, • Yellow brown, • Gravelly [silty/clayey] sand.	0.40{0.80}1.25 *0.376	0.04{0.29}0.60 *0.23 n=4	[Ferruginization present].
[Moderately weathered basalt]	• Slightly moist, • Brown mottled red, • Silty sandy highly to moderately weathered basalt GRAVEL.	SB22 = 0.73 SB23 = 0.40	SB22 = 0.20 SB23 = 0.28 n=2	Only SB22 encountered this layer with SB23 encountering traces of the layer in a riverbank.
Min{Average}Max; * - Standard deviation, [] - Occasional occurrence; n - number of data points				

Certain profiles such as SB23 consists of a colluvial horizon followed by a highly weathered basalt layer without a residual layer. Some profiles terminated in the residual basalt horizon, assumed to be on highly weathered basalt. This occurred at depths where the highly weathered layer was most likely to occur, based on other profiles. **Figure 19** indicate that all horizons of SBProfile 1 consist mostly of silt and sand (silt over all being dominant) with less amounts of gravel. The highly weathered basalt layer contains much less silt than the residual layers, where it contains more gravel and sand.

This is also the case with the residual layer of SB17 which refused on calcrete nodules containing much more gravel than sand and silt, (SB17 is the only auger hole that contained calcrete). The colluvial layer has the highest clay content at 17% which significantly becomes less towards the highly weathered layer with 4.5% clay.

The reverse of this occurs with the gravel content increasing from the colluvial layer to the highly weathered basalt layer, as indicated in **Figure 20**. From **Figure 20** it can be seen that the sand content is approximately equal across the three horizons.

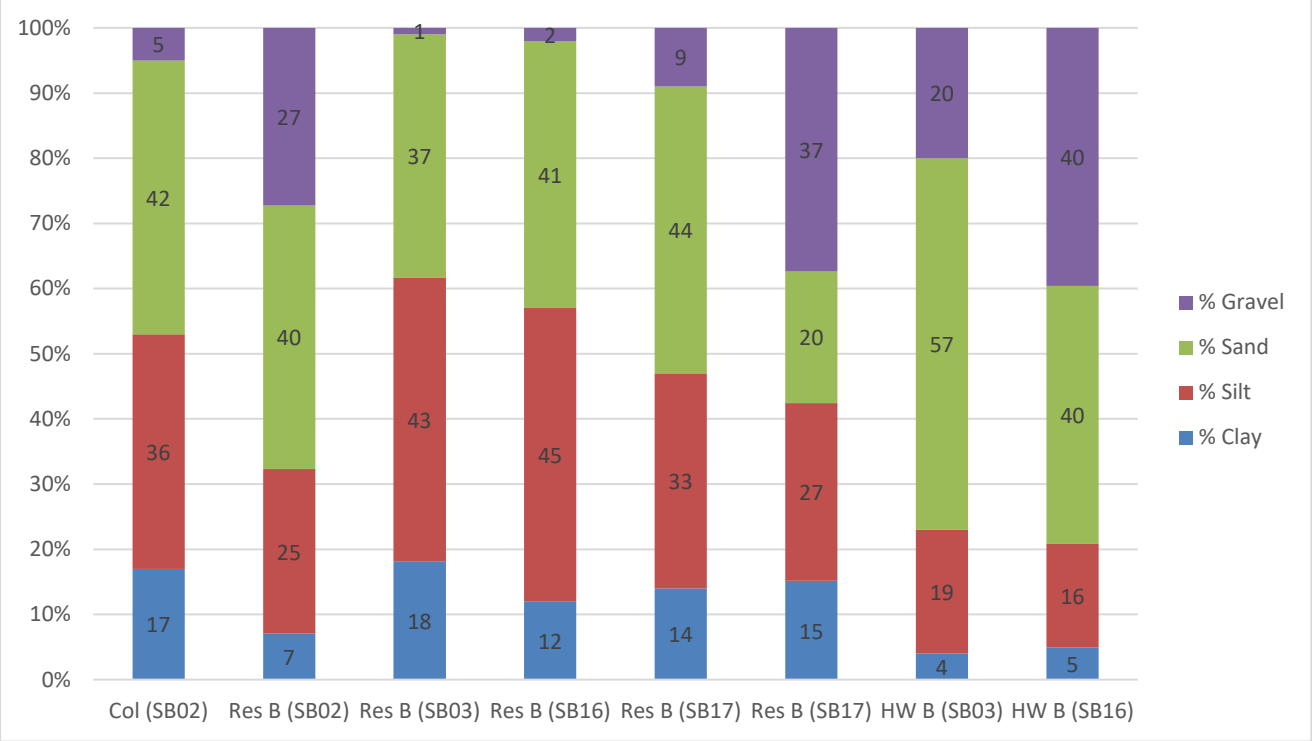

Figure 19: Laboratory soil textures for individual horizons for SBProfile 1.
Col=Colluvium; Res B=Residual Basalt; HW B=Highly Weathered Basalt

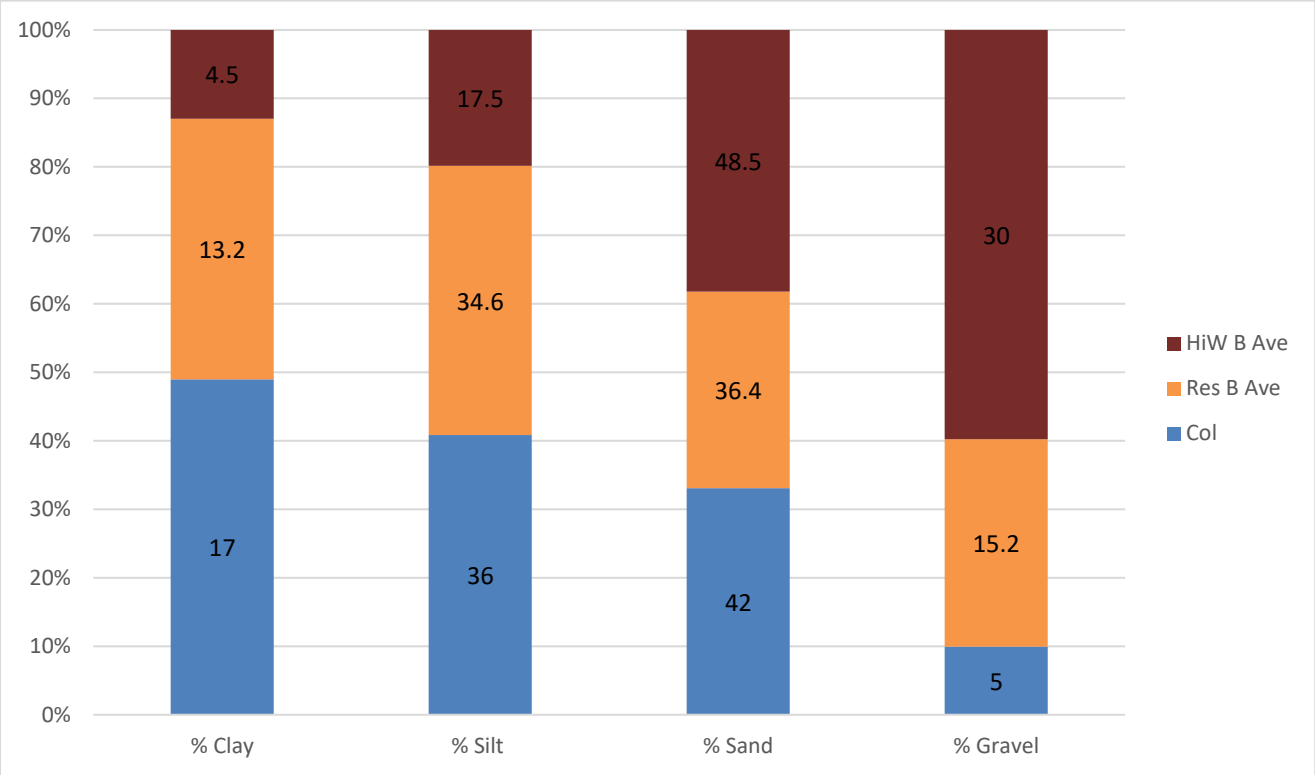

Figure 20: Average soil textures for different horizon for SBProfile 1.
Col=Colluvium; Res B=Residual Basalt; HW B=Highly Weathered Basalt

SBProfile 2: Reworked residual basalt - [Residual basalt] - Highly/Moderately weathered basalt.

Eight similar profiles with the sequence starting with a reworked residual basalt layer and continuing on to one or more of the following layers; residual basalt, highly weathered basalt and/or moderately weathered basalt were encountered and described. This sequence is represented by profiles SB11, SB12, SB15, SB18, SB19, SB20, SB21 and SB25. Summarised below in **Table 4**.

Table 4: Profile description summary for SBProfile 2 - Nhlowa site.

Horizon	**Horizon Description**	**Base of horizon below ground level (m)**	**Horizon Thickness (m)**	**Additional Information**
Reworked residual basalt	• Slightly moist, • Dark brown, • Open root channels, • Gravelly silty SAND.	0.13{0.24}0.32 *0.06	0.13{0.24}0.32 *0.06 n=8	No pedogenic material.

Horizon	**Horizon Description**	**Base of horizon below ground level (m)**	**Horizon Thickness (m)**	**Additional Information**
[Residual basalt]	• Slightly moist, • Light brown to reddish brown, • Silty SAND with Ferricrete nodules as gravel.	0.60{0.61}0.61 *0.001	0.60{0.61}0.61 *0.001 n=2	Ferricrete nodules present only as gravel.
Highly weathered basalt	• Slightly moist, • Light to yellow brown, • [Jointed], • Silty SAND with abundant highly weathered basalt gravel when excavated OR silty sandy GRAVEL.	0.15{0.43}0.80 *0.237	0.02{0.20}0.45* 0.16 n=5	No pedogenic material.
[Moderately weathered basalt]	• Slightly moist, • Light brown mottled orange and yellow, • Jointed, • Sandy coarse GRAVEL of 2cm to 4cm large basalt fragments.	0.30{0.34}0.38 *0.056	0.06{0.065}0.07 *0.01 n=2	No pedogenic material.
Min{Average}Max; * - Standard deviation, [] - Occasional occurrence; n - number of data points				

The residual basalt horizon occurred in auger hole SB11 which continued to the highly weathered basalt layer, where SB15 terminated in the residual basalt layer. Only in auger hole SB11 did the horizon sequence follow the sequence for SBProfile 2, although the residual basalt layer not being the deterministic feature of the layer. The last three horizons (residual to moderately weathered basalt) occurred sporadic in the sequence with the highly weathered basalt horizon present 5 times. The trend of the horizons either terminates in the residual basalt layer or goes from the reworked layer over to the highly weathered or moderately weathered basalt layer not encountering the residual basalt layer. It is important to note that no transported horizon was encountered. A complete sequence example is presented in **Photograph 1**.

No laboratory results are available for the material from this profile sequence.

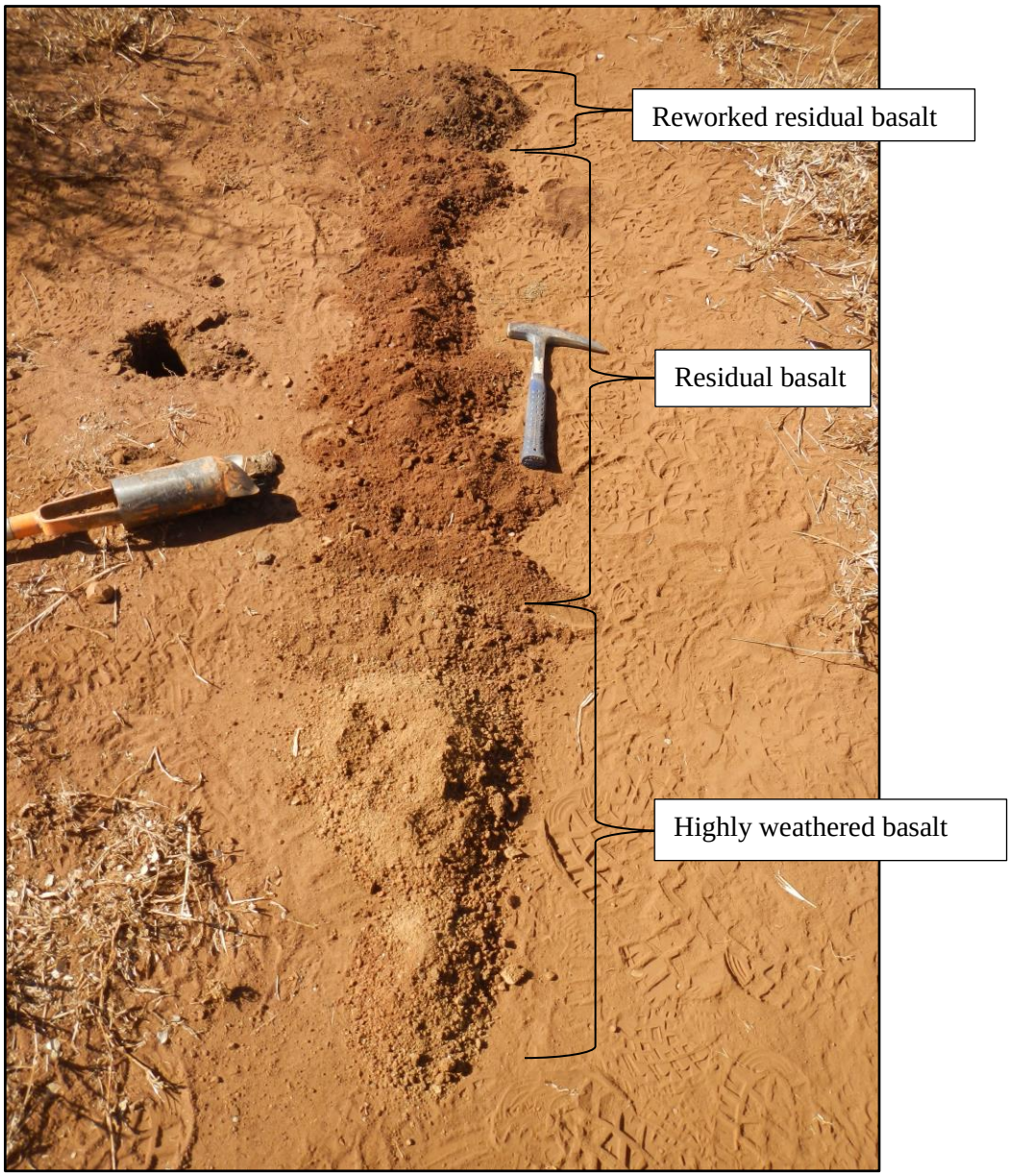

Photograph 1: SB11 example of SBProfile 2.

SBProfile 3: Residual basalt - Highly weathered basalt.

Four similar profiles with the sequence starting with a residual basalt layer and continuing on to highly weathered basalt were described and encountered. Represented by profiles SB26 to SB29. Summarised below in **Table 5**.

Table 5: Profile description summary for SBProfile 3 - Nhlowa site.

Horizon	Horizon Description	Base of horizon below ground level (m)	Horizon Thickness (m)	Additional Information
Residual basalt	• Dry to slightly moist, • Dark brown to black, • [Open root channels], • Clayey silty SAND to silty clayey SAND/sandy CLAY with scattered gravel as Ferricrete nodules and scattered highly weathered basalt possibly from the layer below.	0.33{0.57}0.81 *0.21	0.33{0.57}0.81 *0.21 n=4	Ferricrete nodules are present in each residual layer.
Highly weathered basalt	• Slightly moist, • Yellow brown mottled black, • Gravelly SAND to sandy GRAVEL of highly weathered basalt fragments.	0.54{0.81}1.30 *0.35	0.08{0.24}0.49 *0.17 n=4	Ferricrete staining visible on fragments.
Min{Average}Max; * - Standard deviation, [] - Occasional occurrence; n - number of data points				

The major defining factor in SBProfile 3 was that no cover soil such as colluvium or a reworked horizon was encountered. This could be the most disturbed portions of the site in that the top transported horizon present in SBProfile 1 and reworked horizon in SBProfile 2 has been removed. Only one sample for the residual basalt in auger hole SB29 was available at a depth of 0.81m to 1.30m the results were as follows:

- Clay – 3
- Silt – 19 %
- Sand – 56%
- Gravel – 20%
- PI – 19%

SBProfile 4: Alluvium

Three profiles were encountered and described in a stream or river, represented by profiles SB07, SB13 and SB14. Summarised below in **Table 6**.

Table 6: Profile description summary for SBProfile 4 - Nhlowa site.

Horizon	**Horizon Description**	**Base of horizon below ground level (m)**	**Horizon Thickness (m)**	**Additional Information**
Alluvium	• Slightly moist, • Light to dark greyish brown, • Stiff, • (Sandy clay/sandy gravel) to gravelly SAND.	0.10{0.51}0.94 *0.42	0.10{0.51}0.94 *0.42 n=3	No pedogenic material.
Min{Average}Max; * - Standard deviation, [] - Occasional occurrence; n - number of data points				

Profiles SB07 and SB13 refused due to coarse gravel in the profile, SB13 refused close to surface. One foundation indicator sample was taken at SB07 0.11m to 0.81m and provided the following soil texture information: Clay 16%, Silt 18%, Sand 38% and Gravel 27%.

5.1.2 Mooiplaas Profiles — Lebombo Basalt Profiles

NBProfile 1: Colluvium - residual soil.

Five similar profiles with the sequence that starts with a colluvium horizon and progresses to one or more of the following horizons; pebble marker; residual soil and/or highly weathered basalt were encountered and described. The sequence represented by profiles NB01 to NB04 and NB26. Summarised below in **Table 7**.

Table 7: Profile description summary for NBProfile 1 - Mooiplaas site.

Horizon	**Horizon Description**	**Base of horizon below ground level (m)**	**Horizon Thickness (m)**	**Additional Information**
Colluvium	• Slightly moist to moist, • Medium brown to black, • [Clayey silty SAND/sandy silt]; [clayey SILT]; [clayey SAND].	0.25{0.33}0.43 *0.08	0.25{0.33}0.43 *0.08 n=5	Variety of soil texture due to multiple geological origins.
[Pebble marker]	• Slightly moist, • Brown, • Silty SAND with abundant sub-angular and rounded quartz gravel.	SB02=0.39 m SB26=0.47 m	0.04{0.09}0.14 *0.07 n=2	Present in two of the total 5 profiles (NB02 and NB26).

Horizon	**Horizon Description**	**Base of horizon below ground level (m)**	**Horizon Thickness (m)**	**Additional Information**
Residual soil	• Slightly moist, • [Greyish] Brown [mottled orange], • Silty SAND with [calcrete nodules].	0.50{0.50}0.51 *0.006	0.10{0.17}0.26 *0.08 n=3	The residual geological origins encountered here are gabbro and gneiss.
[Highly weathered rock]	• Slightly moist, • Maroonish brown, • Silty fine coarse SAND, highly weathered basalt/gabbro gravel.	0.80m	0.30m	Only NB01 continued to a highly weathered horizon possibly being basalt or gabbro.
Min{Average}Max; * - Standard deviation, [] - Occasional occurrence; n - number of data points				

This profile sequence is variable and limited in that it consists of different geological origins such as gabbro, rhyolite, sandstone and basalt. This conglomerate of rock types together occurs at the North West corner of the site. The colluvial layer here, originates from the mixture of different weathering rates of all the different rock types juxtaposed together.

It is important to note that the profile sequences following do not contain a colluvial layer which represents the majority of the basalt site. No samples were retrieved for this profile type.

NBProfile 2

Profile sequence 2 is split into two sub divisions and not each into their own profile sequence. The starting/first horizons are close to identical and differ only in the continuation of the profile sequence into other horizons or early termination of the profile in a horizon. The early termination a result of hand auger refusal.

27 similar profiles were encountered and described with the sequence starting at a reworked residual basalt horizon that progresses to one or more of the following layers; residual basalt; highly weathered basalt and/or moderately weathered basalt.

NBProfile 2A: Reworked residual - residual basalt.

This sequence is represented by 20 of the 27 profiles by NB05, NB07 to NB11, NB13, NB14, NB16 to NB25, NB29 and NB33. An excavated example of NBProfile 2A is in Photograph 2 below and the profile summarised below in **Table 8**.

Table 8: Profile description summary for NBProfile 2A - Mooiplaas site.

Horizon	**Horizon Description**	**Base of horizon below ground level (m)**	**Horizon Thickness (m)**	**Additional Information**
Reworked residuum	• Slightly moist, • Black to dark brown, • Sandy SILT/silty SAND to [clayey silt], scattered to minor calcrete nodules and concretions.	0.21{0.37}0.61 *0.115	0.21{0.37}0.61 *0.115 n=20	6 of the 20 profiles contained calcrete in this horizon.
Residual basalt	• Slightly moist, • Greyish brown/light brown mottled white, • Silty SAND [sandy SILT] with abundant calcrete nodules and concretions, calcified horizon.	0.29{0.68}1.07 *0.21	0.07{0.32}0.63 *0.16 n=20	All 20 profiles contained calcrete in this horizon.
Min{Average}Max; * - Standard deviation, [] - Occasional occurrence; n - number of data points				

The reworked residual basalt horizon contains <10% gravel with the exception of NB05 containing 18% gravel. The majority of this horizon contains silty sand to sandy silt material, overall sand being in the majority. The underlying residual basalt layer contain higher amounts of gravel, 15% to 54%, which in this case is attributed to the calcrete nodules and concretions on which the hand auger refused, and the profile terminated. The soil textures are displayed in **Figure 21**. The residual basalt layer contains more sand than silt in all four auger holes sampled. Two of the auger holes from the reworked residual basalt horizon (NB05 and NB11) has higher sand and silt than their underlying residual basalt layer. The other two auger holes (NB19 and NB20) has less sand in the reworked residual layer than in the residual layer (although still a higher silt content), this creates a 50% split between sand and silt dominance with sand slightly in the majority.

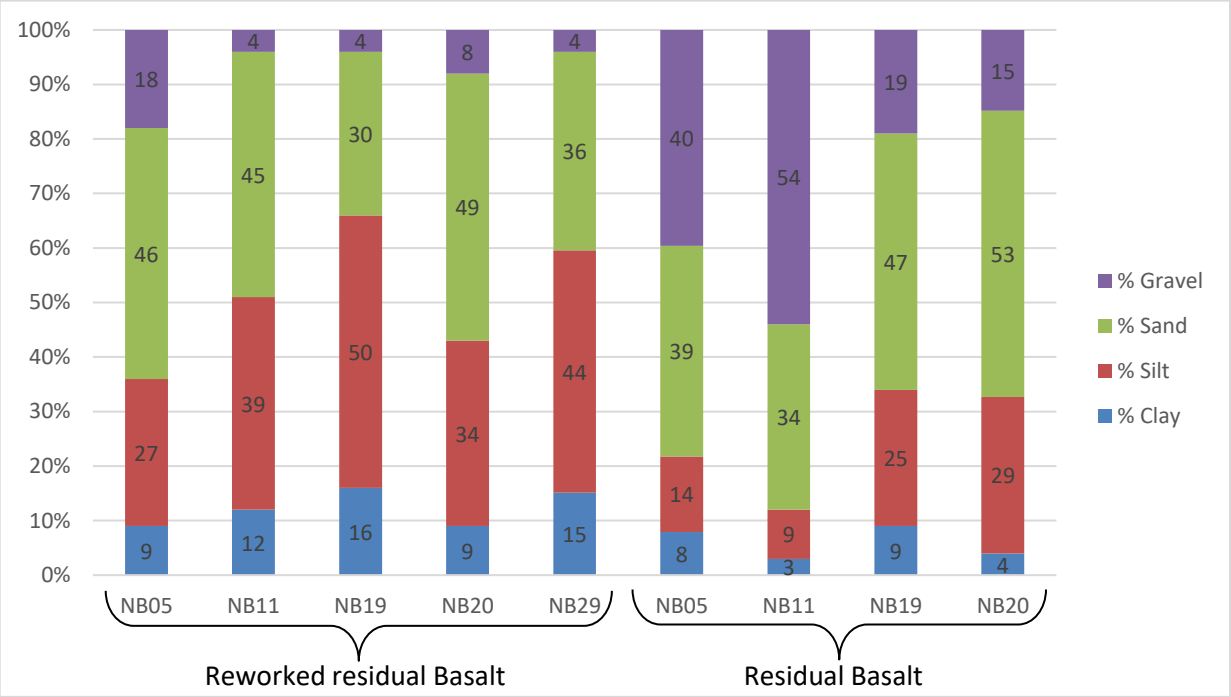

Figure 21: Laboratory soil textures for individual horizons for NBProfile 2A.

The reworked residual basalt contains more silt as well as clay than the residual basalt layer with averages of 38.8% and 12.2% respectively as opposed to the residual basalt averages of 19.25% and 6%. **Figure 22** below shows that the percentage clay and silt are higher in the reworked residual basalt than the residual basalt layer which has undergone less weathering. This could also be attributed to the high presence of calcrete in the residual basalt layer, by limiting increased weathering activity through cementation compared to the reworked residual basalt layer.

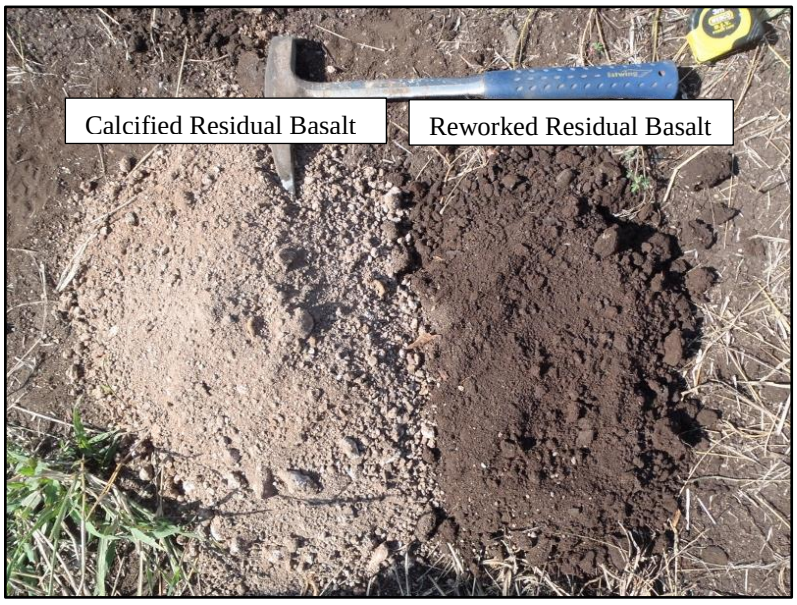

Photograph 2: NB29 example of NBProfile 2A.

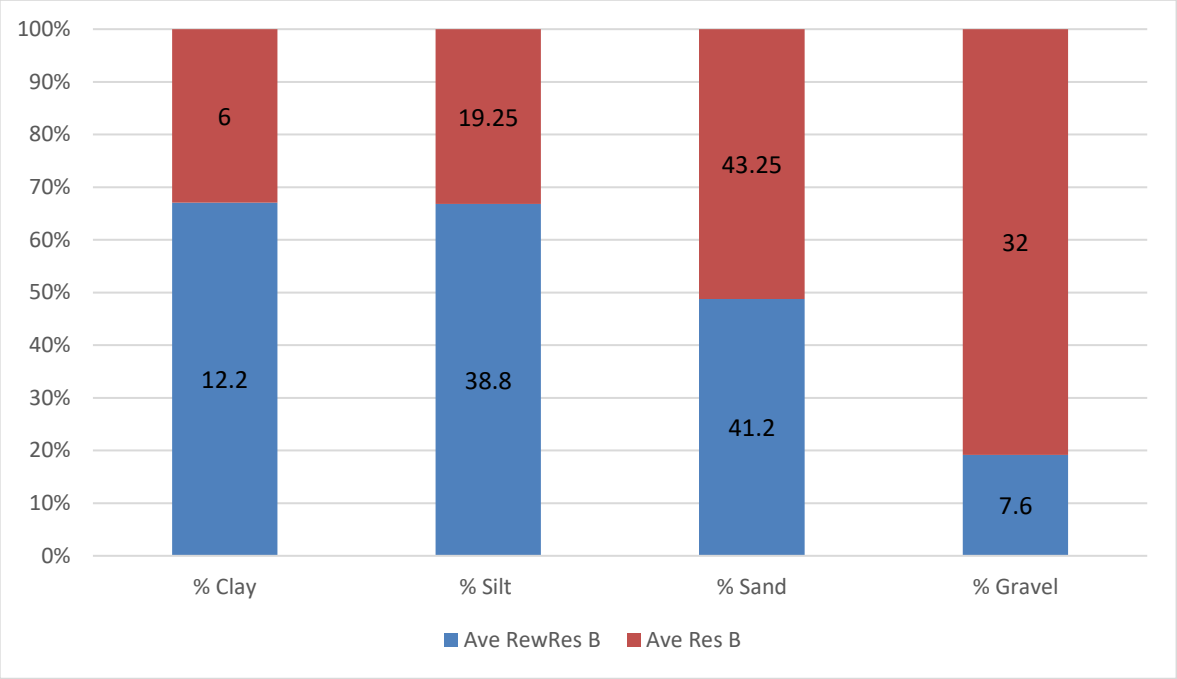

Figure 22: Average soil textures for different horizons for NBProfile 2A.
RewRes B=Reworked Residual Basalt; Res B=Residual Basalt

NBProfile 2B: Reworked residual - Residual basalt - Highly weathered basalt.

This sequence is represented by 7 of the 27 profiles viz. NB06, NB12, NB15, NB27A&B, NB28 and NB34. Profile summarised below in **Table 9**.

Table 9: Profile description summary for NBProfile 2B - Mooiplaas site.

Horizon	**Horizon Description**	**Base of horizon below ground level (m)**	**Horizon Thickness (m)**	**Additional Information**
Reworked residuum	• Slightly moist, • Black to dark brown, • Sandy SILT / [silty SAND] to [clayey silt], scattered calcrete nodules and concretions.	0.15{0.35}0.60 *0.18	0.15{0.35}0.60 *0.18 n=6	Only 1 of the 6 profiles contained calcrete in this horizon.
Residual Basalt	• Slightly moist, • Greyish brown/light brown mottled white, • Silty SAND [sandy SILT] with scattered to abundant calcrete nodules and concretions, calcified horizon.	0.35{0.78}1.48 *0.42	0.20{0.50}1.17 *0.41 n=6	6 of the total 7 profiles contained calcrete. The one profile did not encounter the residual layer.

Horizon	**Horizon Description**	**Base of horizon below ground level (m)**	**Horizon Thickness (m)**	**Additional Information**
Highly weathered basalt	• Slightly moist, • Light greyish brown [dark grey], • Clayey silty fine to coarse SAND GRAVEL [gravelly sand], gravel of highly weathered basalt when augered.	0.45{1.86}3.0 *1.13	0.05{1.47}2.65 *1.12 n=7	Calcrete nodules in 2 of the 7 profiles and calcrete veins encountered in NB27 and NB28 profiled in a quarry.
[Moderately weathered basalt]	• Dark grey, • Jointed and fractured, • Medium hard rock, calcrete veins encountered as streaks and patches in NB27 and NB28.	3 m	2.16{2.49}2.65 *0.28 n=3	NB27A, NB27B and NB28 were profiled in a quarry from and open face. (NB27A shown in Photograph 3)
Min{Average}Max; * - Standard deviation, [] - Occasional occurrence; n - number of data points				

NBProfile 2A terminated in the residual basalt layer, presumably refused on abundant calcrete nodules and concretions or highly weathered basalt. Therefore, the sequence did not continue on to the highly weathered basalt horizon. NBProfile 2B contained mostly scattered to moderately abundant nodules and limited concretions making it possible to auger through to the highly weathered basalt horizon.

Figure 23 displays the soil textures of NBProfile 2B, it portrays similar trends as **Figure 21** for NBProfile 2A in that the gravel content increases from the reworked residual basalt to the residual basalt which represents the increase in calcrete nodule formation. The gravel averages for the reworked residual and residual basalts are 18.25% and 39% respectively. The clay and silt content for the reworked residual basalt of NBProfile 2B such as for NBProfile 2A is still much higher than the residual basalt, with the clay and silt content for the reworked residual horizon at 10.25% and 32.75% respectively compared to the residual basalt horizon at 3.75% and 17.25% respectively.

NBProfile 2A contains a higher content of fines collectively through the profile as well as individually per horizon, than NBProfile 2B as portrayed by **Figure 24**.

The total average percentage fines (silt and clay) for the reworked residual layer for NBProfile 2A is 51% and the residual basalt 25.25%. The reworked residual layer of NBProfile 2B contains 43% fines and the residual basalt layer 21%.

Photograph 3: Highly to moderately weathered medium hard rock Basalt with calcrete streaks (Profile in Quarry).

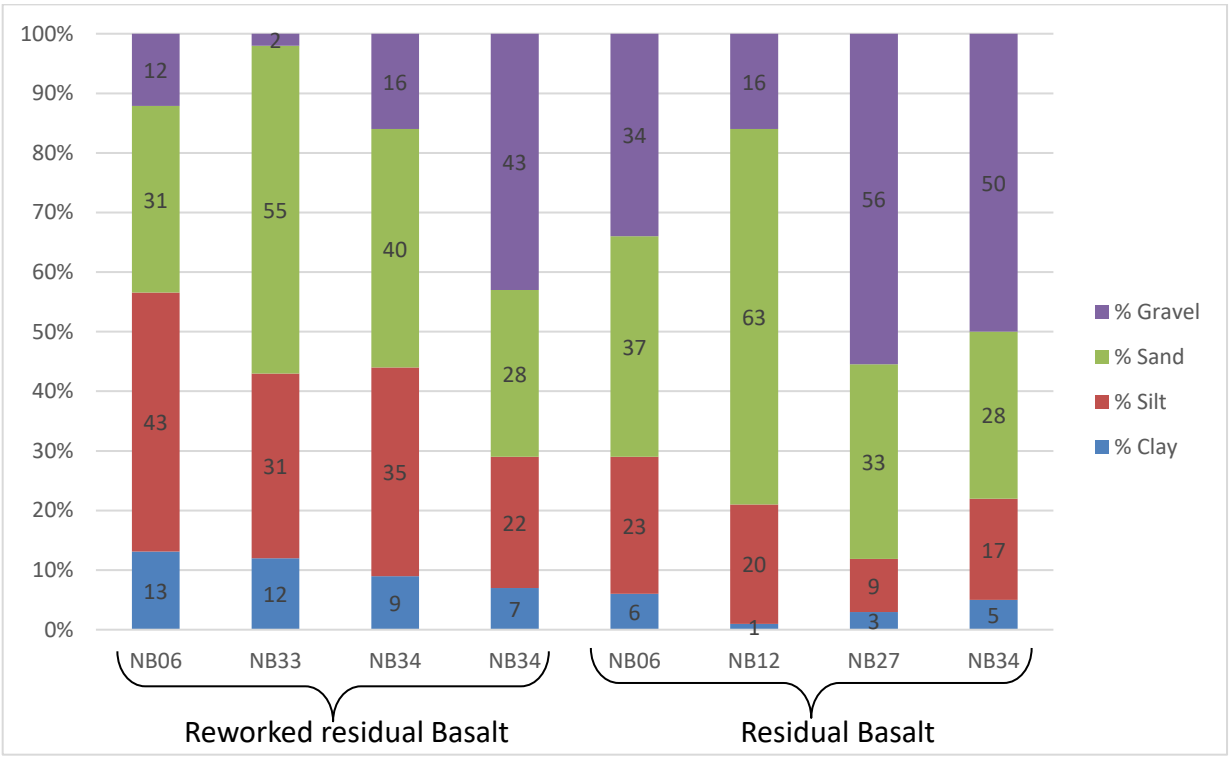

Figure 23: Laboratory soil textures for individual horizons for NBProfile 2B.

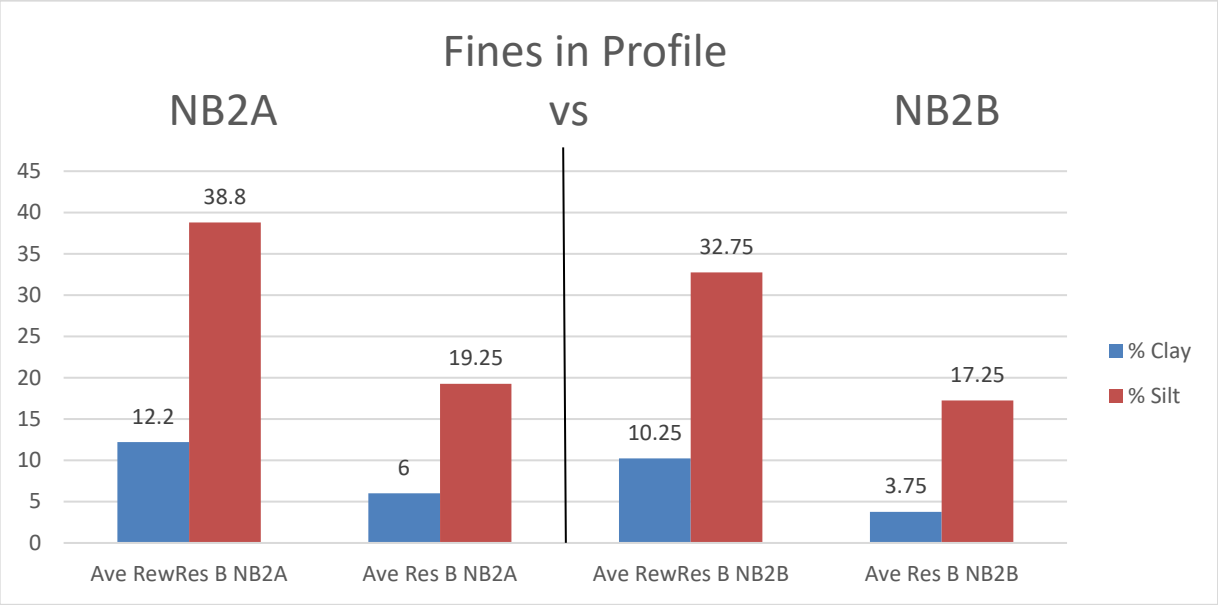

Figure 24: Average clay and silt content for NBProfile 2A vs NBProfile 2B.
RewRes B=Reworked Residual Basalt; Res B=Residual Basalt

NBProfile 3: Alluvium

Three profiles were encountered and described in a stream or river. The alluvial horizon was underlain by either the reworked residual basalt or residual basalt layer represented by profiles NB30 to NB32. Profile summarised below in **Table 10**.

Table 10: Profile description summary for NBProfile 3 - Mooiplaas site.

Horizon	**Horizon Description**	**Base of horizon below ground level (m)**	**Horizon Thickness (m)**	**Additional Information**
Alluvium	• Slightly moist, • Brown to dark grey to black, • Silty sand to clayey SILT, and gravel.	0.24{0.58}0.90 *0.33	0.24{0.58}0.90 *0.33 n=3	Gravel is of mixed origin and calcrete nodules on surface but not in the horizon.
Reworked residual Basalt	• Grey streaked and mottled orange and mottled white, • Sandy SILT, scattered calcrete nodules.	Horizon occurred at 0.90 - 1.20	0.30	Horizon only encountered in profile NB31.
Residual basalt	• Grey brown mottled and streaked orange brown, • Sandy SILT, scattered calcrete nodules.	0.64{0.80}0.72 *0.11	0.03{0.3}0.56 *0.37 n=2	Horizon encountered in profiles NB30 and NB32.

Min{Average}Max;
* - Standard deviation,
[] - Occasional occurrence;
n - number of data points

Profile NB30 was profiled at a first order stream and NB31 in a second order stream. NB30 refused on calcrete concretions from a possible reworked residual basalt horizon where NB32 also refused on calcrete nodules in the residual basalt horizon. Two sieve analysis tests were done on auger hole NB32 at 0.00m to 0.24m for the alluvial layer and at 0.24m to 0.80m for the underlying calcified residual basalt. The results provided the following soil texture information for the alluvial layer: Clay 20%, Silt 25%, Sand 42% and Gravel 13%; and for the calcified residual basalt layer: Clay 29%, Silt 20%, Sand 37% and Gravel 15%.

5.1.3 Siloam — Sibasa Basalt Profiles

The profiles at Siloam represents the Sibasa basalts through eight profiles (TP01-TP08) excavated by a LuiGong 777 TLB to a depth of between 1.50m and 3.20m. Only one profile sequence with some differences in the horizons are described and summarised below in **Table 11**.

Table 11: Profile description summary for Sibasa basalts - Siloam site.

Horizon	**Horizon Description**	**Base of horizon below ground level (m)**	**Horizon Thickness (m)**	**Additional Information**
Colluvium	• Slightly moist to moist, • Dark brown/brown, • Stiff [soft, very stiff], • Open structured and slightly slickensided, • Sandy clayey SILT / [sandy silt] to [silty CLAY], minor to abundant gravel.	0.65{1.04}1.90 *0.41	0.65{1.04}1.90 *0.41 n=8	No pedogenic material encountered.
Reworked pebble marker / residuum	• Slightly moist, • Red/maroon brown mottled black/white/red, • Dense to [very dense, stiff], • Open structured, • Silty sandy GRAVEL/sandy gravelly SILT [clayey silt with abundant gravel] with abundant sub-angular cobbles.	1.45{1.76}2.35 *0.35	0.45{0.58}0.75 *0.14 n=5	Ferricrete nodules encountered in TP01, TP02 and TP04.

Horizon	**Horizon Description**	**Base of horizon below ground level (m)**	**Horizon Thickness (m)**	**Additional Information**
Residual basalt	• Slightly moist, • Yellow brown mottled/patched black, • Dense to very dense, • [Slightly] pinholed structured, • Silty/sandy GRAVEL to sandy gravelly SILT [clayey silt with abundant gravel] with abundant rounded to sub-rounded basalt cobbles, [Scattered Ferricrete nodules].	1.45{1.76}2.35 *0.58	0.15{1.01}1.85 *0.62 n=8	Ferricrete encountered in TP01, TP02 and TP04. TP08 contains patches of highly to completely weathered basalt.
[Completely weathered basalt]	• Wet, • Light brown, • Firm to medium dense, • Relic rock structure, • Sandy clayey SILT, scattered highly to completely weathered basalt gravel.	Horizon occurred at 2.50-3.00m	0.50m	No pedogenic material encountered.
Min{Average}Max; * - Standard deviation, [] - Occasional occurrence; n - number of data points				

The investigated site is too small with no distinct large differences to distinguish more than one profile type. The typical sequence encountered during excavation was colluvium underlain by a reworked pebble marker and residuum, residual basalt and one profile continued into completely weathered basalt. Photograph 4 displays a basic soil profile on site.

The colluvial horizon contained the highest amount of clay with an average (standard deviation) of 26.50% (15.02%) followed by the residual layer with 14.83% (9.26%). The highest percentage of fines are also present in the colluvial layer with an average of 50.75% followed by the residual layer at 35.49%. The high fines content most likely attributed to the site being located close to the footlope of the mountain. The reworked pebble marker as expected, contained the highest gravel content at an average of 51%.

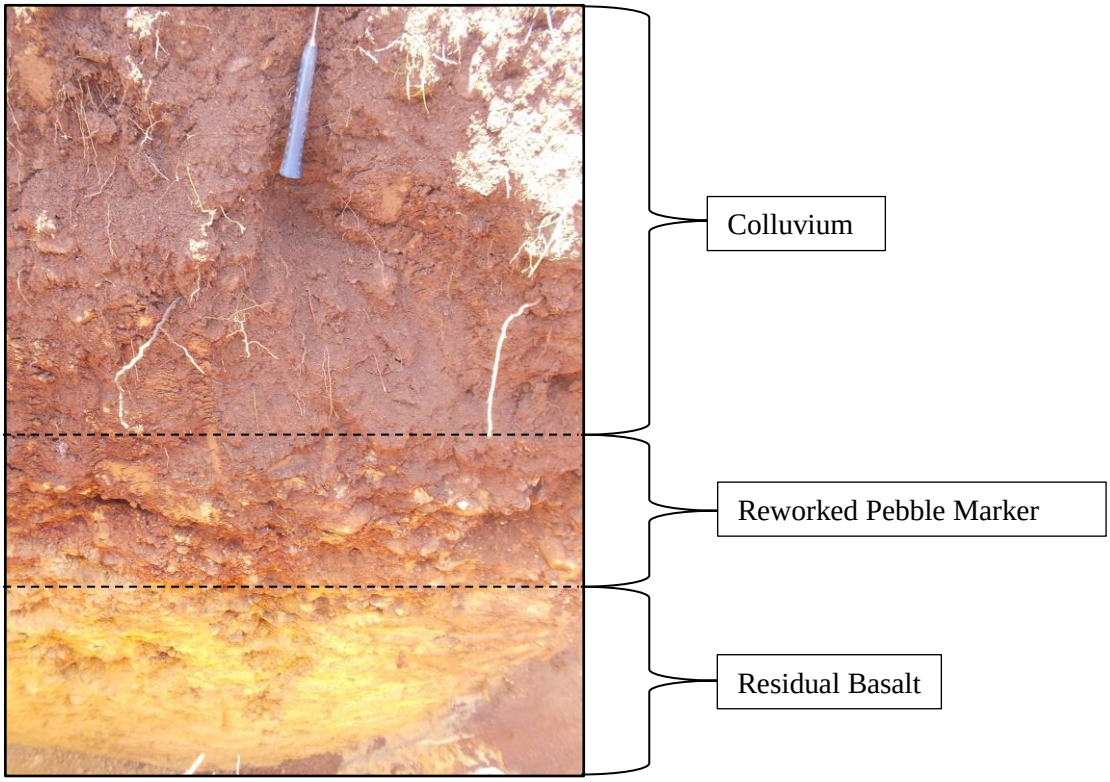

Photograph 4: Typical Sibasa Basalt profile example, TP01.

5.1.4 Roedtan — Springbok Flats Basalt Profiles

The profiles at Roedtan represents the Springbok Flats basalt excavated by a JCB 3CX TLB down to a depth of between 2.10m to 2.50m with an average depth of 2.30m. Only one profile sequence with some differences in the horizons are described as the profiles encountered were constant across the site. Summarised below in **Table 12**.

Table 12: Profile description summary for Springbok Flats basalts - Roedtan site.

Horizon	**Horizon Description**	**Base of horizon below ground level (m)**	**Horizon Thickness (m)**	**Additional Information**
Colluvium	• Slightly moist to moist, • Maroon/red brown, • Medium dense to dense, • Pinholed structured, • Clayey silty SAND.	0.26{0.33}0.40 *0.05	0.26{0.33}0.40 *0.05 n=8	No pedogenic material encountered.

Horizon	**Horizon Description**	**Base of horizon below ground level (m)**	**Horizon Thickness (m)**	**Additional Information**
Calcified residual basalt	• Slightly moist, • Red/orange brown mottled/patched white, • Medium dense to dense, • Open [pinholed] structured, • Silty gravelly SAND/silty sandy GRAVEL with gravel of weathered basalt and calcrete concretions and nodules.	0.55{0.83}1.20 *0.24	0.29{0.50}0.85 *0.21 n=8	Calcrete encountered in TP02 to TP07. Patches of horizontally layered and fractured completely/highly weathered basalt,
Completely to Highly weathered Basalt	• Slightly moist, • Streaked orange brown and black mottled white, • Dense to soft rock, • Fractured and horizontally layered, • Silty sandy GRAVEL with gravel of weathered basalt, [patches of moderately weathered basalt], [patches of calcification.]	1.10{1.75}2.50 *0.47	0.50{0.92}1.80 *0.45 N=5	Calcrete nodules encountered in TP01.
[Highly to Moderately weathered Basalt]	• Slightly moist, • Streaked black and orange, • Highly fractured and horizontally layered, • Soft rock to medium hard rock, • Excavates to sandy GRAVEL with gravel of moderately weathered basalt.	2.40{2.43}2.50 *0.06	0.60{0.83}1.30 *0.40 n=3	Calcrete encountered only as scattered patches.

Min{Average}Max;
* - Standard deviation,
[] - Occasional occurrence;
n - number of data points

The basic profile horizon sequence was colluvium, calcified residual basalt, completely weathered basalt, highly weathered basalt with patches of moderately weathered basalt in the latter two horizons. These latter two horizons are described as a combination such as completely to highly weathered basalt due to mixed portions of both completely and highly weathered basalt present in the horizon. In some profiles a definite distinction could be made although due to the undulated weathering in the horizon this was not the majority of the time. The dominant soil texture in these profiles is gravel and sand in the residual and weathered basalt horizons. The sand content in the calcified residual basalt is higher than the completely/highly weathered basalt horizon with an average (standard deviation) of 36.33% (6.66%) and 27% (4.47%) respectively. The high gravel content in the calcified residual basalt layer is attributed to the calcrete nodules

and concretions as well as weathered basalt gravel: Ave. 48% and Stdev. 8.71%. Although this is still less than the weathered basalt horizons that has a highly fractured structure and excavates to mostly gravel: Ave. 67.20% and Stdev. 5.58%. The fines content is extremely low in both these horizons at <5% present.

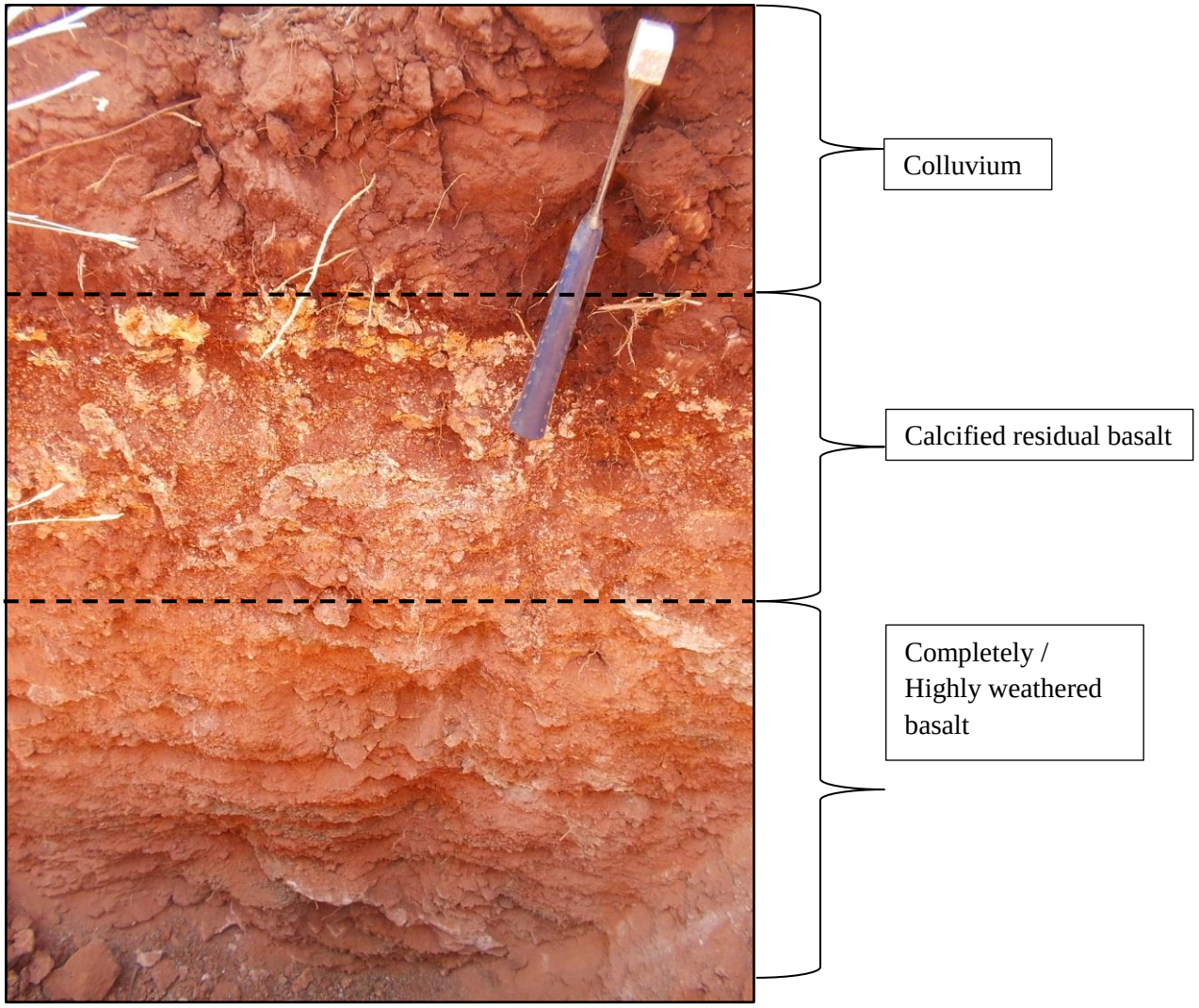

Photograph 5: Typical Springbok Flats Basalt profile example, TP02.

5.1.5 Codrington — Springbok Basalt Profiles

Only one profile was described in an open quarry as a reference point to the Springbok Flats basalt in the Roedtan site. Profule summarised below in **Table 13**, and typical profile depicted in **Photograph 6**.

Table 13: Profile description summary for Springbok Flats basalts - Codrington site.

Horizon	Horizon Description	Base of horizon below ground level (m)	Horizon Thickness (m)	Additional Information
Residual basalt	• Dry, • Dark brown mottled white, • Loose to soft, • Shattered, • Silty clayey fine SAND/silty sandy CLAY (with calcrete nodules and concretions).	1.00m	1.00m n=1	Calcrete encountered in top residual horizon
Highly weathered basalt	• Dry, • Olive brown speckled white & orange, • Loose, • Intact, • Gravelly silty SAND.	2.00m	1.00m	No calcrete encountered.
Min{Average}Max; * - Standard deviation, [] - Occasional occurrence; n - number of data points				

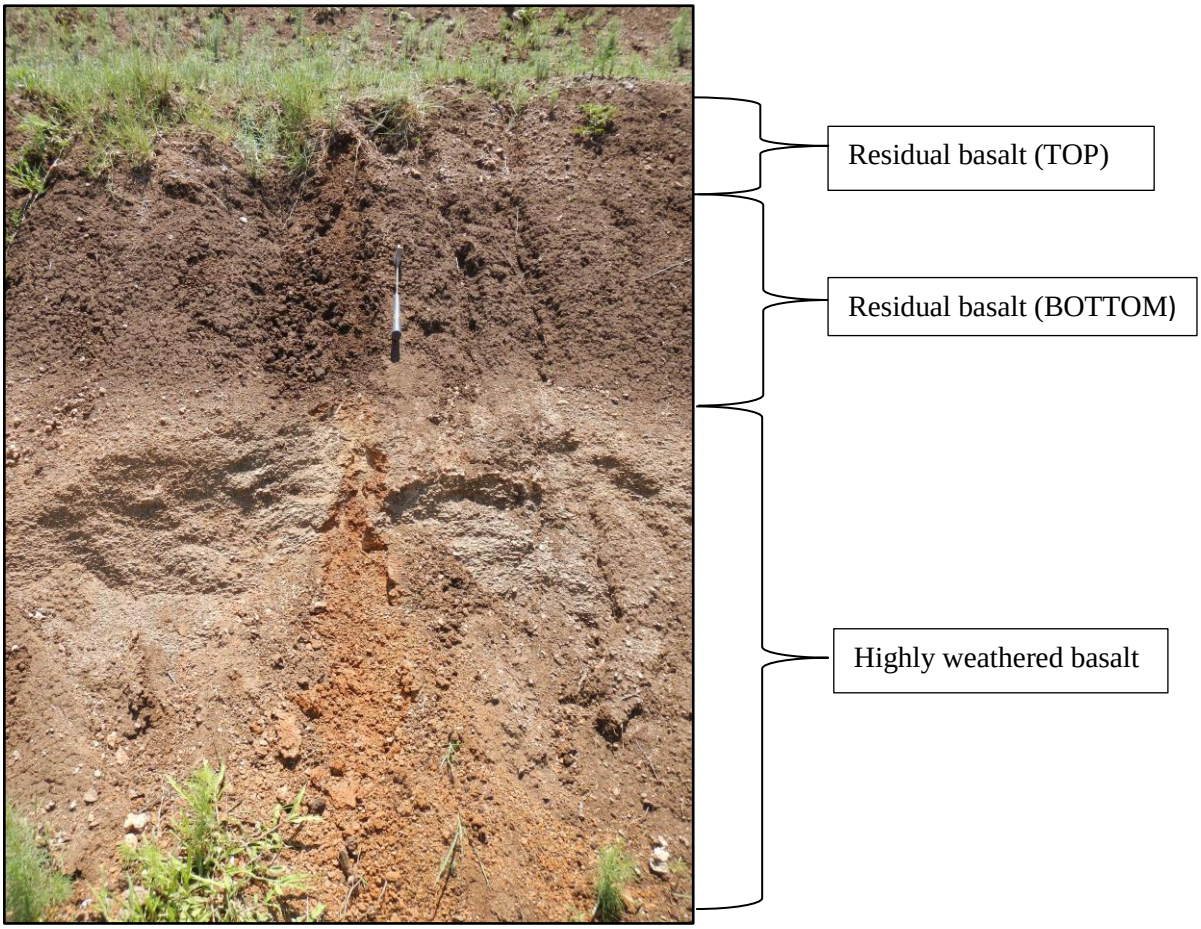

Photograph 6: Basic profile example at Codrington, S01.

5.2 Chemical and Mineralogical Analysis

As indicated above the basalt from the Nhlowa site is mostly or entirely underlain by the Sabie River formation, which according to Duncan and Marsh (2006) are tholeiitic (olivine poor) basalt in composition. The Mooiplaas site is partly or entirely underlain by the Letaba Formation, picritic (olivine rich) basalt. The basalt magma series can be divided into two groups *viz.* alkaline and subalkaline, where the subalkaline group is further divided into tholeiitic and calc-alkaline basalt. A summary of the characteristics of tholeiitic basalt from the subalkaline subgroup and alkaline group can be seen above in **Chapter 1** in **Figure 1**.

The alkaline basalts area characterized by having a lower silica content (silica-undersaturated) and have higher contents of alkalis such as sodium (Na_2O) and potassium (K_2O) than the tholeiitic basalts series. The tholeiitic basalt series contain higher iron content whereas the calc-alkaline comprises of more magnesium and alkalis (Na_2O) than tholeiitic basalt, as portrayed by the AMF diagram in

Figure **2**.

The basalts of the Springbok Flats according to SACS (1980, cited in Marsh 1984) was originally correlated to the Letaba formation of the Lebombo Group. This name was collectively given to all basalts that were located below the rhyolites in Lebombo. Although after additional investigations it was found that the Springbok Flats were chemically and petrographically different to the Letaba Formation basalts. Additional data presented by Marsh (1984) indicated the Springbok Flats are more closely associated to the Sabie River Formation and Lesotho Formation, although having a stronger supporting correlation to the former.

The AMF diagram in **Figure 25** indicates where the Nhlowa, Mooiplaas and Springbok Flats basalts at Codrington plot according to the XRF data gathered. From the profile descriptions above it can be observed that the Nhlowa and Mooiplaas sites do not weather similarly and in turn creates different profiles and soil characteristics. One notable difference between the two profiles is the formation of different pedocretes *viz.*, ferricrete at Nhlowa in the south and calcrete at Mooiplaas in the north.

This can be accredited to differences in parent rock mineralogy as well as different climates conditions (such as rainfall and/or evaporation), this contributes to different soil forming processes as a generalization on Weinert's N value (Brink, 1979).

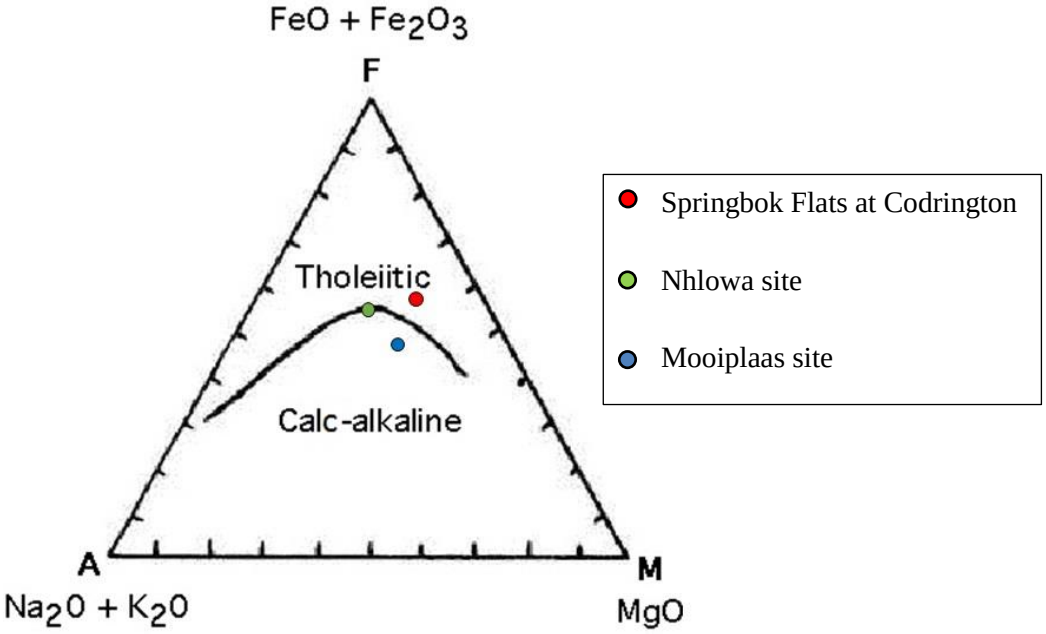

Figure 25: The Karoo basalts plotted on the AMF diagram for Tholeiitic and calc-alkaline basalt determination (adapted from Winter, 2001).

Smith et al. (2013) indicate that the northern Mooiplaas site receives less annual rainfall than the southern Nhlowa site. The average rainfall for the Mooiplaas site is 480mm/annum (to the closest 10mm/annum) and the Nhlowa site 610mm/annum. Rainfall records between 1940-1941 and 2010-2011 from stations near the sites were used in calculating the average rainfall.

The Siloam site has similar rainfall as the Nhlowa site and the Springbok Flats Basalts of Roedtan and Codrington have similar lower rainfall to the Mooiplaas site. The Siloam, Roedtan and Codrington sites also differ in that the soil profiles at the Siloam site contain ferricrete whereas those at the Roedtan and Codrington sites contain calcrete similarly to the Nhlowa and Mooiplaas site respectively.

5.2.1 XRF Analysis — Rock

5.2.1.1 Mooiplaas and Nhlowa

The Mooiplaas rock analyses had six rock samples available in contrast to Nhlowa with only two samples, for the latter from a jointed rock mass and one containing visible amygdales. From a chemical/elemental point of view as displayed by Table 14 and **Figure 26** no key differences in the major elements (Fe and Ca) of the sampled parent rocks from the two sites can be distinguished. Key differences in respect to the Fe and Ca contents present is in excess and contribution to calcrete formation at the Mooiplaas site in the northern basalts, and ferricrete formation at the Nhlowa site in the southern basalts. The Fe and Ca contents between the two sites are very similar. With the Fe contents of the Mooiplaas and Nhlowa site at 12.29% and 12.43% and the Ca contents at 8.81% and 7.71% respectively.

The abovementioned indicates the amount of Fe and Ca in the parent rock, is not in excess in either of the rocks from the sites. From this information the amount of Fe and Ca in the rock possibly being in excess at one site to the other is not the determining factor for different pedogenic formation. It is reasonable to believe the distinctive pedogenic formations between the two sites are possibly not determined by excess of one element to the other. The differences in type of mineralogy and weathering properties in different climatic environments all contribute to different pedogenic formations. The type and intensity of weathering these different mineral assemblages undergo determines which elements get transported or precipitated.

Notable differences in the elemental concentrations between the Mooiplaas and Nhlowa basalt rock is evident for Al and Mg. The average Al concentrations are higher in the Nhlowa basalt rock at 14.60% than the Mooiplaas basalt rock at 10.86%, where the reverse occurs with the average Mg concentrations of 5.22% in the Nhlowa basalt rocks and 8.38% for the Mooiplaas basalt rocks. The alkali content of the parent rocks between the two sites are very similar when considering the averages. When considering the standard deviation at the Mooiplaas site for the Na_2O content, the Mooiplaas site contains rock samples with higher sodium contents.

Table 14: Average rock element concentrations for the Mooiplaas and Nhlowa sites.

	Rock samples			
	Mooiplaas		Nhlowa	
XRF (wt%)	Average	Standard Deviation	Average	Standard Deviation
SiO_2	46.64	4.40	50.89	1.27
TiO_2	2.95	0.54	2.21	1.53
Al_2O_3	10.86	1.59	14.60	0.03
CaO	8.81	1.21	7.71	1.12
Fe_2O_3	12.29	0.73	12.43	0.04
MnO	0.18	0.03	0.16	0.05
MgO	8.38	3.76	5.22	1.88
Na_2O	3.81	2.67	3.32	0.28
K_2O	1.56	0.77	2.16	1.15
P_2O_5	0.54	0.28	0.40	0.37
Cr_2O_3	0.06	0.06	0.02	0.01
NiO	0.04	0.03	0.00	0.00
V_2O_5	0.06	0.00	0.05	0.003
ZrO_2	0.03	0.02	0.03	0.03
CuO	0.02	0.01	0.00	0.00
LOI	3.25	2.85	2.36	0.56
TOTAL	99.49	0.25	101.56	0.42
Y (ppm)	29.17	8.76	36.07	14.15
Zr (ppm)	336.17	117.17	282.23	272.15
	Higher value than other site			
	Lower value than other site			
	Similar values between sites			

The less mobile element Titanium (Ti) for the two sites are very similar with the Mooiplaas site slight higher, average concentration of 2.93% and Nhlowa of 2.21%. The lower standard deviation of the Ti of the Mooiplaas site indicates a more constant concentration in the rock samples and the Nhlowa site with very high or low concentrations. The trace elements Yttrium (Y) and Zirconium (Zr) for the two sites somewhat do drastically differ from each other. The Y concentration of the Mooiplaas site is 29.17ppm which is lower than the Nhlowa site at 36.07ppm. The Mooiplaas site has more constant concentrations of Y from a minimum of 19ppm to a maximum of 38ppm.

The same trend for the Mooiplaas site occurs with Zr where the concentrations are 336.17ppm with very similar concentrations in all the samples with a minimum at 213ppm and maximum at 465ppm. The Zr concentrations for the Nhlowa site are similar to Ti whereby it has either very high or low values, in the case for Zr 474.66ppm to 89.79ppm.

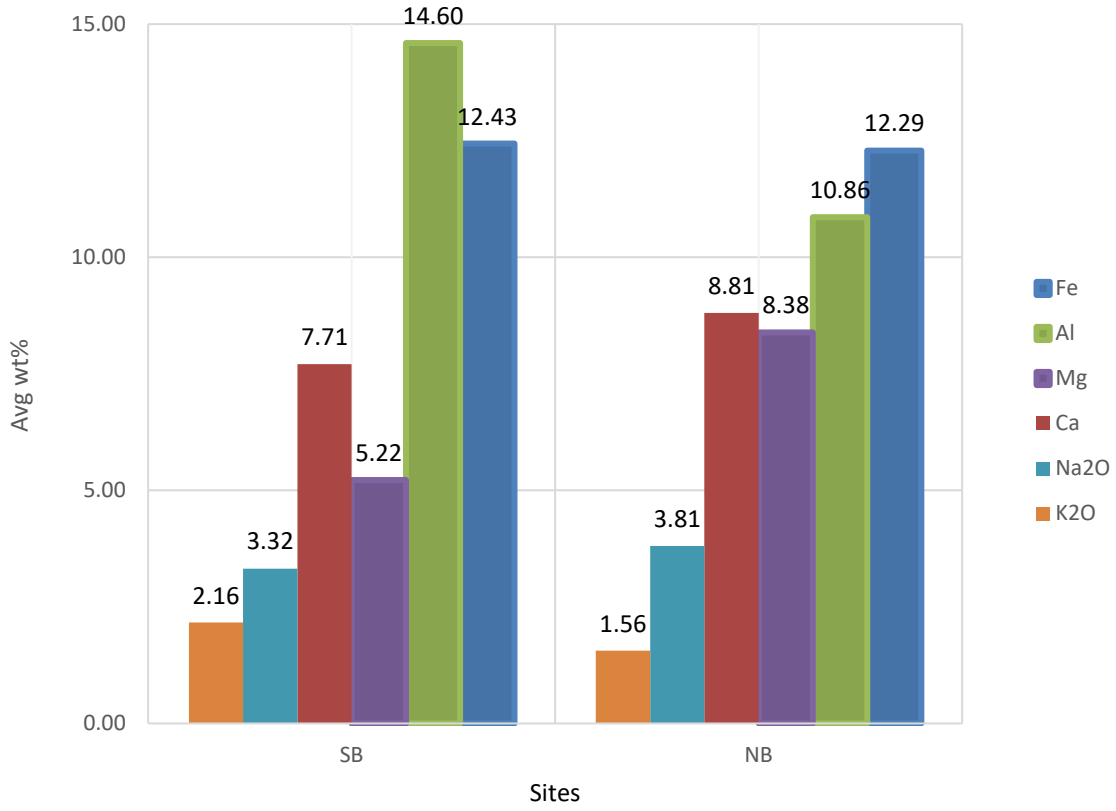

Figure 26: Major element change between Nhlowa (SB - southern basalts) and Mooiplaas (NB - northern basalts) sites.

5.2.1.2 Codrington

No fresh or weathered rock samples were tested for the Sibasa basalts at Siloam as well as for the Springbok Flats basalts at Roedtan. For the Springbok Flats basalt at Codrington one highly weathered basalt sample was taken from profile at 1.00m to 2.00m as well as a slightly weathered rock sample. The Ca content for the Codrington site in both rock samples are higher than the Mooiplaas and Nhlowa sites, the highly weathered basalt at 10.08% and the slightly weathered basalt at 9.86%, only 1.00% to 2.00% higher.

The Fe content for the Codrington site samples are less than the KNP sites with 1.00% to 1.50%, the highly weathered basalt at 10.70% and the slightly weathered basalt at 11.09%.

The Mg and Al contents of the highly and slightly weathered basalt for the Springbok flats at Codrington are very similar, Mg at 5.84% and 6.21% and Al at 14.33% and 14.85% respectively. These values are also very similar to the Nhlowa site values of Mg 5.22% and Al 14.60%. The Mooiplaas site has lower Al contents at 10.86% and higher Mg contents of 8.38% than the Codrington site representing the Springbok flats basalt.

The alkali contents of Na_2O and K_2O are much lower than both of the KNP supersites especially the K_2O content. The K_2O content for the highly and slightly weathered basalt of the Springbok Flats are 0.51% and 0.46% respectively, whereas Nhlowa is 2.16% and Mooiplaas is 1.56%. The Na_2O content for the highly weathered basalt at the Codrington site is 1.91% and the slightly weathered basalt is 2.12%; this is 1.20% to 1.90% less than at Mooiplaas and Nhlowa. These values together with all other individual XRF data can be viewed in **Appendix B**.

The Ti, Y and Zr concentrations of the highly and slightly weathered basalt samples are very similar to their respective samples. The Ti content of the highly weathered basalt is 0.93% and slightly weathered basalt is 0.97%, which is much lower than the KNP supersites.

The trace elements Y for the highly weathered basalt and slightly weathered basalt are very similar to each other, the same for Zr. The Y for the highly weathered basalt is 21.00ppm and slightly weathered basalt is 23.00ppm. The Zr content is 107ppm for the highly weathered basalt and 105ppm for the slightly weathered basalt. The Y content at Codrington is similar to the averages of the Mooiplaas site but less than the Nhlowa site. The Zr content at Codrington is generally much less than both the KNP sites with some samples slightly higher.

5.2.2 XRD Analysis — Rock

5.2.2.1 Mooiplaas and Nhlowa

Table 15 below indicates the average XRD concentrations for rock samples from the two KNP supersites. Mineral percentages per rock sample differ at times for example by 16% from each other (indicated by the standard deviations), this as a result that certain minerals aren't always present in the rock. Differences between the mineral configurations of the KNP supersites are as follows: the pyroxene mineral Augite [$(Ca,Na)(Mg,Fe,Al,Ti)(Si,Al)_2O_6$] is only present in the northern basalt rocks at Mooiplaas, whereas Diopside (commonly $MgCaSi_2O_6$, part of the solid solution series with Augite) is only found in the southern basalt rocks at Nhlowa.

The Mg endmember of pyroxene, Enstatite ($MgSiO_3$), was also only found in the southern basalt rocks. Olivine was found to be only present in the northern basalt rocks in two samples, as Forsterite the Mg endmember. The rock sample at Codrington representing the Springbok Flats basalts also only contain Augite and no Diopside or Enstatite, similar to the northern basalt samples although it contains no Forsterite (olivine).

The northern basalt rocks from the Mooiplaas site differ largely from each other across the site in mineral content, this is indicated by **Table C4**, **Appendix C** depicting the individual XRD rock sample results. Rock samples from Outcrop 4 and 5 show similar mineral assemblages and concentrations although differ almost completely from the other samples. For example. rocks taken at auger hole NB17 and NB29 also indicates similar mineral assemblages and concentrations to each other. These two rock pairs (from outcrops and auger holes) at Mooiplaas differ from each other in the following aspects:

- The outcrop samples contain the minerals Magnetite, Hematite and Hornblende whereas the rocks at NB17 and NB29 do not.
- The outcrop rock samples do not contain any feldspar minerals such as Plagioclase, Orthoclase or Microcline whereas the rock samples at NB17 and NB29 contain high concentrations of Plagioclase (29.86% to 37.20% respectively), although Outcrop 4 contains the feldspathoid mineral Nepheline.

- The outcrop rock samples do not contain any feldspar minerals, in turn they contain other tectosilicate minerals such as Analcime ($NaAlSi_2O_6 \cdot H_2O$) (Outcrop 4 at 11.53% and Outcrop 5 at 11.98%) and Natrolite ($Na_2Al_2Si_3O_{10} \cdot 2H_2O$) (Outcrop 4 at 12.25% and Outcrop 5 at 14.40%).
- The Mg endmember of Olivine (Forsterite) is also only present in the rock samples from NB17 and NB29 (2 out of the 6 samples).

The southern basalt rocks from the Nhlowa site contain minerals such as Chlorite and already mentioned Enstatite, which are not present in the northern basalt rocks from the Mooiplaas site. The southern basalt rock samples do not contain the tectosilicate minerals of Analcime and Natrolite although they do contain Plagioclase and Microcline.

According to Figure 1 a tholeiitic basalt contains no olivine (olivine poor), no alkali feldspar, Microcline and Orthoclase, but contains Augite. The southern basalt rocks which should class as a tholeiitic basalt, plots on the border of the tholeiitic and calc-alkaline boundary. These rocks do in fact not contain Olivine as a tholeiitic basalt should. Although is also in contrast to a tholeiitic basalt which does not contain Augite and does contain Microcline an alkali feldspar.

The northern basalt rocks plot in the calc-alkaline section of the AMF diagram in **Figure 25**, which is described as Mg rich and higher in alkalis (Na_2O+K_2O). The northern basalt rocks which is described as picritic (olivine rich) only contain olivine in 2 of the 6 rock samples, contains Augite in all 6 samples and also contain Orthoclase an alkali feldspar. The XRF data also indicate that the Mooiplaas site has higher Mg than the Nhlowa site. Individual XRD data can be viewed in **Appendix C**.

Table 15: Average mineral concentrations for the Mooiplaas and Nhlowa sites.

	Rock samples				
	Mooiplaas			Nhlowa	
XRD (wt%)	Average	Standard Deviation		Average	Standard Deviation
Augite	42.15	13.61		0.00	0.00
Diopside	0.00	0.00		15.65	22.13
Chlorite	0.00	0.00		20.51	3.25
Muscovite	0.93	1.68		4.07	5.76
Enstatite	0.00	0.00		2.09	2.96
Goethite	0.00	0.00		0.00	0.00
Kaolinite	0.00	0.00		0.00	0.00
Ilmenite	1.26	2.01		0.00	0.00
Magnetite	3.40	3.93		0.00	0.00
Hematite	0.62	0.98		0.71	1.00
Hornblende	1.20	2.95		2.23	3.15
Forsterite	5.57	9.49		0.00	0.00
Microcline	0.00	0.00		15.96	22.57
Orthoclase	1.59	3.89		0.00	0.00
Plagioclase	11.18	17.47		31.22	3.51
Quartz	0.00	0.00		2.16	3.05
Smectite	9.38	22.98		0.00	0.00
Titanite	0.00	0.00		5.42	7.66
Calcite, magnesian	0.82	2.02		0.00	0.00
Palygorskite	0.00	0.00		0.00	0.00
Anatase	0.00	0.00		0.00	0.00
Analcime	4.48	5.79		0.00	0.00
Actinolite	1.54	3.76		0.00	0.00
Natrolite	12.82	19.49		0.00	0.00
Nepheline	2.32	5.68		0.00	0.00
Laumonite	0.75	1.84		0.00	0.00
Total	100.00	-		100.00	-
	Higher value than other site				
	Lower value than other site				

5.2.2.2 Codrington

The highly and slightly weathered basalt from the Springbok Flats samples are already altered containing 35.85% and 23.96% of a secondary mineral Smectite, whereas the Mooiplaas site only contained one sample with Smectite of 56.29%. The remaining five rock samples and the Nhlowa site contain no smectite.

This is a possible indication for why the Springbok Flats have such low Augite concentrations of 19% to 24% and the average found at the Mooiplaas site is 42.15%. The rock sample from Codrington only contains Augite with no Diopside or Enstatite, similar to the northern basalt samples although contain no Forsterite (olivine) which the Mooiplaas site does.

5.2.3 XRF Analysis — Soil

5.2.3.1 Mooiplaas and Nhlowa

Figure 27 and **Figure 28** below indicate and focus on different Fe and Ca concentrations in the profile sequence between the Mooiplaas and Nhlowa supersites at the KNP. This portrays different processes and conditions of leaching, precipitation and transportation of Fe and Ca in the profiles and individual horizons between the two sites.

For the Nhlowa site high Fe content is found in the different horizons attributed to the presence of ferricrete. The Fe content increases from the underlying parent rock upwards through the profile to the colluvial horizon. A possible mechanism is Fe that gets leached out of the underlying parent rock and precipitated in and through the profile by fluctuating shallow seasonal seepage water which leads to ferricrete formation. The cementation of Fe sesquioxides in the soil to form ferricrete results in a higher concentration of Fe in the residual and highly weathered basalt layers than Fe content in the parent rock. With a high Fe concentration in the colluvial layer as well it indicates that the Fe concentration is possibly also attributed to transported Fe, such as with the formation of laterite. The Ca content decreases from the underlying parent rock upwards to the colluvial layer in contrast to the increase in Fe. The average Ca content in the rock samples is less than the Fe content portrayed in **Figure 27**.

The Mg concentrations also decrease from the parent rock up through the profile. This indicates that certain Ca and Mg bearing minerals weather more readily in the high rainfall area of the Nhlowa site, which results in Ca and Mg mobilizing early in the eluviation process.

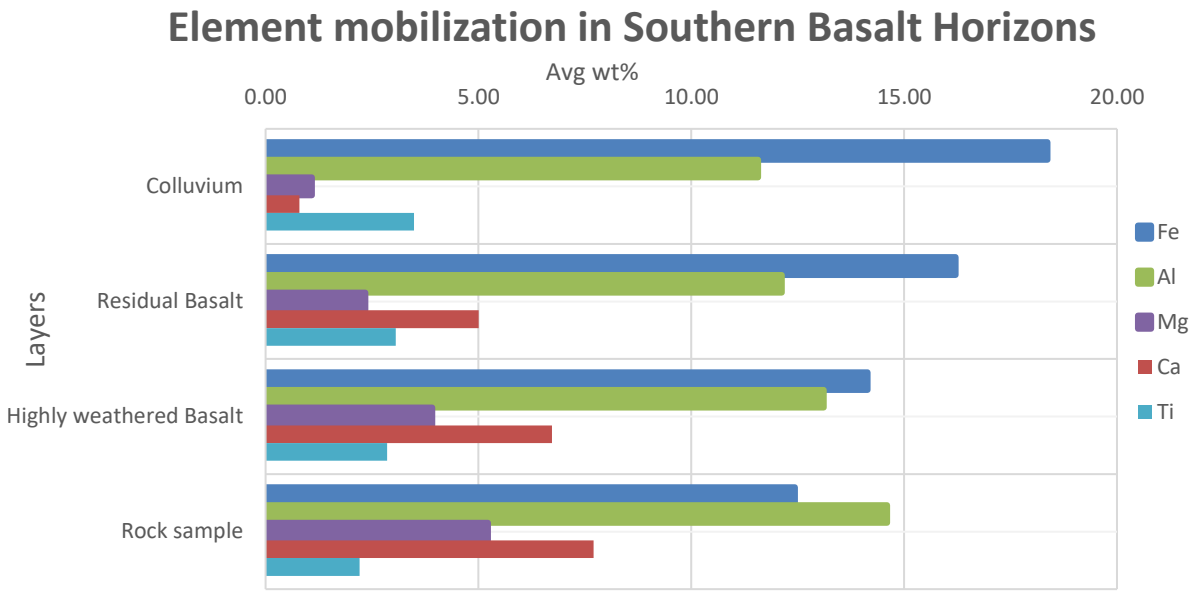

	Rock sample	Highly weathered Basalt	Residual Basalt	Colluvium
Fe	12.43	14.14	16.21	18.37
Al	14.60	13.11	12.13	11.57
Mg	5.22	3.92	2.34	1.09
Ca	7.71	6.72	5.01	0.80
Ti	2.21	2.86	3.06	3.49

Figure 27: Major element mobilization in Southern Basalt horizons (Nhlowa).

In contrast to the Nhlowa site, Fe gets leached out and transported at the Mooiplaas site whereas Ca gets precipitated in the soil profile which leads to calcrete formation, **Figure 28**. The calcrete concentration is focused in the residual basalt and highly weathered basalt layer which is higher than the parent rock's concentration similar to the Fe concentration in the Nhlowa site. Calcium concentrations drop below the parent rock's level in the reworked residual basalt and colluvial layers where erosion processes transport the Ca away more readily. This strengthens the likelihood that an increase in concentrations in the profile is introduced from other sources as well.

From **Figure 28**, one can see that the Al concentration at the Mooiplaas site decreases from the parent rock to the residual basalt layer similarly to the Nhlowa site. From the residual basalt horizon, the Al concentrations increases most likely due to Al input from transported sources. The Mg concentrations initially increase form the parent rock to the highly weathered rock, further on the concentrations decrease through the horizons up to the colluvial layer.

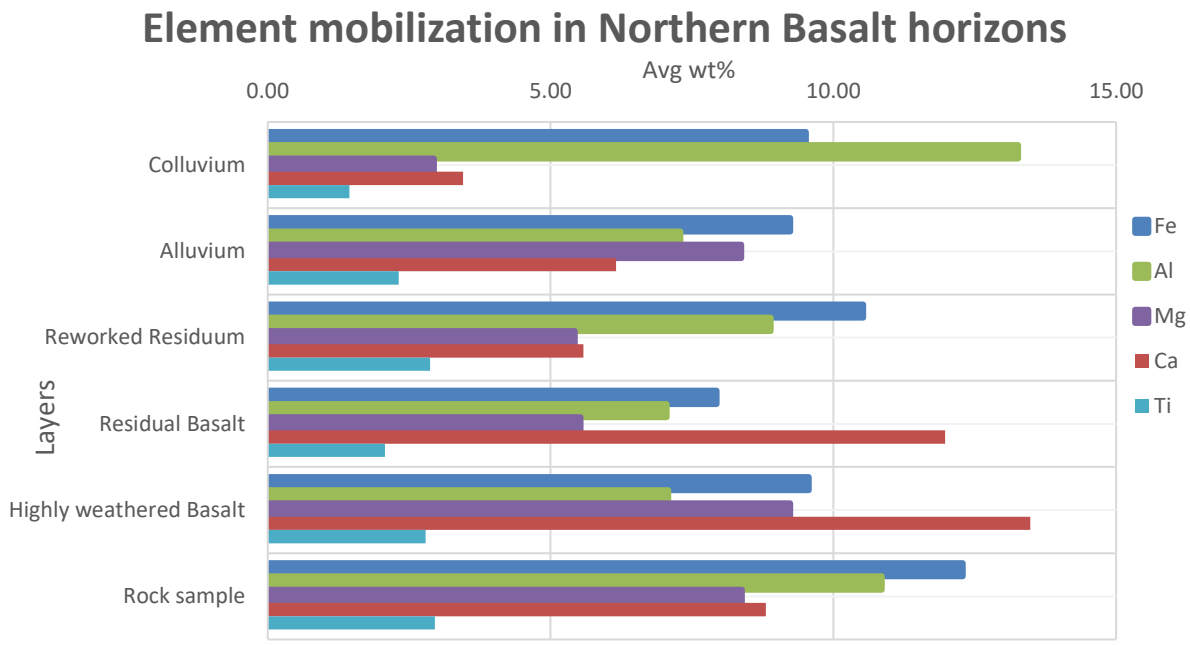

	Rock sample	Highly weathered Basalt	Residual Basalt	Reworked Residuum	Alluvium	Colluvium
Fe	12.29	9.57	7.94	10.53	9.24	9.52
Al	10.86	7.08	7.05	8.89	7.30	13.27
Mg	8.38	9.24	5.53	5.43	8.37	2.94
Ca	8.81	13.48	11.98	5.58	6.16	3.45
Ti	2.95	2.79	2.08	2.87	2.32	1.44

Figure 28: Major element mobilization in Northern Basalt horizons (Mooiplaas).

A decrease in the Na content occurs in both the Mooiplaas and Nhlowa sites, the decrease at the Mooiplaas site from parent rock to highly weathered basalt is drastic, from 3.81% to 0.80% and the drop to the residual layer only slight at 0.60%. The drop at the Nhlowa site is not as drastic with the parent rock at 3.52% to the highly weathered basalt at 1.85% and residual basalt at 0.90%. The K content at Nhlowa decreases in a similar manner as the Na, although at the Mooiplaas site the K content increases above the parent rocks concentration.

The standard deviations for the Ti content for both sites are mostly around 1.00% and some >0.50%. The Ti content in both the Mooiplaas and Nhlowa sites behave similarly to the Fe content. At the Nhlowa site Ti increases from the parent rock to the colluvial layer similar to Fe. The Ti content similar to the Fe content at the Mooiplaas site decreases from the parent rock to the residual horizon.

The Ti increases in the reworked residual horizon and decreases again in the colluvial horizon. The Y and Zr content in both sites show an increase and decrease from the parent rock upwards through the profile, **Table 16**. Although some standard deviations are large at 10ppm to 14ppm for Y and 100ppm to 200ppm for Zr, a mobilization of these elements are still occurring from the parent rock through the profile.

Table 16: Movement of average trace element concentrations of the sites.

Element	Horizon	Nhlowa	Mooiplaas	Codrington	Siloam
Y (ppm)	Reworked residual	-	30.88	-	-
	Residual	44.29	24.67	25	29.57
	Highly Weathered	50.08	24.60	21	-
	Rock	36.07	38.00	*23	-
Zr (ppm)	Reworked residual	-	372.63	-	-
	Residual	340.76	311.47	174	149.86
	Highly Weathered	307.80	319.61	107	-
	Rock	282.02	465.00	*105	-
* Sample was slightly weathered					

5.2.3.2 Codrington and Siloam

The average Fe content in the residual basalt horizon of the Sibasa basalts at Siloam is 14.45% with a minimum of 12.88% and maximum of 17.18%. In the Springbok Flats basalt at Codrington, the top residual horizon has 14.80% Fe and the underlying residual horizon has 9.07% Fe. For the highly weathered basalt at Codrington the Fe content is 10.70% with the slightly weathered rock at 11.09%.

The Fe content in the residual basalt horizon of the Sibasa basalts at Siloam are very similar to the southern basalts at Nhlowa, for the average highly weathered basalt the Fe content is 14.14% and for the average residual basalt it is 16.21%. The highly weathered basalt at Codrington is closer to the average highly weathered basalt at the Mooiplaas site of 9.57%.

The Na and K content at Codrington behaves similarly to Mooiplaas where the Na content decreases and the K content increases although only slightly. Profile TP08 at Siloam indicates a decrease of Na and K from 3.00m up to 0.70m through the profile similarly to Nhlowa, see **Appendix B**.

The Y and Zr in both the Codrington and Siloam site shows and increase upwards through the profile. At Codrington the Y first decreases from the slightly weathered basalt to the highly weather basalt, afterwards it increases again although slightly in the top residual horizon, **Table 16**. The Zr content at Codrington increases from 105ppm for the slightly weathered basalt to 202ppm at the top residual horizon. As for the Siloam site the average Y content also increases from the residual to colluvial horizon with 29.57ppm to 34.67ppm. Excluding the colluvial horizon (a transported horizon) and considering the in-situ material such as the residual basalt an increase is still noticed.

TP08 consists of three different residual horizons sampled at 0.70m to 1.10m, 2.00m to 2.50m and 2.50m to 3.00m, the Y first decreases but ultimately still increases from the bottom horizon to the top from 27ppm, 23ppm to 32ppm. The same occurs with the Zr content where it decreases from 119ppm to 115ppm and then increases to 184ppm. This portrays the mobility of both these elements. In TP05 an increase of both Y and Zr occurs in the two residual basalt horizons. Yttrium increases from 29ppm at 1.70m to 32ppm at 0.80m and Zirconium increases from 156ppm to 167ppm at these same depths, individually displayed in **Table B7**, **Appendix B**.

The region of Siloam and the Nhlowa site receives similar high rainfall of approximately 600mm/annum. Compared to the lower rainfall regions such as Mooiplaas and Springbok Flats at the Codrington site (no XRF was conducted at Roedtan) an approximate 400mm/annum is received. This attributes to the similar high Fe contents of the Nhlowa and Siloam site and presence of ferricrete in the profile.

Similarly, with the low average Ca contents in the residual basalt horizon at Siloam with 6.35% and Nhlowa with 5.01%. Likewise, with the low Fe content of the Codrington and Mooiplaas site. Although no XRF was taken at Roedtan in order to compare Ca percentages, through visual inspection it was noticed that both horizons contained large extents of calcification in the profile. See **Tables B1 to B7**, **Appendix B** for individual data values.

5.2.4 XRD Analysis — Soil

5.2.4.1 Mooiplaas and Nhlowa

Some contrasting/peculiar information was found from the results between the rock samples and weathered profile samples for the KNP supersites. Plagioclase and Quartz are present in relatively high percentages in the residual and highly weathered basalt horizons at the Mooiplaas site, where little to nothing was present in the rock samples from the site. Especially Quartz which is not present in any of the 6 rock samples from the Mooiplaas site, is however present in more than 80% of the reworked residual basalt, residual basalt and highly weathered basalt horizons, portrayed in **Table C2 to Table C4**, **Appendix C**.

A similar situation occurs at the Nhlowa site where the results from rock sample SB10A only indicates 4.31% Quartz present in the rock and 0.0% in SB10J, whereas all the samples from the residual and highly weathered basalt horizons contain high percentages of Quartz. The highly weathered basalt has 4% to 10% Quartz and the residual basalt 22% to 66%. Some of the Quartz in the residual basalt could be attributed to a reworked component between the colluvial and residual layer at both the Nhlowa and Mooiplaas site. This a high possibility in the reworked residual basalt layer at the Mooiplaas site.

The parent rock from the Mooiplaas site, based on the XRD results, only contain the pyroxene mineral Augite, and the rock samples from the Nhlowa site Diopside. The weathered profile horizons of the Mooiplaas site in contrast to the rock samples contain more Diopside (present in more samples) than Augite. For example, the residual basalt layers of the Mooiplaas site contains Diopside in 12 of the 17 samples with minimum concentrations of 3.86% and maximum of 24.20%. The Augite and Diopside concentrations in the weathered horizons are notably lower than the Augite concentrations in the parent rock. This can be attributed to the inherent instability of these minerals resulting in progressive weathering.

The percentage of the clay mineral Smectite in a sample from a horizon can be used, to some degree, to determine the extent of weathering which has taken place, or that weathering has occurred. From the parent rock to the weathered horizons; this would be the breakdown of original/primary minerals in the parent rock to secondary minerals.

Smectite is present in almost every sample of the weathered horizons from the Mooiplaas site. The Nhlowa site does not have this high occurrence of the clay mineral, containing Smectite of 18.22% in only one sample. For the Mooiplaas site the reworked residual basalt horizon contains the highest smectite content. The residual basalt and highly weathered basalt contain very similar amounts to each other based on the averages and standard deviations, which is less than the reworked residual basalt. The minimum and maximum percentages of smectite for these horizons are as follows (not including 0.00%):

- Reworked residual basalt – 38.83% and 65.92%;
- Residual basalt – 22.05% and 57.47%;
- Highly weathered basalt – 25.85% and 52.43%.

The averages of these horizons are displayed in **Table 17** with individual data sets in **Tables C1-C4**, **Appendix C**. The samples from the Nhlowa site lacks other clay minerals except the phyllosilicate mineral chlorite.

Based on the results, the Smectite clay mineral may originate from the weathering and break down of Augite, Plagioclase, Magnetite, Hematite, Forsterite and the tectosilicates Analcime and Natrolite. Given that the Smectite content increases as these other minerals decrease. This is especially notable at Mooiplaas with the likelihood that Augite weathers to Smectite. From the parent to highly weathered rock, the Augite content drastically decreases, while the Smectite content drastically increases, see **Table 17**. Nhlowa site which does not contain any Augite results in having drastically less to no Smectite. The tectosilicates mentioned above are only present in the Mooiplaas basalt parent rock mineral assemblages, and not present in any of the weathered horizons or in the Nhlowa basalt rocks.

5.2.4.2 Codrington and Siloam

The residual basalt horizon at Siloam contain a range of Quartz contents from minimum of 3.77% to a maximum of 27.37% similar to the Nhlowa site, although with not such a large range from minimum to maximum. Whereas the Quartz content at Codrington has a similar trend as the Mooikloof site where the highly and slightly weathered basalt at Codrington has low Quartz content of 3.14% and 5.13% respectively and increases dramatically in the top and bottom residual basalt layer of 34.95% and 20.39% respectively.

The presence of pyroxene in the residual basalt at Siloam is occasional, with one sample containing Diopside and two with Augite. No Diopside is present in the Codrington samples although the Augite content decreases from the slightly weathered basalt of 24.73% to the highly weathered basalt of 19.59%, with the bottom and top residual basalt of 14.52% and 0.00% respectively. The Plagioclase content also decreases drastically in the Codrington sample from the slightly weathered basalt to residual basalt. The Plagioclase in the residual basalt at Siloam has a similar range to its Quartz content with a minimum Plagioclase of 3.20% and maximum of 26.45%, no rock sample was tested at Siloam.

Table 17: Mineral summary across horizons for Plagioclase, Diopside, Augite and Smectite.

Sites	Minerals (wt%)	Reworked Residual Basalt	Residual Basalt	Highly Weathered Basalt	Parent Rock
Mooiplaas	Plagioclase	9.18	8.30	17.22	11.18
	Diopside	5.63	9.42	10.36	0.00
	Augite	5.55	1.97	6.99	42.15
	Smectite	41.34	36.7	36.89	9.38
Codrington	Plagioclase	-	9.04	41.42	*43.95
	Diopside	-	0.00	0.00	*0.00
	Augite	-	7.26	19.59	*24.73
	Smectite	-	38.78	35.85	*23.96
Nhlowa	Plagioclase	-	12.88	38.74	31.22
	Diopside	-	1.19	17.96	15.65
	Augite	-	0.00	0.00	0.00
	Smectite	-	4.56	29.67	0.00
Siloam	Plagioclase	-	11.78	-	-
	Diopside	-	3.09	-	-
	Augite	-	0.79	-	-
	Smectite	-	40.77	-	-

*Sample was slightly weathered already.

The Smectite content in the Codrington samples increases as the Plagioclase and Augite content decrease, this suggests the decomposition of primary minerals such as Plagioclase and Augite to a secondary mineral Smectite, see **Table 17**. The highest Smectite content is in the top residual basalt at 51.19%, this horizon also has the lowest Plagioclase content with no Augite.

The Smectite contents in the residual basalt at Siloam are less than two orders of magnitude from each other with a min of 40.18% and max of 53.28% with one sample containing no Smectite. Although this sample does contain high amounts of Chlorite also a type of secondary mineral. Either smectite is the dominant secondary mineral to form from these minerals or all the other clay minerals have been transported out of the profile in each horizon which seems unlikely.An incongruous mineral occurring in the residual basalt at Siloam is the presence of Epidote in low to relatively high quantities of minimum 5.10% and maximum of 23.57%. Epidote is mostly formed by metamorphism and hydrothermal activity. The individual data can be viewed in **Tables C6 and C7, Appendix C**.

5.3 Engineering Parameters

5.3.1 Atterberg Limits

Table 18 below portrays the average and standard deviation values of the Atterberg Limits for the residual horizons of the study sites. The average for the Mooiplaas site is the collective residual basalt horizons for the site's 2 main profile types *viz.* NBProfile 2A and NBProfile 2B. This was done since the individual averages for these profile types were very similar, individual data can be viewed in **Appendix A**.

Table 18: Residual horizon Atterberg Limit averages from all sites.

Residual horizon									
Site	**Nhlowa**		**Mooiplaas**		**Roedtan**		**Siloam**		**Codrington**
	Average	**Standard Deviation**	**Average**	**Standard Deviation**	**Average**	**Standard Deviation**	**Average**	**Average**	**No Data**
% Clay	13,20	4,09	4,88	2,70	3,00	1,00	14,83	9.26	
% Silt	34,60	9,10	18,25	7,34	12,33	2,31	20,67	7.79	
% Sand	36,40	9,50	41,75	11,72	36,33	6,66	32	13.25	
% Gravel	15,20	16,04	35,50	17,19	48,00	8,72	27,5	21.80	
Liquid Limit (%) (LL)	48,60	11,67	50,63	8,90	31,33	2,08	53,67	7.79	
Plasticity index (%) (PI)	23,20	6,02	21,50	4,31	13,33	4,04	28,5	5.47	
Linear shrinkage (%) (LS)	11,30	3,03	10,25	1,83	5,83	1,26	12,33	1.63	

Table 19 indicates that the Siloam site has the highest average clay percentage followed by the Nhlowa site. Although for Siloam this high average is created by one very high clay percentage value from TP08 at 0.70-1.10, with a clay content of 33%.

When this value is excluded the average clay percentage of the Nhlowa site is 11.20%. Aside from this the highest fines content (clay and silt) is present at the Nhlowa site. The Mooiplaas and Roedtan sites both have lower fines content and higher gravel and sand than the Siloam and Nhlowa sites. The Nhlowa and Siloam sites are located in the more humid areas of South Africa with similar climatic environments, the climatic N-value for Nhlowa is between 2.62-2.78 and the N-value for Siloam is 1.60-2.21.

The aforementioned range of N-values promotes decomposition or chemical weathering. This correlates to the high fines content encountered at these sites as well as the high liquid limit and plasticity index. Considering the standard deviations, maximums and minimums of the two site, they portray very similar values for these properties.

Mooiplaas and Roedtan falls in similar climatic environments with similar rainfall and evaporation, the N-value for Mooiplaas is between 3 and 4 and for Roedtan between 3 and 5. These N-values indicate a sub-arid environment where disintegration/physical weathering would be more dominant with some form of decomposition still taking place. This correlates with the low fines content and high gravel and sand encountered.

The Roedtan site is slightly more arid (closer to N=5) which is portrayed in the higher coarse material and lower fines compared to the Mooiplaas site. In contrast to be located in a more arid environment, the Mooiplaas site has similar LL and PI to the Nhlowa and Siloam sites with 50.63% and 21.50% respectively. This could be attributed to the high smectite clay content present in the residual basalt from the Mooiplaas site, as well as from the powder calcrete (as calcite and magnesian is at 21.64%), calcrete characteristically having high LL and PI with low swelling clays.

The higher smectite and in turn higher LL and PI could be attributed to the lower evaporation rate present at the Mooiplaas site (1700-1900mm) compared to the Roedtan site (1800-2000). The Roedtan site has the lowest clay content and PI which would be expected in this more arid site.

Table 19: Completely to highly weathered basalt Atterberg Limit averages.

Completely to highly weathered basalt					
Site	**Nhlowa**		**Roedtan**		**Codrington**
Depth (m) / **Origin**	**Average**	**Standard Deviation**	**Average**	**Standard Deviation**	
% Clay	4,5	0,71	0,6	0,89	**No DATA**
% Silt	17,5	2,12	5,2	0,84	
% Sand	48,5	12,02	27	4,47	
% Gravel	30	14,14	67,2	5,59	
Liquid Limit (%)	44	11,31	30,8	4,71	
Plasticity Index (%)	19,5	7,78	10,4	2,7	
Linear shrinkage (%)	9,5	3,54	4	1,22	

Table 19 above portrays the Atterberg Limits for the completely to highly weathered basalt horizons between the Nhlowa and Roedtan sites. These two sites respectively represent a high rainfall/humid area and a low rainfall more arid area. As would be expected the Nhlowa site, a humid area, has higher fines, LL, LS and PI than the Roedtan site a more arid area. The liquid limit and plasticity index for the completely to highly weathered basalt of the two sites are relatively similar to the values for the residual basalt horizon presented in **Table 18:** Residual horizon Atterberg Limit averages from all sites., differing by 3% to 4%.

5.3.2 Compaction data

Table 20 and **Table 21** below portrays the CBR and Mod. AASHTO compaction data for the Sibasa basalts at Siloam and the Springbok Flats basalts at Roedtan. All the horizons tested for the Siloam site classify as a G9 according to the COLTO classification system (COLTO, 1998). This is due to the high PI and very low compactive strength of the material.

In contrast to the Siloam site, the completely to highly weathered basalt and calcified residual basalt both classify as G7 material according to the COLTO classification system. This is attributed to the low PI contents and good compaction strength of the material on the Roedtan site. The highly weathered basalt at Roedtan classifies as a G8 according to the COLTO classification system (COLTO, 1988). This is due to the low compactive strength of the material at 93% and 95% even though the PI is relatively low and acceptable.

Table 20: Mod. AASHTO and CBR test results for the Sibasa Basalts at Siloam.

Test pit no	Sample depth (m)	Material description	PI	MOD. AASHTO			CBR VALUES at% Mod. AASHTO					Soil Classes		
				MDD (kg/m3)	OMC (%)	Swell%	90	93	95	98	100	USCS	AASHTO	COLTO
TP01	1.50-2.50	Residual basalt	21	1880	12,9	1,4	4	5	6	7	8	SC	A-7-6 (5)	G9
TP02	1.10-1.60	Reworked pebble marker/ residuum	30	1993	11,5	1,2	4	5	5	6	7	GC	A-2-7 (3)	G9
TP06	1.00-2.00	Reworked pebble marker/ residuum	32	1836	12,3	6,1	1	2	2	2	3	SM	A-2-7 (4)	G9
MDD – Maximum Dry Density; OMC – Optimum Moisture Content, PI – Plasticity Index														

Table 21: Mod. AASHTO and CBR test results for the Springbok Flats basalts at Roedtan.

Test pit no	Sample depth (m)	Material description	PI	MOD. AASHTO			CBR VALUES at% Mod. AASHTO					Soil Classes		
				MDD (kg/m3)	OMC (%)	Swell%	90	93	95	98	100	USCS	AASHTO	COLTO
TP04	1.50-2.30	Completely to highly weathered basalt	10	2120	10,6	0,0	27	33	38	61	86	SW	A-2-4 (0)	G7
TP05	0.50-1.10	Calcified residual basalt	14	2039	10,6	0,0	24	30	35	48	61	SC	A-2-6 (0)	G7
TP07	1.00-2.00	Highly weathered basalt	12	2057	10,3	0,0	8	10	12	15	17	SP-SM	A-2-6 (0)	G8
MDD – Maximum Dry Density; OMC – Optimum Moisture Content, PI – Plasticity Index														

From the data presented here the presence of the abundant calcrete in the calcified residual horizon shows that it aids in achieving high compaction and CBR values similar to the completely to highly weathered horizon at the Roedtan site.

6. SUMMARY

This chapter will provide a short summary on the results acquired during this study. This was incorporated owing to the large data set from multiple sites.

The investigation covered 5 different low relief basalt sites for different rainfall intensities and evaporation rates, underlain by different geological lithologies. Two sites in high rainfall areas and three in low rainfall areas were investigated. The first high rainfall area is, the Southern Basalt Research Supersite (Nhlowa) in the Kruger National Park which represents the Lebombo Group basalt, with an average precipitation of 610mm/annum and evaporation of 1600-1700mm/annum. The second high rainfall site is in Siloam which represents the Sibasa Group basalt, with a precipitation range of 680-810mm/annum and evaporation of 1300-1500mm/annum. These two sites classify as humid to sub-humid area with their climatic N-value as, Nhlowa site N=2.62-2.78 and Siloam N=1.60-2.20.

The first low rainfall area is the Northern Basalt Research Supersite (Mooiplaas site) which also represents the Lebombo Group basalt, with an average precipitation of 480mm/annum and evaporation of 1700-1900mm/annum. The second site is at Roedtan which represents the basalt in the Springbok Flats Basin, with a range of 344-470mm/annum and evaporation of 1800-2000mm/annum. The last site is at Codrington, also on the Springbok Flats which has a precipitation range of 400-634mm/annum and evaporation of 1700-1800mm/nnuma. These sites classify as sub-humid to slightly arid conditions with their climatic N-value aa, Mooiplaas N=3.54-3.95, Roedtan N=3.00-5.00 and Codrington N=2.68-4.50.

Regionally the most noticeable difference between these sites, particularly between the rainfall intensity groups, are the different pedocrete formations present. The high rainfall and low evaporation sites contain ferricrete whereas the lower rainfall and higher evaporation sites are dominated by calcrete. The humid areas also experienced more chemical decomposition resulting in higher clay contents with higher liquid limit (LL), linear shrinkage (LS) and plasticity index (PI) values. The sub-humid to arid areas experienced more physical weathering or disintegration which results in coarser soil textures and lower Atterberg Limit values.

These two rainfall intensity groups experienced different mineralogical changes and element exchanges due to the different climates they are located in and different underlying geological lithologies.

6.1 Geology and Rock mineralogy

According to Duncan and Marsh (2006) the Nhlowa site is underlain by the Sabie River Formation and depicted as tholeiitic (olivine poor) basalts. The Mooiplaas site is in turn underlain by the Letaba Formation which is described as picritic (olivine rich) basalt. According to Marsh (1984) the basalts in the Springbok Flats Basin is closely related to the Drakensburg Formation, although compositionally and petrographically more to the Sabie River Formation.

With the use of the available rock sample XRF averages and plotting them on an AMF diagram, the Nhlowa site basalts plotted on the boundary of tholeiitic and calc-alkaline. The Mooiplaas site plotted as calc-alkaline and the Springbok Flats basalt sample from Codrington plotted as tholeiitic, **Figure 25**. The Springbok Flats basalt sample plotting as tholeiitic correlates with Marsh (1984) to be compositionally and petrographically similar to the Sabie River formation, which is described as tholeiitic (olivine poor) basalts, no olivine was present in the slightly and highly weathered basalts from Codrington.

Even though the northern basalts in Mooiplaas are described as olivine rich, only two of the six rock samples contained the Mg rich olivine mineral Forsterite. The Nhlowa site does not contain any olivine mineral as described by Duncan and Marsh (2006). The iron and alkali contents of the two sites are very similar; with the Fe_2O_3 content of the Mooiplaas and Nhlowa sites at 12.29% and 12.43% respectively. The alkali content (Na_2O and K_2O) of Mooiplaas at 3.81% and 1.56% and Nhlowa at 3.32% and 2.16%. This only large difference is the average Mg content, whereby in the northern basalts it is higher than the southern basalts at 8.38% to 5.22% respectively. This places the Mooiplaas basalts in the calc-alkaline region of the AMF diagram and the southern basalts on the boundary.

The XRF analyses indicate that the Ca content of the rock samples from the northern and southern basalt sites are very similar with the average Ca content at 8.81% and 7.71% respectively. With the Fe and Ca concentrations very similar between the sites similarly with the Na and K contents they originate from different mineral assemblages and types of minerals between the two sites.

For example the northern basalts contain the pyroxene mineral Augite ($(Ca,Na)(Mg,Fe,Al)(Al,Si)_2O_6$) in all 6 samples, with an average of42.15% and standard deviation of 13.61%. The southern basalts do not contain Augite but does have Diopside ($Ca(Mg,Fe)Si_2O_6$) with an average of 15.65% and standard deviation of 22.13% which contributes different amounts and types of elements as mentioned above. Similarly, the northern basalt rock samples contain minerals which the southern basalt rock samples do not contain. This would be tectosilicates such as Analcime ($NaAlSi_2O_6 \cdot H_2O$), Natrolite ($Na_2Al_2Si_3O_{10} \cdot 2H_2O$) and the already mentioned Mg Olivine endmember Forsterite. These minerals are also not constant in the results from the northern basalt rock samples, certain samples lacking these minerals. The same can be said for the concentrations of Plagioclase, Orthoclase, Magnetite, Hematite and Hornblende.

The basalt rock sample from the Springbok Flats basalt in Codrington also contain Augite (19.59% and 24.73%) although no Olivine, Diopside or Microcline albeit does contain Plagioclase at 43.95%. The Springbok Flats basalt also has extremely low K_2O at 0.46% and slightly higher Na_2O at 2.12% and Fe_2O_3 at 11.09%. Although it has the highest CaO content at 9.86%.

The secondary alteration mineral Smectite was already present in the Springbok Flats highly weathered basalt and slightly weathered basalt samples at 35.85% and 23.96% respectively. This indicates that weathering and alteration has already started and could explain why the Augite mineral is so much less than the Mooiplaas basalts. Smectite was only present in one sample of the Mooiplaas basalts at 56.29% this sample had the lowest Augite content at 26.34%, the Nhlowa site did not contain any Smectite. This indicates that the mineral Augite when weathered is predominantly altered to Smectite and can aid in the determination of the extent of weathering.

6.2 Profile development and weathering

6.2.1 Profile differences

The most pronounced difference between the sites are the distinct different pedogenic formations present. This would be calcrete at the Mooiplaas, Roedtan and Codrington sites with ferricrete at the Nhlowa and Siloam sites. The Nhlowa site is slightly more diverse in different profile types than the Mooiplaas site. The Siloam, Roedtan and Codrington sites only have 1 profile type due to the close proximity and similarity of the test pits.

The high rainfall and low evaporation sites of Nhlowa and Siloam experienced dominantly chemical decomposition, both these sites located in areas of N<3. The Nhlowa site has 4 profile types with the following horizon assemblages, **Table 3** to **Table 6**:

1. SBProfile 1: Colluvium-residual basalt – highly weathered basalt,
2. SBProfile 2: Reworked residual basalt – scattered residual basalt – highly or moderately weathered basalt,
3. SBProfile 3: Residual basalt – highly weathered basalt,
4. SBProfile 4: Alluvial profile.

The profiles are mostly characterized by the presence of more fines than coarse material excluding the highly weathered basalt gravel fragments excavated. Ferricrete nodules are mostly found in the residual basalt horizon although not in high concentrations or fully developed, some ferruginization was visible on the highly weathered basalt gravel excavated.

One profile type was given to the Siloam site with the sequence of colluvium – reworked pebble marker/residuum – residual basalt. The residual basalt horizon has a fines content of approximately 35%. Ferricrete nodules were not present in every test pit and was only located in the reworked and residual basalt layers.

The Mooiplaas site was divided into 3 profile types with the following horizon assemblages, **Table 7** to **Table 10**:

1. NBProfile 1: Colluvium – residual basalt,
2. NBProfile 2A: Reworked residual – residual basalt,
3. NBProfile 2B: Reworked residual – residual basalt – highly weathered basalt,
4. NBProfile 3 the alluvial profile.

The majority of the horizon characteristics from the profiles of the Mooiplaas site are very similar resulting in the NBProfile 2 split of 2A and 2B. These two profile types are seemingly identical with minor differences in their horizon characteristics and profile succession, termination occured in different horizons due to refusal on calcrete nodules/concretions and highly weathered basalt. Although if refusal did not occur profile succession would seemingly be similar to identical. The profiles from the Nhlowa site are not as alike to each other in profile succession as the Mooiplaas site, although analogous horizon characteristics are present as well as a similar profile succession. Calcrete formations in the Mooiplaas profiles are concentrated in the residual basalt horizon although also present in lesser extent in the reworked residual basalt horizon. Silt and sand is the main soil texture across the reworked and residual basalt horizons with high gravel content from hard calcrete concretions.

Roedtan is the site with the lowest rainfall and highest evaporation rate and has a dominant gravel and sand texture in the residual basalt layer and weathered basalt horizons when excavated with a TLB. The basic profile horizon sequence encountered was colluvium – calcified residual basalt - completely weathered basalt – highly weathered basalt (with patches of moderately weathered basalt in the latter two horizons). The residual basalt horizon is specifically labelled as calcified due to the abundance of calcrete formations (nodules, concretions and streaks) present. The high gravel content in the residual basalt horizon is attributed to the calcrete nodules and concretions as well as weathered basalt gravel. This indicates the dominant presence of physical disintegration over chemical decomposition with the fines content at less than 5%.

Only one profile was described at Codrington to serve as extrapolative data for the Springbok Flats basalt. The profile encountered had two residual basalt horizons underlain by a highly weathered basalt layer.

The top residual basalt horizon contained calcrete nodules and concretions with a clayey sand texture whereas the underlying residual basalt horizon had no calcrete and was clay dominant.

6.2.2 Element exchange

The most pronounced difference in element exchange between the Mooiplaas and Nhlowa site is the Fe and Ca contents. The Nhlowa site has approximately twice as much Fe in the residual basalt horizon at an average of 16.21% compared with the Mooiplaas site at an average of 7.94%, this is attributed to the presence of ferricrete in the Nhlowa profile. The average Fe content of the Nhlowa site increases from the parent rock at 12.43% up to the colluvial layer with 18.37%. The reverse occurs at the Mooiplaas site where average Fe content is decreased from the parent rock at 12.29% to 7.94% in the residual basalt layer, the reworked and colluvial layers are similar to the highly weathered basalt layer at around 9.50%.

The residual and highly weathered basalt of the Mooiplaas site has a higher average Ca content of 11.98% and 13.48% respectively than the parent rock at 8.81%. The highest Ca concentration is in the highly weathered basalt horizon is likely attributed to the Ca in the rock together with the calcification in the highly weathered rock structure. Calcium concentrations drop below the parent rock's level at the reworked residual basalt and colluvial horizons, these concentrations are lower than the Fe content in the same horizons which indicates that Ca is readily mobilized from the system by erosion. The average Ca content of the Nhlowa site decreases from the parent rock at 7.71%, highly weathered basalt 6.72%, residual basalt 5.01% then drastically to the colluvial layer at 0.80%.

The high Fe content range in the residual basalt horizon of the Siloam site (14.45% to 17.18%) is similar to that of the Nhlowa site of 13.79% to 18.74%. Siloam has similar low and high ranges of Ca contents to the Nhlowa site, with 3.20% to 10.05% for Siloam and 1.20% to 10.70% for Nhlowa. The Codrington site has slightly higher Fe content in the residual basalt horizon of 9.07% and 14.80% compared to the Mooiplaas site with an average 7.94%, although the average Fe in the highly weathered basalt horizons are very similar at 10.70% for Codrington and 9.57% for Mooiplaas.

The Codrington site has a slightly similarity to Mooiplaas where increase in the Ca content occurs from the slightly weathered basalt to the highly weathered basalt. Although no XRF information was gathered at Roedtan in order to compare the Ca contents, based on just visual inspection, Roedtan would have the higher Ca content compared to Mooiplaas.

The Mooiplaas site has lowest average Fe content at 7.94% in the residual basalt horizon with the highest at Nhlowa with 16.21%. The average Fe content for Siloam and Codrington site are between these two sites, with Codrington at 11.94% and Siloam at 14.45%. The Mooiplaas site has the highest average Ca content in the residual basalt horizon of all the sites at 11.98% followed by the Codrington site with 7.42%, the Siloam site with 6.35% and the Nhlowa site with the lowest at 5.01%.

Moon and Jayawardane (2004) and Bih Che et al. (2012) indicated that in the initial weathering of basaltic rock from parent to slightly weathered to highly weathered rock etc. a loss and depletion of the main elements of Mg, Fe and Ca are experienced. Both in the Mooiplaas and Nhlowa site a depletion of Mg is noticed although the Ca and Fe contents differ dependant on the site. The average Ca and Fe contents in the parent rocks of the Mooiplaas is 8.81% and 12.29% respectively and 7.71% and 12.43% at the Nhlowa sites respectively. Even though the parent rocks of these two sites have similar starting Ca and Fe contents their profile concentrations follow opposite enrichments and depletions. The Ca content at the Nhlowa site steadily decreases from parent rock to residual basalt whereas the Fe content drastically increases by approximately 4%. The opposite occurs at the Mooiplaas site where the Fe content decreases (as sharply as it increases at the Nhlowa site) and the Ca content increases from the parent rock to the highly weathered and residual basalt horizons.

The Y and Zr content in both sites show an increase and decrease from the parent rock upwards through the profile. Although some standard deviations are large 10ppm to 14ppm for Y and 100ppm to 200ppm for Zr a mobilization of these elements are still occurring from the parent rock through the profile. The Zr content at Codrington increases from 105ppm for the slightly weathered basalt to 202ppm at the top residual horizon. As for the Siloam site the average an increase if Y from the parent rock to residuum.

TP08 at Siloam indicates an overall increase in Y of 27ppm, 23ppm to 32ppm upwards through the profile sampled from different depths. The same occurs with the Zr content where it decreases from 119 pp to 115ppm and then increases to 184ppm. This indicates the mobility of both elements, previously thought to be immobile. In TP05 an increase of both Y and Zr also occurs, 29ppm to 32ppm and 156ppm to 167ppm respectively.

6.2.3 Mineralogical changes

The following mineralogical changes were noticed that occurred with these elemental changes. The parent rock from the Mooiplaas site contained only the pyroxene mineral Augite and the Nhlowa site only Diopside. The weathered profile horizons of the Mooiplaas site in contrast to the rock samples contains more Diopside in total of individual samples than Augite. Also conflicting with the parent rock concentrations is the residual basalt layers of the Mooiplaas site, which contains Diopside in 12 of the 17 samples at a minimum of 3.86% and maximum of 24.20%. Diopside was also present in the highly weathered basalt of the Mooiplaas site.

The Augite and Diopside concentrations collectively in the weathered horizons are notably lower than the Augite concentrations in the parent rock. No Augite was encountered in the Nhlowa site and the Diopside content decreased greatly from the parent rock to the residual basalt horizon, 31.30% to 4.75% respectively, with Diopside not present in every sample.

Smectite is present in almost every sample of the weathered horizons from the Mooiplaas site. The Nhlowa site does not have this high occurrence of the clay mineral, with Smectite of 18.22% in only one sample. For the Mooiplaas site the reworked residual basalt horizon contains the most Smectite, indicating the most active weathered horizon. The residual basalt and highly weathered basalt contain very similar amounts based on the averages and standard deviations but still less than the reworked residual basalt. The minimum and maximum percentages of these horizons are (not including 0.00%): Reworked residual basalt 38.83% and 65.92%; Residual basalt 22.05% and 57.47%; highly weathered basalt 25.85% and 52.43%.

The samples from the Nhlowa site lacks any other clay minerals except the phyllosilicate mineral chlorite. Based on the results, the Smectite clay mineral results from the weathering and breakdown of Augite, Plagioclase, Magnetite, Hematite, Forsterite and the tectosilicates Analcime and Natrolite. It was observed that the Smectite content increases as the content of these minerals decrease. This is especially notable at Mooiplaas with Augite weathering to Smectite. From parent rock to highly weathered rock the Augite content drastically decreases (42.15% to 6.99%) whereas the Smectite content increases drastically (9.38% to 36.89%). The Nhlowa shite which does not contain any Augite results in very few amounts of Smectite. The tectosilicates mentioned are only present in the northern basalt parent rock mineral assemblages and not in the southern basalts.

The presence of pyroxene in the residual basalt at Siloam is scarce, with one sample containing Diopside and two with Augite. No Diopside is present in the Codrington samples although the Augite content decreases from the slightly weathered basalt of 24.73% to the bottom residual basalt of 14.52%, the top residual basalt contains no Augite. The Plagioclase content also decreases in the Codrington sample from very high percentage to very low.

The slightly weathered basalt contains 43.95% Plagioclase which decreases to 6.96% in the top residual horizon. The Smectite content in conjunction with this increases as the Plagioclase and Augite content decreases further indicating the transformation of these primary minerals to Smectite during decomposition. The Smectite content in the slightly weathered basalt is 23.96% and 51.19%. in the top residual horizon.

The Plagioclase in the residual basalt at Siloam is very low at 3.20% to 26.45% compared with very high Smectite contents of 40.18% to 53.28%. Siloam also has much more Chlorite content although low when paired with Smectite, the Chlorite ranges from 3.37% to 8.98%. The one sample that does not have Smectite contains higher Chlorite content at 27.71% and this sample in turn has no Augite or Diopside and very low Plagioclase at 6.53%.

The release and mobilization of elements in different stages are a result of an amalgamation of different factors. These factors are influenced by different weathering rates and mineral breakdowns which is attributed to the high diversity of minerals present between rocks of different climatic environments.

6.3 Engineering Geology

The Nhlowa and Siloam sites have the highest fines content which correlates with the humid environment they are located in. The average clay and silt content of the Nhlowa site is 13.20% and 34.60%, the Siloam site has slightly higher clay content of 14.83% although a lower silt content 20.67%. This relates to the expected high LL, PI and LS of the sites. the Nhlowa site averages are 48.60%, 23.20% and 11.30% respectively. The Siloam site has similar values of 53.67%, 28.50% and 12.33% respectively.

The drier more sub-humid to slightly arid environments of Mooiplaas and Roedtan do have lower fines content. With the clay and silt at Mooiplaas at 4.88% and 18.25% and at Roedtan at 3.00% and 12.33% respectively. These sites are dominated by high sand and gravel contents, the sand and gravel in excess of 35%. The Roedtan has the highest gravel content at 48% and Mooiplaas the highest sand at 41.75%. The Atterberg limits for these two sites are low with a PI of 13.33% at Roedtan. Although the Mooiplaas site has similar LL, PI and LS to the more humid Nhlowa and Siloam sites despite having much lower clay and higher sand and gravel contents than them. This could be attributed to the high calcrete content containing Palygorskite paired with the high smectite present in the horizon. The higher rainfall and lower evaporation compared to Roedtan could also aid in creating this skewed effect.

The LL, PI and LS for the completely to highly weathered basalt for the Nhlowa and Roedtan sites are very similar to their residual basalt values, only being slightly less. The fines content for Nhlowa are still relatively high with clay of 4.50% and silt at 17.50% whereas the Roedtan site has almost no clay at 0.60% and very low silt of 5.20%.

The better compaction characteristics are found at the sub-arid area Roedtan when compared to the humid area of Siloam. The calcified residual basalt and completely to highly weathered basalt at Roedtan classifies as G7 material according to the COLTO classification system. This material had low PI of 10 to 14 with adequate compressive strength at 95% Mod. ASSHTO. Compared to the Roedtan the residual basalt material of Siloam only classifies as G9, this rating is supported by the high PI of 21 to 32 and low compressive strength of the material.

7. Conclusion

With the completion of this study a better understanding of the weathering trends and soil development for low relief basalts have been achieved. Even though low relief basalts do not contain distinct noticeable topography, such as crests, mid-slopes and foot-slopes, differences in profile development and weathering are influenced by the flat lying nature and climatic aspects.

7.1 Profile development

The research sites were naturally divided into high rainfall and low evaporation sites such as for Nhlowa and Siloam, and low rainfall high evaporation sites for Mooiplaas, Roedtan and Codrington.

- The vertical profile succession from the Mooiplaas site is more uniform than those on the Nhlowa site. Although analogous horizon characteristics are present to provide similar profile successions such as reworked residuum – residual basalt – highly weathered basalt.
- The Nhlowa site portrayed a more sporadic presence and absence of horizons in the profile succession than the Mooiplaas site. This indicates higher weathering variability across the site due to the higher rainfall and lower evaporation.
- Ferricrete nodules are mostly found in the residual basalt horizon although not in high concentrations or fully developed, some ferruginization was visible in the highly weathered basalt gravel.

- As a result of lower rainfall and higher evaporation the Mooiplaas site has a very uniform profile succession across the site, this results in the NBProfile2 type split into

2A and 2B. These two profile types are seemingly identical with minor differences in their horizon characteristics and profile succession, termination occurred in different horizons due to refusal on abundant calcrete formations or highly weathered basalt. It reasonably to assume that if refusal did not occur profile succession would seemingly be similar to identical.

- Silt and sand is the main soil texture for the Mooiplaas site across the reworked and residual basalt horizons with high gravel content resulting from hard calcrete concretions.
- Calcrete formations in the Mooiplaas profiles are concentrated in the residual basalt layer although also present in the reworked residual basalt layer in lesser extent.

- The high rainfall sites of Nhlowa and Siloam have, as expected due to similar climatic environments, very similar profile horizon successions with similar high fines contents. Ferricrete was also present at both sites although not constant throughout the profile and across the site.
- At Siloam ferricrete nodules were not present in every test pit and was only located in the reworked and residual basalt layers.

- Both Roedtan and Mooiplaas have low rainfall and high evaporation although the effect of physical disintegration and lack of chemical weathering is much more noticeable at Roedtan than Mooiplaas where some chemical weathering is still present. Furthermore, the Roedtan profile is dominated by a very thin residual horizon before continuing to highly weathered rock.
- This is also evident in the lower fines and higher gravel content throughout the profiles at Roedtan compared to the Mooiplaas site.
- The degree of calcification present at Roedtan is also the most pronounced and can be attributed to having a lower rainfall and higher evaporation compared to Mooiplaas.

- A specific trend noticed between the sites are that the high rainfall and low evaporation sites, Nhlowa and Siloam, contain ferricretes in the profiles.
- The low rainfall and high evaporation sites, Mooiplaas, Roedtan and Codrington contain calcrete with the more arid site Roedtan containing the highest calcrete content.

- The above two statements agree with the generalization made with Weinert's N-value that sub-humid areas (N=2) preferentially form ferricretes and sub-arid to arid areas (N=5) form calcrete (Brink, 1979 and 1985) and (Netterberg 1969 and 1971 cited in Brink, 1985).
- The above mentioned was also noticed in the enrichment and depletion of Fe and Ca in soils from these sites.

7.2 Element analysis

The elemental exchange focus for weathering from parent rock to residual soil was placed on specific major elements *viz.* Na, K, Ca, Fe, Al and Mg. As well as specific elements and trace elements previously thought to be immobile, Y, Zr and Ti.

- Moon and Jayawardane (2004) indicated in their study that a loss in major elements (Mg, Fe, Ca, Na) occur with a significant decrease from fresh to moderately weathered rock and smaller losses to residual soil.
  - Only Na and Mg indicated a decrease in concentration from fresh rock to residual soil in all the study sites, Na being the only element that showed a large decrease in concentration from fresh to weathered rock.
  - In contrast to the study of Moon and Jayawardane (2004), the high rainfall sites (Nhlowa and Siloam) experience an increase in Fe content and decrease in Ca content. The reverse occurs in the lower rainfall sites (Mooiplaas and Codrington) where Ca increases, and Fe decreases from fresh to weathered rock and/or residual soil.
  - Although, this still indicates mobilization of the major elements in and out of the system with respect to enrichment and depletion of the elements, and not just depletion as with the case in the study of Moon and Jayawardane (2004).

- Certain elements and trace elements such as Ti, Y and Zr have thought to be immobile during the alteration and weathering of crystalline basalt.
  - Mobility of all three these elements have been noted in all the study areas.
  - The Y content both indicates a depletion and enrichment between the sites and horizons. At Mooiplaas Y and Zr portrays a slight depletion, whereas at Nhlowa an increase and decrease of Y content occurs from parent to highly weathered rock and then residual soil, Zr is locally enriched or depleted.

- The aforementioned is similar to the study of Hill et al. (2013) in northeast Ireland which experienced a marked decrease of Y and increase of Zr, where Zr is locally depleted.
- At Siloam and Codrington, a decrease then increase in Y occurs, with Zr at Codrington increasing upward through the profile. Bih Chi et al. (2012) noticed during their study on basalt in the humid-tropics in SW Camaroon an increase in Yttrium through the profile as well.
- Bih Chi et al. (2012) experienced notable mobility of Ti aand Zr in their study where Hill et al. (2013) noticed an increase in Ti and Zr with laterite formation.
- The abovementioned trend was also noted at Nhlowa having ferricretes with a slight increase in Ti and Zr content. Although Ti content showed a decrease at Mooiplaas upward through the profile.

7.3 Mineralogy

The main focus for the mineralogical aspect between the sites were the link between primary and secondary minerals. Where decreases in primary mineral content and an increase in secondary minerals especially smectite clays indicate weathering extent.

- Houston and Smith (1997) determined the degree of alteration of basalt by comparing a primary mineral (Plagioclase) in basalt to a weathered product or secondary mineral (Smectite) in basalt from New South Wales Australia.
  - The aforementioned was also observed in the samples from the study sites that a lower Plagioclase concentration occurred upward through the profile with an increase in smectite. A low Plagioclase content in a sample also correlated with a high Smectite content, compared to the original concentrations in the parent rocks.
  - Although, the decrease in Plagioclase content was not significant or proportionate to the increase in smectite concentrations, e.g. the Nhlowa site had a decrease in plagioclase content (present in every sample) with only some smectite detected in scattered samples, even in the residual soil.
  - High smectite content is however present in the Mooiplaas and Codrington site with a marginal lower Plagioclase content.

- The dramatic increase in smectite content at these two sites were mostly attributed to the weathering of Augite. This was observed with the drastic decrease of Augite content from parent to highly weathered rock paired with a high increase of Smectite.
- If a high Smectite content was present together with Augite in the sample the Plagioclase content would be less than the overall average between the samples. Indicating a combination of the weathering of Plagioclase and Augite to produce Smectite with Augite preferentially weathering.

➢ The previous statement's occurrence was also described in the studies by Moon and Jayawardane (2004) on the Karamu Basalts in New Zealand and by Hill et al. (2013) in northeast Ireland. Where they found that after initial weathering, Fe-rich Smectites are the replacement product of weathered Olivine and Augite and Al-rich Smectites the replacement product of weathered Plagioclase. This indicates a combination of the weathering of Plagioclase and Augite to create Smectite with Augite weathering preferentially.

- A similar trend was observed in certain residual basalt samples which has no Augite and relatively high Plagioclase and high Smectite, where in samples with low Augite content had less Plagioclase but still high Smectite content.
- The rock samples from the Nhlowa site indicated not to have any Augite in the parent rock and the Plagioclase did not preferentially weather to Smectite, this is shown by the very low Smectite content in the samples. Some scattered samples did however contain Smectite which could point to the possibility of the original rock weathering to the residual sample containing some Augite and having it favourably weather over Plagioclase.

➢ The study of Bih Chi et al. (2012) on basaltic soils in humid tropic climates in south-western Cameroon, concentrated on the weathering of Olivine, Pyroxene, Amphibole and calcic Plagioclase as the principal minerals weathering from fresh rock to soil.

- In all the study sites, very little to no Olivine and Amphibole were present, this meant that the main weathering minerals here were Pyroxene and Plagioclase. Klein and Dutrow (2007) commented that Olivine usually occurs as phenocrysts. Also that Olivine will be very scarce in a sample due to being the most unstable mineral on surface and weathers preferentially before other minerals.

7.4 Engineering Data

The mechanical tests done were merely to provide engineering property information on the weathered products of low relief basalts. This was compared to existing data for the residual soils of Drakensburg and Sibasa basalt Formations in order to highlight differences or similarities.

- Brink, 1983 on pages 156 to 157 provides tables of expected values for residual basalt of the Drakensburg Formation in Lesotho and the Letaba Formation of the Lebombo Group in Komatipoort.
  - The Mooiplaas site underlain by the Letaba Formation has slightly higher average Liquid Limit and Plasticity Index than the residual soil at Komatipoort.
  - When the low relief high rainfall sites (Nhlowa and Siloam) are compared to the mountainous and high rainfall environment of the Drakensberg the LL and PI of the study sites are much higher.
  - The average LL and PI in a valley setting below 2 500m in Lesotho are 38.8% and 13% whereas Nhlowa has a much higher LL and PI of 48.6% and 23.20% and Siloam at 53.67% and 28.5% respectively. This indicates that the weathering intensity on flat lying basalts are higher than in mountainous and valley settings even with very high rainfall conditions.
  - The only site which has similar LL and PI to the valley setting of the Drakensberg is Roedtan at 31.33% and 13.33% possibly due to the flat lying nature of the site. A possible reason to this is that even with low rainfall, water will stay in the rock and soil long enough to simulate a degree of chemical weathering conditions similar to the high rainfall and high runoff in a mountain and valley setting.
  - At Roedtan the compaction effort at 95% Mod. AASHTO for the calcified residual basalt is 35 and the completely weathered basalt 38. This is relatively close to the valley and mountain settings, with values of 45 and 47.
  - The LL of 41% to 64% and PI of 21% to 37% for the residual Sibasa basalts at Siloam very similar to the values provided in Brink (1981) at the Nzhelele dam in Venda, with a LL of 35% to 62% and PI of 5% to 26%, although closer to the higher values.
  - For the residual basalt at Nzhelele dam in Venda, Brink (1981) provides values of 6 to 59 for a compaction effort of 95% Mod. ASSHTO whereas at Siloam values of 2 to 6 was achieved.

It is not sufficient to only gather information and understand the effect of weathering of a single setting on a specific rock type. Understanding the effects of weathering on low relief as well as mountainous basalt in variable climatic conditions are crucial to comprehend the behaviour of basalt as well as other rock types during the complex process of weathering. As displayed in this study a moderate shift in climate in terms of rainfall and evaporation can have far reaching effects on the residual soil development on basalt. Effects such as substantial differences in pedocrete formation between high and low rainfall areas to the type of soil formation from very gravelly or dominated by fines are noticeable even for similar low relief areas with slight mineralogical differences.

Future studies should set out to investigate both low and high relief areas in different climatic conditions together in order to produce collective information with the intention of creating possible new investigation techniques that are time and cost effective.

8. Acknowledgements

First and foremost, I would like to thank SANparks for such an unbelievable opportunity to conduct an investigation in the magnificent Kruger National Park. It is an extremely rare opportunity, and experience which I will never forget. Secondly to my supervisor Prof. Louis van Rooy for seeing the potential in me to be able to undertake such an investigation, as well as for all the assistance and guidance you gave me during this challenging MSc. To the Environment and Engineering Geology Honours class of 2012 at the University of Pretoria, and all who assisted me in gathering the data for this massive investigation, I thank you. Not that spending time in the Kruger National Park for the data gathering was such a punishment.

Second to last thank you to my mother Engela van Staden for constantly checking up on my progress with this MSc, just to make sure I was not getting too relaxed and forgetful. Even more than that, the example she set for me on how to strive forward and do your utmost best is unmatched and I could not have asked for a better role model. Lastly, thank you to my wife to be, Gwendylin Lawson, for all your unwavering support, love and motivation through the good, difficult and “tuff” times. With you by myside I know I would be able to achieve anything, I lava you very much.

9. References

- AFCAP/MOZ/091, (2012). Identification and Mapping of Calcrete Deposits in Inhambane Province and Preparation of a Calcrete Classification System and Specifications for the Use of Calcrete in Road Construction in Mozambique, Africa Community Access Program (AFCAP). Technical Review Report No. RPN 2326, Crown Agents, UK Department for International Development.
- Ameyan, O. (1996). Quality of Land Facets as Soil Mapping Units in an Area of Northern Nigeria, Geoform, Vol. 17, No.1, p.97-107.
- Barker, O.B., Brandl, G., Callaghan, C.C., Eriksson, P.G. and van der Neut, M. (2006). The Soutpansberg and Waterberg groups and the Blouberg formation. In: Anhaeusser C.R., Johnson M.R. and Thomas R.J. (Eds). The Geology of South Africa, Geological society of South Africa, Johannesburg and Council for Geoscience, Pretoria, p.303-306.
- Barker, F., (1979). Trondjemites, Dacites, and Related Rocks, Volume 6 Developments in Petrology, Elsevier, U.S. Geological Survey, Denver, Colorado, USA.
- Bell, F.G. and Haskins, D.R., (1997). A geotechnical overview of Katse Dam and Transfer Tunnel, Lesotho, with a note on basalt durability, Elsevier, Engineering Geology (46). p.175-198.
- Bih Che, V., Fontijn K., Ernst, G.G.J., Kervyn, M., Elburg, M., Van Ranst, E. and Suh. C.E., (2012). Evaluating the degree of weathering in landslide-prone soils in the humid tropics: The case of Limbe, SW Cameroon, Elsevier, Geoderma 170, 378-389.
- Botha, G. and Porat, N., (2007). Soil chronosequence development in dunes on the southeast African coastal plain, Maputaland, South Africa, Elsevier, Quaternary International 162-163, p.111-132.
- Brandl, G., Cloete, M. and Anhaeusset, C.R., (2006). Archaean Greenstone Belts. In: Anhaeusser C.R., Johnson M.R. and Thomas R.J. (Eds). The Geology of South Africa, Geological society of South Africa, Johannesburg and Council for Geoscience, Pretoria, Chapter 2, p.9-30.
- Brink, A.B.A. (1979). Engineering Geological of South Africa: The first 2 000million years of geological time, Building Publications, Volume 1, Chapter 1, p.30-31.
- Brink, A.B.A. (1983). Engineering Geological of South Africa: The Karoo Sequence, Building Publications, Volume 3, Chapter 6, p.151-159.
- Brink, A.B.A. (1985). Engineering Geological of South Africa: Post-Gondwana Deposits, Building Publications, Volume 4, Chapter 10, p.286-307.
- Brink A.B.A and Bruin R.M.H (2002), Guidelines for Soil and Rock Logging in South Africa, 2nd Impression 2002, eds. A.B.A Brink and R.M.H. Bruin, Proceedings, Geoterminology Workshop organised by AEG, SAICE and SAIEG, 1990.
- Bristow, J.W. and Cox, K.G. (1984). Volcanic rocks of the Lebombo-Nuanetsi-Sabi zone: classification and nomenclature in: Petrogenesis of the VolcanicRocks of the Karoo Province, Geological Society of South Africa Special Publication 13 (edited by A.J. Erlank), p. 69-75.
- Cawthorn, R.G., Eales, H.V., Walraven, F., Uken, R. and Watkeys, M.K., (2006). The Bushveld Complex. In: Anhaeusser C.R., Johnson M.R. and Thomas R.J. (Eds). The

Geology of South Africa, Geological society of South Africa, Johannesburg and Council for Geoscience, Pretoria, Chapter 11, p.261-269.

- Chief Directorate National Geo-spatial Information of South Africa: reprojected and collar-cropped for seamless mosaic. MrSid file format, Topographical map 2331 AB, 1: 50 000, Limpopo series, http://www.madmappers.com/details.php?MS=16&MP=125.
- Chief Directorate National Geo-spatial Information of South Africa: reprojected and collar-cropped for seamless mosaic. MrSid file format, Topographical map 2331 CB, 1: 50 000, Limpopo series, http://www.madmappers.com/details.php?MS=16&MP=67.
- Chief Directorate National Geo-spatial Information of South Africa: reprojected and collar-cropped for seamless mosaic. MrSid file format, Topographical map 2230 CC, 1: 50 000, Limpopo series, http://www.madmappers.com/details.php?MS=16&MP=94.
- Chief Directorate National Geo-spatial Information of South Africa: reprojected and collar-cropped for seamless mosaic. MrSid file format, Topographical map 2531 BB, 1: 50 000, Mpumalanga series, http://www.madmappers.com/details.php?MS=17&MP=149.
- Chief Directorate National Geo-spatial Information of South Africa: reprojected and collar-cropped for seamless mosaic. MrSid file format, Topographical map 2531 BD, 1: 50 000, Mpumalanga series, http://www.madmappers.com/details.php?MS=17&MP=150.
- Chief Directorate National Geo-spatial Information of South Africa: reprojected and collar-cropped for seamless mosaic. MrSid file format, Topographical map 2429 CA, 1: 50 000, Limpopo series, http://www.madmappers.com/details.php?MS=16&MP=30.
- Chief Directorate National Geo-spatial Information of South Africa: reprojected and collar-cropped for seamless mosaic. MrSid file format, Topographical map 2528 AA, 1: 50 000, Limpopo series, http://www.madmappers.com/details.php?MS=16&MP=60.
- Chief Directorate National Geo-spatial Information of South Africa: reprojected and collar-cropped for seamless mosaic. MrSid file format, Topographical map 2528 AB, 1: 50 000, Gauteng series, http://www.madmappers.com/details.php?MS=14&MP=34.
- Coetzee, F., (1978). Nylstroom Geological sheet 2428, 1:250 000, Geological series, RSA Department of Mines.
- Coetzee, F., (1978). Pretoria Geological sheet 2528, 1:250 000, Geological series, RSA Department of Mines.
- Coetzee, L.E., (1985). Tzaneen Geological sheet 2330, 1:250 000, Geological series, RSA Department of Mineral and Energy Affairs.
- COLTO (1998 Edition) Standard Specifications for road and Bridge works for State Road Authorities.
- Connallon, C.B. and Schaetzel R.J., (2017). Geomorphology of the Chippewa River delta of Glacial Lake Saginaw, central Lower Michigan, USA, Elsevier, Journal of Geomorphology (290), p.128-141.
- Duncan A.R. and Marsh J.S. (2006). The Karoo Igneous Province. In: Anhaeusser C.R., Johnson M.R. and Thomas R.J. (Eds), The Geology of South Africa, Geological society of South Africa, Johannesburg and Council for Geoscience, Pretoria. p.501-505.

- Eggleton, R.A., (2001). The Regolith Glossary: Surficial Geology, Soils and Landscapes. CRC LEME, Kensington, Australia.
- Engidasew, T.A. and Barbieri, G., (2014). Geo-engineering evaluation of Termaber basalt rock mass for crushed stone aggregate and building stone from Central Ethiopia, Elsevier, Journal of African Earth Sciences (99), p.581-594.
- Eriksson, P.G., Alterman, W. and Hartzer, F.J., (2006). The Transvaal Supergroup and its Precursors. In: Anhaeusser C.R., Johnson M.R. and Thomas R.J. (Eds), The Geology of South Africa, Geological society of South Africa, Johannesburg and Council for Geoscience, Pretoria, Chapter 10, p.239-255.
- Gold, D.J.C., (2006). The Pongola Supergroup. In: Anhaeusser C.R., Johnson M.R. and Thomas R.J. (Eds), The Geology of South Africa, Geological society of South Africa, Johannesburg and Council for Geoscience, Pretoria, Chapter 5, p.140-143.
- Google Earth 6.0. 2015. Kruger National Park Southern Basalt Research Supersite, 25º 14’ 13.9’’ S 31º 55’ 05.56’’ E, Eye altitude 10.85km, US Dept. of State Geographer, CNES/Astrium (2015), AfriGIS (Pty) Ltd. (2015), Digital Globe (2015), [17 July 2015].
- Google Earth 6.0. 2015. Kruger National Park Southern Basalt Research Supersite with 2530 Barberton 1:250 000 Geological map overlay, 25º 15’ 21.59’’ S 31º 51’ 56.47’’ E, Eye altitude 28.06km, US Dept. of State Geographer, CNES/Astrium (2015), AfriGIS (Pty) Ltd. (2015), Digital Globe (2015), [17 July 2015].
- Google Earth 6.0. 2015. Kruger National Park Northern Basalt Research Supersite, 23º 28’ 47.49’’ S 31º 24’ 36.39’’ E, Eye altitude 23.48km, US Dept. of State Geographer, Cnes/Spot Image (2015), CNES/Astrium (2015), [17 July 2015].
- Google Earth 6.0. 2015. Kruger National Park Northern Basalt Research Supersite with 2330 Tzaneen 1:250 000 Geological map overlay, 23º 30’ 42.85’’ S 31º 16’ 10.50’’ E, Eye altitude 56.24km, US Dept. of State Geographer, Cnes/Spot Image (2015), CNES/Astrium (2015), [17 July 2015].
- Google Earth 7.0. 2016. Siloam Hospital, 22º 53’ 50.66’’ S 30º 11’ 49.63’’ E, Eye altitude 2.25km, AfriGIS (Pty) Ltd. (2016), CNES/Astrium (2015), [03 February 2016].
- Google Earth 7.0. 2015. Siloam Hospital with 2330 Tzaneen 1:250 000 Geological map overlay, 22º 53’ 50.66’’ S 30º 11’ 49.63’’ E, Eye altitude 26.82km, Digital Globe (2016), [03 February 2016].
- Google Earth 7.0. 2016. Roedtan proposed police station location, 24º 36’ 18.86’’ S 29º 04’ 56.48’’ E, Eye altitude 2.34km, AfriGIS (Pty) Ltd. (2016), Digital Globe (2015), [03 February 2016].
- Google Earth 7.0. 2016. Roedtan proposed police station location with 2428 Nylstroom 1:250 000 Geological map overlay, 24º 49’ 30.35’’ S 28º 40’ 55.48’’ E, Eye altitude 94.04km, AfriGIS (Pty) Ltd. (2016), Digital Globe (2015), [03 February 2016].
- Google Earth 7.0. 2016. Codrington Quarry, 28º 02’ 49.69’’ S 28º 18’ 34.85’’ E, Eye altitude 4.42km, AfriGIS (Pty) Ltd. (2016), Digital Globe (2015), [03 February 2016].
- Google Earth 7.0. 2016. Codrington Quarry with 2528 Pretoria 1:250 000 Geological map overlay, 24º 49’ 30.35’’ S 28º 40’ 55.48’’ E, Eye altitude 94.04km, AfriGIS (Pty) Ltd. (2016), Digital Globe (2015), [03 February 2016].

- Guidelines for Soil and Rock Logging in South Africa, 2nd Impression 2001, eds. A.B.A. Brink and R.M.H. Bruin, Proceedings, Geoterminology Workshop organised by AEG, SAICE and SAIEG, 1990.
- Hill, I.G., Worden, R.H. and Meighan, I.G., (2013). Yttrium: The Immobility-mobility transition during basaltic weathering, The Geological Society of America, v. 28, p.923-926.
- Houston, E.C. and Smith, J.V., (1997). Assessment of rock quality variability due to smectitic alteration in basalt using X-ray diffraction analysis, Elsevier, (46) p.19-32.
- Johnson, M.R., van Vuuren, C.J., Visser, J.N.J., Cole, D.I., Wickens, H. de V., Christie, A.D.M., Roberts, D.L. and Brandl, G. (2006). Sedimentary rocks of the Karoo Supergroup. In: Anhaeusser C.R., Johnson M.R. and Thomas R.J. (Eds), The Geology of South Africa, Geological society of South Africa, Johannesburg and Council for Geoscience, Pretoria, p.485-487.
- Klein, C. and Dutrow, B., (2007). The 23rd edition of the manual of Mineral Science, John Wiley & Sons, Inc., Chapter 19 and 21.
- Limpopo DFED, 2004, Limpopo State of the Environment Report (Phase 1), Limpopo Department of Finance and Economic Developemnt.
- Liu, Z., Cai, Z.C., Wang, J.F., (1996). Microelements of Soils in China: Nanjing. Jiangsu Science and Technology Press.
- Masoud, Z., Akbar, A., and Khan, A. H., (2013). High quality and cost effective drilling systems for prebored pressuremeter testing, Elsevier, Soils and Foundations, Volume 53, Issue 6, p.903-9090.
- Marsh, J. (1984). Karoo Basalts of the Springbok Flats, Transvaal: Geochemistry and Correlation, 20th Geological Congress of the Geological Society, p.91.
- McCarthy T. and Rubidge B. (2005). The story of Earth and Life, Struik, Cape Town. p.209-211.
- McCarthy, T.S., (2006). The Witwatersrand Supergroup. In: Anhaeusser C.R., Johnson M.R. and Thomas R.J. (Eds), The Geology of South Africa, Geological society of South Africa, Johannesburg and Council for Geoscience, Pretoria, Chapter 7, p.155-158.
- McNally, G.H., (2003). Soil and Rock Construction Material, E & FN Spon, London and New York, p.65-69.
- Middleton, B.J. and Bailey A.K., (2008). Water Resources of South Africa, 2005 Study (WR2005), WRC report number TT 381/08, Version 1.
- Moon and Jayawardane, V. and Jayawardane, J., (2004). Geotechnical and geochemical changes during early stages of weathering of Karamu Basalt, New Zealand, Elsevier, (74) p.57-72.
- Netterberg, F. (1969). The Geology and Engineering Properties of South African Calcretes: Engineering properties and specifications for roads, Volume 3, University of the Witwatersrand.
- Netterberg, F. (1971). Calcrete in Road Construction, South African Council for Scientific and Industrial Research, Volume 10 of Bulletin: National Institute of Road Research.

- Paige-Green, P., (2007). Durability testing of basic crystalline rocks and specification for use as road base aggregate, Springer.
- SAexplorer, 2000-2014. [online]. [Accessed 1 December 2015]. Available from World Wide Web: http://www.saexplorer.co.za/south-africa/climate/roedtan_climate.asp.
- SABS [South African Bureau of Standards], (2012). Geotechnical Investigations for Township Development. Draft South African National Standard SANS 634. SABS Standards Division, Pretoria.
- SACS (SOUTH AFRICA COMMITTEE FOR STRATIGRAPHY) (1980) Stratigraphy of South Africa Part 1: Lithostratigraphy of the Republic of South Africa, South West Africa/Namibia and the Republics of Bophuthatswana, Transkei and Venda. Handbook Geological Survey South Africa, Pretoria.
- Sato, H., Aramaki, S., Kusakabe, M., Hirabayashi, J., Sano, Y., Nojiri, Y., Tchoua, F., 1990. Geochemical difference of basalts between polygenetic andmonogenetic volcanoes in the central part of the Cameroon Volcanic line. Geochemical Journal 24, 357–370.
- Smit, IPJ, Riddell, ES, Cullum, C & Petersen, R. (2013). Kruger National Park research supersites: Establishing long-term research sites for cross-disciplinary, multiscaled learning. Koedoe 55(1).
- Sumner, P.D., Hall, K.L., van Rooy, J.L. and Meiklejohn, K.I., (2009). Rock weathering on the eastern mountains of southern Africa: Review and insights from case studies, Elsevier, Journal of African Earth Sciences (55), p.236-244.
- Tatsumi, Y. and Suzuki, T., (2009). Tholeiitic vs Calc-alkalic Differentiation and Evolution of Arc Crust: Constraints from Melting Experiments on a Basalt from the Izu–Bonin–Mariana Arc, Journal of Petrology (50), p.1575-1603.
- Van der Westhuizen, W.A., de Bruiyn, H. and Meintjies, P.G., (2006). The Ventersdorop Supergroup. In: Anhaeusser C.R., Johnson M.R. and Thomas R.J. (Eds), The Geology of South Africa, Geological society of South Africa, Johannesburg and Council for Geoscience, Pretoria, Chapter 8, p.189-196.
- Van Rensburg, H.M.L., (1986). Barberton Geological sheet 2530, 1:250 000, Geological series, RSA Department of Mineral and Energy Affairs.
- Van Rooy JL (1994) Aggregate selection criteria for Drakensberg basalt, Kingdom of Lesotho. In: Proceedings of the 7th Int Cong of Int Ass Engng Geol, Lisbon, 3245–3250
- Venter, F.J., (1990). 'A classification for land management planning in the Kruger National Park', PhD Thesis. Pretoria, University of South Africa. Chapters 6 and 10.
- Weinert, H.H. (1980). The Natural Road Construction Materials of Southern Africa. H & R Academia Publ., Pretoria.
- Widdowson, M., (2003). Ferricrete. In: Goudie, A.S. (Eds), Encyclopedia of Geomorphology, Routledge, p.365-367.
- Wilkinson, K.J., (1981). Messina Geological sheet 2230, 1:250 000, Geological series, RSA Department of Mineral and Energy Affairs.
- Winter, J.D., (2001). An Introduction to Igneous and Metamorphic Petrology, Prentice Hall, Chapter 8 to 10.

Appendix A

Grading Analysis and Atterberg Limits

Table A1: Grading and Atterberg Limits of the Mooiplaas site for NBProfile 2A and alluvium.

NBProfile 2A															
Test pit	**NB05**	**NB11**	**NB19**	**NB20**	**NB29**	**Average**	**Standard Deviation**	**NB05**	**NB11**	**NB19**	**NB20**	**Average**	**Standard Deviation**	**NB32**	**NB32**
Depth (m)	**0.00-0.25**	**0.00-0.24**	**0.00-0.44**	**0.00-0.44**	**0.00-0.21**			**0.44-0.67**	**0.32-0.58**	**0.44-0.95**	**0.44-1.07**			**0.0-0.24**	**0.24-0.80**
Origin	**Reworked Residual Basalt**							**Residual Basalt**						**Alluvium**	**Calcified Residual Basalt**
% Clay	9	12	16	9	15	12.20	3.27	8	3	9	4	6.00	2.94	20	29
% Silt	27	39	50	34	44	38.80	8.87	14	9	25	29	19.25	9.32	25	20
% Sand	46	45	30	49	36	41.20	7.92	39	34	47	53	43.25	8.42	42	37
% Gravel	18	4	4	8	4	7.60	6.07	40	54	19	15	32.00	18.31	13	15
Liquid Limit (%)	43	48	73	44	63	54.20	13.22	51	44	65	40	50.00	10.98	50	83
Plasticity Index (%)	17	20	37	17	27	23.60	8.53	24	20	29	18	22.75	4.86	22	38
Linear shrinkage (%)	9	11	18	10	14	12.40	3.65	11	10	13	9	10.75	1.71	9	14
PRA	A-7-6	A-7-6	A-7-5	A-7-6	A-7-5	-	-	A-2-7	A-2-7	A-7-5	A-6	-	-	A-7-6	A-7-5
Unified classification	SC	ML	MH	SM	MH	-	-	SC	SC	SM	SC	-	-	SC	MH

PRA - Public Road Administration; USCS - Unified Soil Classification System

Table A2: Grading and Atterberg Limits of the Mooiplaas site for NBProfile 2B.

NBProfile 2B												
Test pit	**NB06**	**NB33**	**NB34**	**NB34**	**Average**	**Standard Deviation**	**NB06**	**NB12**	**NB27**	**NB34**	**Average**	**Standard Deviation**
Depth (m)	**0.0-0.48**	**0.00-0.25**	**0.00-0.30**	**0.30-0.60**			**0.40-0.88**	**0.50-1.48**	**0.15-0.35**	**0.60-0.90**		
Origin	**Reworked Residual Basalt**						**Residual Basalt**					
% Clay	13	12	9	7	10.25	2.75	6	1	3	5	3.75	2.22
% Silt	43	31	35	22	32.75	8.73	23	20	9	17	17.25	6.02
% Sand	31	55	40	28	38.5	12.12	37	63	33	28	40.25	15.61
% Gravel	12	2	16	43	18.25	17.52	34	16	56	50	39.00	17.93
Liquid Limit (%)	67	41	50	55	53.25	10.84	61	47	43	54	51.25	7.93
Plasticity Index (%)	31	16	24	26	24.25	6.24	25	17	17	22	20.25	3.95
Linear shrinkage (%)	16	8	11	13	12.00	3.37	12	8	8	11	9.75	2.06
PRA	A-7-5	A-7-6	A-7-6	A-2-7	-	-	A-7-5	A-2-7	A-2-7	A-2-7	-	-
Unified classification	MH	CL	CL	SC	-	-	SM	SM	SC	SM	-	-

PRA - Public Road Administration; USCS - Unified Soil Classification System

Table A3: Grading and Atterberg Limits of the Nholwa site.

	Profile SB01												Profile SB02
Test pit	**SB02**	**SB02**	**SB03**	**SB16**	**SB17**	**SB17**	**Average**	**Standard Deviation**	**SB03**	**SB16**	**Average**	**Standard Deviation**	**SB16**
Depth (m)	**0-0.12**	**0.12-0.55**	**0.24-0.32**	**0.38-0.65**	**0.0-0.64**	**0.64-0.84**			**0.71-0.94**	**0.65-1.03**			**0.65-1.03**
Origin	**Colluvium**	**Residual Basalt**							**Highly Weathered Basalt**				**Residual Basalt**
% Clay	17	7	18	12	14	15	13.20	4.09	4	5	4.50	0.71	3
% Silt	36	25	43	45	33	27	34.60	9.10	19	16	17.50	2.12	21
% Sand	42	40	37	41	44	20	36.40	9.50	57	40	48.50	12.02	56
% Gravel	5	27	1	2	9	37	15.20	16.04	20	40	30.00	14.14	20
Liquid Limit (%)	33	47	37	43	48	68	48.60	11.67	36	52	44.00	11.31	42
Plasticity Index (%)	14	21	17	21	24	33	23.20	6.02	14	25	19.50	7.78	19
Linear shrinkage (%)	7	9.5	8	11	12	16	11.30	3.03	7	12	9.50	3.54	9
PRA	A-6	A-7-6	A-6	A-7-6	A-7-6	A-7-5	-	-	A-2-6	A-2-7	-	-	A-2-7
Unified classification	CL	SC	CL	CL	CL	GM	-	-	SC	SC	-	-	SC

PRA - Public Road Administration; USCS - Unified Soil Classification System

Table A4: Grading and Atterberg Limits of the Sibasa Basalts at Siloam (Transported).

Test pit	**TP01**	**TP03**	**TP04**	**TP05**	**Average**	**Standard Deviation**	**TP01**	**TP02**	**Average**	**Standard Deviation**
Depth (m)	**0.0-0.7**	**0.0-1.0**	**0.0-1.0**	**0.0-0.6**			**1.0-1.4**	**1.1-1.6**		
Origin	**Colluvium**						**Reworked Pebble Marker/ Residuum**			
% Clay	8	22	43	33	26.5	15.02	11	11	11.00	0.00
% Silt	14	33	22	28	24.25	8.18	18	15	16.50	2.12
% Sand	35	43	29	37	36.00	5.77	21	22	21.50	0.71
% Gravel	43	2	6	2	13.25	19.92	50	52	51.00	1.41
Liquid Limit (%)	41	44	54	46	46.25	5.56	48	46	47.00	1.41
Plasticity Index (%)	22	23	28	30	25.75	3.86	26	30	28.00	2.83
Linear shrinkage (%)	11	13	13.5	14	12.88	1.31	13	13	13.00	0.00
PRA	A-2-7	A-7-6	A-7-6	A-7-6	-	-	A-2-7	A-2-7	-	-
Unified classification	GC	CL	CH	CL	-	-	GC	GC	-	-

PRA - Public Road Administration; USCS - Unified Soil Classification System

Table A5: Grading and Atterberg Limits of the Sibasa Basalts at Siloam (Residual horizon).

Test pit	TP01	TP03	TP05	TP06	TP08	TP08	Average	Standard Deviation
Depth (m)	1.5-2.5	1.5-2.0	0.8-1.2	1.0-2.0	0.7-1.1	2.0-2.5		
Origin	Residual Basalt							
% Clay	8	9	11	15	33	13	14.83	9.26
% Silt	32	17	12	15	28	20	20.67	7.79
% Sand	40	20	21	24	33	54	32	13.25
% Gravel	20	54	56	16	6	13	27.5	21.8
Liquid Limit (%)	46	51	49	64	49	63	53.67	7.79
Plasticity Index (%)	21	26	28	32	27	37	28.5	5.47
Linear shrinkage (%)	10	12	13	15	12	12	12.33	1.63
PRA	A-7-6	A-2-7	A-2-7	A-2-7	A-7-6	A-7-6	-	-
Unified classification	SC	GC	GC	SM	CL	SC	-	-

PRA - Public Road Administration; USCS - Unified Soil Classification System

Table A6: Grading and Atterberg Limits of the Springbok Flats Basalt at Roedtan**.**

Test pit	TP02	TP02	TP05	TP06	Average	Standard Deviation	TP02	TP04	TP05	TP06	TP07	Average	Standard Deviation
Depth (m)	0.0-0.3	0.5-0.9	0.5-1.1	0.4-0.8			1.0-1.5	1.5-2.3	1.5-2.0	1.4-1.8	1.0-2.0		
Origin	Colluvium	Calcified Residual Basalt					Completely to Highly Weathered Basalt						
% Clay	15	2	3	4	3.00	1.00	0	0	0	1	2	0.60	0.89
% Silt	18	15	11	11	12.33	2.31	6	4	5	6	5	5.20	0.84
% Sand	66	44	32	33	36.33	6.66	32	21	24	28	30	27.00	4.47
% Gravel	1	38	54	52	48.00	8.72	62	75	71	65	63	67.20	5.59
Liquid Limit (%)	24	29	32	33	31.33	2.08	27	27	29	33	38	30.80	4.71
Plasticity Index (%)	10	9	14	17	13.33	4.04	8	10	9	10	15	10.40	2.70
Linear shrinkage (%)	4	4.5	6	7	5.83	1.26	3	3	4	4	6	4.00	1.22
PRA	A-4	A-2-4	A-2-6	A-2-6	-	-	A-2-4	A-2-4	A-2-4	A-2-4	A-2-6	-	-
Unified classification	SC	SC	SC	SC	-	-	SP-SC	SW	SP-SC	SP-SC	SP-SM	-	-

PRA - Public Road Administration; USCS - Unified Soil Classification System

Appendix B

XRF Results

Table B1: Major and Trace Elements, XRF Results at Mooiplaas for the Transported Horizons.

XRF (wt %)	Colluvium				Alluvium				
Test pit	NB01	NB03	Average	Standard Deviation	NB30	NB31	NB32	Average	Standard Deviation
Depth (m)	0.00-0.40	0.00-0.25			0.00-0.38	0.00-0.40	0.00-0.24		
SiO_2	60.98	56.41	58.70	3.23	51.48	49.80	45.33	48.87	3.18
TiO_2	1.61	1.28	1.44	0.24	2.76	2.13	2.06	2.32	0.38
Al_2O_3	13.16	13.37	13.27	0.15	9.17	7.39	5.34	7.30	1.92
Fe_2O_3	9.52	9.51	9.52	0.00	11.54	9.54	6.64	9.24	2.46
MnO	0.13	0.17	0.15	0.03	0.15	0.12	0.10	0.13	0.02
MgO	1.77	4.11	2.94	1.65	6.06	8.92	10.13	8.37	2.09
CaO	2.31	4.59	3.45	1.61	4.04	4.32	10.12	6.16	3.43
Na_2O	1.35	1.13	1.24	0.15	1.29	0.70	1.30	1.10	0.34
K_2O	1.91	1.27	1.59	0.45	1.84	1.45	1.25	1.51	0.30
P_2O_5	0.10	0.10	0.10	0.00	0.25	0.33	0.16	0.25	0.09
Cr_2O_3	0.05	0.07	0.06	0.01	0.11	0.09	0.07	0.09	0.02
NiO	0.03	0.04	0.04	0.00	0.06	0.05	0.03	0.05	0.01
V_2O_5	0.04	0.03	0.04	0.00	0.05	0.04	0.05	0.05	0.00
ZrO_2	0.04	0.02	0.03	0.01	0.04	0.04	0.04	0.04	0.00
CuO	0.01	0.00	0.00	0.00	0.01	0.01	0.00	0.01	0.00
LOI	6.00	8.21	7.10	1.56	11.31	14.71	17.70	14.57	3.20
Total	99.01	100.32	99.66	0.92	100.17	99.65	100.31	100.04	0.35
Y	22	16	19.00	4.24	25	23	22	23.75	1.50
Zr	250	149	199.50	71.42	284	236	269	269.25	23.63
ppm									
As	0	0	0.00	0.00	0	0	0	0.00	0.00
Cu	78	64	71.00	9.90	95	85	51	77.00	23.07
Ga	16	14	15.00	1.41	14	12	9	11.67	2.52
Mo	2	0	1.00	1.41	1	1	2	1.33	0.58
Nb	10	7	8.50	2.12	17	14	11	14.00	3.00
Ni	201	190	195.50	7.78	415	332	219	322.00	98.38
Pb	9	3	6.00	4.24	1	1	8	3.33	4.04
Rb	63	44	53.50	13.44	42	35	34	37.00	4.36
Sr	188	115	151.50	51.62	265	414	1263	647.33	538.36
Th	0	0	0.00	0.00	0	0	0	0.00	0.00
U	0	0	0.00	0.00	0	0	3	1.00	1.73
W*	49	34	41.50	10.61	20	12	46	26.00	17.78
Y	22	16	19.00	4.24	25	23	22	23.33	1.53
Zn	58	67	62.50	6.36	83	86	50	73.00	19.97
Zr	250	149	199.50	71.42	284	236	269	263.00	24.56

Results indicated with a * should be considered semi-quantitative.

Table B2: Major and Trace Elements, XRF Results at Mooiplaas for the Reworked Residual Basalt Horizon.

XRF (wt %)	Reworked Residual Basalt																	
Test pit	NB06	NB07	NB11	NB11	NB12	NB15	NB17	NB19	NB20	NB22	NB24	NB29	NB31	NB33	NB34	NB34	Average	Standard Deviation
Depth (m)	0.00-0.48	0.00-0.30	0.00-0.24	0.24-0.32	0.00-0.31	0.00-0.40	0.00-0.30	0.00-0.44	0.00-0.40	0.00-0.47	0.00-0.35	0.00-0.21	0.90-1.20	0.00-0.25	0.00-0.30	0.30-0.60		
SiO_2	-	44.80	47.52	-	45.40	41.71	57.20	53.11	35.76	57.94	54.67	56.24	43.83	52.55	53.04	48.92	49.48	6.58
TiO_2	-	2.75	3.02	-	2.52	2.80	2.80	2.96	2.22	3.40	3.47	3.09	1.82	2.78	3.26	3.27	2.87	1.07
Al_2O_3	-	6.86	7.44	-	11.20	9.12	9.10	8.78	6.48	10.40	11.35	11.60	6.16	8.55	9.37	8.07	8.89	3.46
Fe_2O_3	-	8.93	11.95	-	13.24	9.79	10.80	11.88	6.87	11.20	11.87	12.32	7.98	9.80	10.79	9.98	10.53	3.95
MnO	-	0.14	0.17	-	0.20	0.14	0.18	0.17	0.09	0.16	0.14	0.15	0.10	0.15	0.17	0.13	0.15	0.06
MgO	-	3.82	9.99	-	7.10	3.02	2.99	4.35	2.93	2.70	2.91	2.32	10.35	6.40	5.04	12.06	5.43	3.26
CaO	-	15.02	8.38	-	9.89	2.08	2.48	2.78	2.63	2.18	1.83	1.76	9.32	7.98	4.87	6.93	5.58	4.08
Na_2O	-	0.43	0.72	-	6.24	0.37	0.72	0.27	0.54	0.50	0.68	0.50	0.39	0.61	0.55	0.43	0.93	1.54
K_2O	-	0.97	0.91	-	1.27	3.13	2.38	1.25	2.40	4.16	3.51	2.51	0.97	0.88	2.67	2.47	2.11	1.07
P_2O_5	-	0.21	0.26	-	0.48	0.27	0.27	0.14	0.24	0.31	0.26	0.19	0.16	0.13	0.34	0.50	0.27	0.11
Cr_2O_3	-	0.09	0.17	-	0.01	0.10	0.13	0.11	0.07	0.14	0.13	0.12	0.08	0.13	0.12	0.13	0.11	0.04
NiO	-	0.04	0.08	-	0.01	0.06	0.05	0.06	0.04	0.06	0.06	0.05	0.04	0.05	0.06	0.08	0.05	0.02
V_2O_5	-	0.04	0.05	-	0.06	0.04	0.05	0.05	0.03	0.05	0.05	0.05	0.06	0.04	0.05	0.05	0.05	0.01
ZrO_2	-	0.04	0.04	-	0.03	0.07	0.05	0.04	0.04	0.07	0.08	0.06	0.03	0.02	0.05	0.05	0.05	0.02
CuO	-	0.00	0.01	-	0.02	0.01	0.01	0.01	0.00	0.01	0.01	0.01	0.00	0.01	0.01	0.01	0.01	0.01
LOI	-	17.12	9.81	-	2.59	25.96	8.83	12.21	38.97	6.91	7.41	8.79	18.90	9.48	9.54	5.96	13.03	9.57
Total	0.00	101.26	100.53	0.00	100.25	98.66	98.01	98.17	99.33	100.18	98.44	99.75	100.20	99.57	99.93	99.04	99.52	0.96
Y	30	23.00	24.00	25.00	27.00	37.00	28.00	26.00	35.00	35.00	39.00	31.00	18.00	24.00	42.00	50.00	30.88	8.29
Zr	369	255.00	310.00	301.00	258.00	581.00	309.00	299.00	488.00	510.00	565.00	389.00	211.00	203.00	437.00	477.00	372.63	123.38

ppm																		
As	0	0	0	0	0	0	0	0	0	1	0	0	0	3	2	5	0.69	1.45
Cu	97	61	94	91	72	105	81	84	80	89	94	96	60	66	87	93	84.38	13.45
Ga	18	11	14	13	13	19	13	15	18	18	20	18	10	14	18	23	15.94	3.57
Mo	2	1	2	2	1	5	2	2	3	5	5	2	0	10	15	16	4.56	4.88
Nb	22	13	15	12	12	31	21	15	22	31	25	19	11	12	25	25	19.44	6.80
Ni	393	265	547	590	382	565	356	434	431	474	508	383	278	338	464	280	418.00	102.32
Pb	8	3	1	1	2	14	4	4	11	15	13	5	1	4	12	12	6.88	5.14
Rb	48	24	24	20	29	74	47	37	54	73	65	57	27	21	50	51	43.81	18.31
Sr	242	182	260	322	185	472	229	128	511	439	529	239	713	225	398	774	365.50	192.98
Th	0	0	0	0	0	3	0	0	0	5	4	0	0	16	22	24	4.63	8.26
U	0	0	0	0	0	0	0	0	0	0	0	0	0	1	6	12	1.19	3.25
W*	41	21	20	6	52	15	44	20	55	60	28	35	23	329	286	101	71.00	95.42
Y	30	23	24	25	27	37	28	26	35	35	39	31	18	24	42	50	30.88	8.29
Zn	99	68	87	88	91	104	87	90	96	94	96	96	51	74	105	118	90.25	15.69
Zr	369	255	310	301	258	581	309	299	488	510	565	389	211	203	437	477	372.63	123.38

Results indicated with a * should be considered semi-quantitative.

Table B3: Major and Trace Elements, XRF Results at Mooiplaas for the Residual Basalt Horizon.

XRF (wt %)	Residual Basalt																		
Test pit	NB01	NB03	NB06	NB07	NB11	NB12	NB12	NB17	NB19	NB20	NB22	NB23	NB24	NB24	NB29	NB32	NB34	Average	Standard Deviation
Depth (m)	0.4-0.5	0.25-0.50	0.48-.88	0.3-0.73	0.32-0.58	0.31-0.50	0.50-1.48	0.30-0.42	0.44-0.95	0.44-1.07	0.47-0.96	0.59-0.83	0.35-0.70	0.70-0.80	0.21-0.64	0.24-0.80	0.60-0.80		
SiO_2	-	49.61	-	70.51	-	71.55	38.16	22.20	35.14	39.92	44.81	44.98	55.65	48.38	36.40	46.35	42.85	46.18	13.16
TiO_2	-	3.51	-	0.12	-	0.27	1.60	1.05	2.17	2.83	2.88	3.19	3.32	2.33	2.07	0.80	2.91	2.08	1.14
Al_2O_3	-	9.17	-	2.15	-	5.42	6.90	3.69	5.95	6.70	7.74	7.90	9.53	7.61	6.62	11.51	7.80	7.05	2.36
Fe_2O_3	-	12.01	-	0.70	-	1.63	9.55	4.59	9.04	8.20	8.47	9.48	9.85	9.51	8.00	10.46	9.64	7.94	3.30
MnO	-	0.15	-	0.01	-	0.01	0.11	0.13	0.14	0.11	0.10	0.12	0.10	0.15	0.12	0.29	0.13	0.12	0.07
MgO	-	9.77	-	0.03	-	0.35	7.63	2.47	7.16	7.63	5.66	9.04	7.04	4.79	5.27	2.94	7.62	5.53	3.07
CaO	-	7.59	-	0.01	-	0.10	16.89	34.59	18.82	16.39	14.25	11.82	5.13	3.66	19.74	5.18	13.50	11.98	9.34
Na_2O	-	2.12	-	0.18	-	0.39	0.64	0.23	0.30	0.18	0.38	0.93	1.15	0.51	0.67	0.31	0.60	0.61	0.52
K_2O	-	1.52	-	0.99	-	2.71	1.05	0.62	0.60	3.10	4.00	2.68	3.16	1.66	1.31	0.48	1.65	1.82	1.11
P_2O_5	-	0.54	-	0.03	-	0.05	0.22	0.15	0.22	0.41	0.44	0.40	0.43	0.32	0.28	0.05	0.33	0.28	0.16
Cr_2O_3	-	0.11	-	0.00	-	0.00	0.08	0.05	0.09	0.09	0.10	0.12	0.11	0.10	0.07	0.09	0.12	0.08	0.04
NiO	-	0.04	-	0.00	-	0.00	0.05	0.03	0.05	0.06	0.04	0.08	0.05	0.05	0.03	0.02	0.07	0.04	0.02
V_2O_5	-	0.06	-	0.00	-	0.01	0.03	0.02	0.03	0.04	0.04	0.05	0.05	0.04	0.03	0.03	0.05	0.03	0.02
ZrO_2	-	0.06	-	0.05	-	0.03	0.02	0.02	0.03	0.06	0.06	0.07	0.07	0.03	0.04	0.02	0.04	0.04	0.02
CuO	-	0.01	-	0.01	-	0.00	0.00	0.00	0.00	0.00	0.00	0.01	0.01	0.01	0.00	0.01	0.01	0.01	0.00
LOI	-	4.12	-	25.20	-	18.16	17.22	30.84	19.93	14.84	12.10	9.55	3.79	20.53	18.55	20.29	11.93	16.22	7.53
Total	0.00	100.38	0.00	100.00	0.00	100.70	100.14	100.65	99.68	100.56	101.06	100.42	99.45	99.67	99.21	98.82	99.25	82.35	0.67
ppm																			
As	0	-	0	-	0	0	0	0	0	0	0	0	0	0	0	0	2	0.13	0.52
Cu	82	-	82	-	88	57	55	39	67	68	61	89	83	48	64	57	93	68.87	16.45
Ga	16	-	13	-	15	10	12	5	11	13	15	15	18	11	11	10	16	12.73	3.26
Mo	1	-	4	-	3	1	1	2	1	5	3	5	5	3	1	0	14	3.27	3.41
Nb	8	-	25	-	13	10	7	10	10	21	26	25	20	12	11	10	22	15.33	6.92
Ni	198	-	324	-	705	295	372	225	436	498	316	629	400	239	260	268	505	378.00	150.98
Pb	10	-	8	-	9	4	0	2	0	8	10	14	11	8	3	2	12	6.73	4.53
Rb	58	-	17	-	20	20	12	15	13	35	47	41	42	25	21	31	34	28.73	13.81
Sr	168	-	622	-	425	167	286	192	237	312	442	1078	960	566	488	1296	446	512.33	345.85
Th	1	-	1	-	0	0	0	0	0	1	1	1	1	0	0	0	25	2.07	6.36
U	0	-	0	-	0	0	0	0	0	0	0	5	3	0	0	1	9	1.20	2.60
W*	35	-	4	-	12	21	1	7	1	7	16	7	36	25	6	14	171	24.20	42.12
Y	20	-	22	-	23	20	17	26	22	25	27	32	36	21	26	21	32	24.67	5.29
Zn	63	-	76	-	100	66	78	35	76	77	74	88	90	54	66	51	95	72.60	17.47
Zr	210	-	316	-	296	187	137	129	209	406	419	546	553	304	298	269	393	311.47	131.70

Results indicated with a * should be considered semi-quantitative.

Table B4: Major and Trace Elements, XRF Results at Mooiplaas for the Highly Weathered Basa

XRF (wt %)	Highly Weathered Basalt						
Test pit	NB01	NB12	NB15	NB19	NB34	Average	Standard Deviation
Depth (m)	0.50-0.80	1.48-1.72	0.40-0.45	0.95	0.80-0.90		
SiO_2	49.20	32.96	49.80	35.68	41.74	41.88	7.65
TiO_2	3.45	1.32	3.95	2.24	2.98	2.79	1.03
Al_2O_3	7.33	5.74	8.55	6.02	7.76	7.08	1.19
Fe_2O_3	10.42	8.37	10.25	9.41	9.39	9.57	0.82
MnO	0.13	0.10	0.14	0.13	0.12	0.12	0.02
MgO	14.04	7.12	8.53	8.11	8.39	9.24	2.74
CaO	6.14	21.92	6.06	18.23	15.06	13.48	7.16
Na_2O	1.71	0.65	0.37	0.40	0.84	0.80	0.55
K_2O	2.75	0.78	5.40	0.58	1.58	2.22	1.98
P_2O_5	0.47	0.19	0.64	0.24	0.35	0.38	0.18
Cr_2O_3	0.12	0.07	0.13	0.11	0.11	0.11	0.03
NiO	0.08	0.04	0.06	0.06	0.07	0.06	0.02
V_2O_5	0.05	0.02	0.06	0.04	0.05	0.04	0.01
ZrO_2	0.08	0.02	0.10	0.03	0.04	0.05	0.03
CuO	0.01	0.00	0.01	0.01	0.01	0.01	0.00
LOI	3.38	20.39	4.76	18.52	11.16	11.64	7.74
Total	99.39	99.69	98.82	99.80	99.64	99.47	0.39
ppm							
As	0	0	4	0	0	0.80	1.79
Cu	84	44	94	67	88	75.40	20.22
Ga	15	10	21	11	15	14.40	4.34
Mo	0	1	8	2	16	5.40	6.69
Nb	5	7	44	8	20	16.80	16.30
Ni	160	329	516	453	476	386.80	144.75
Pb	8	0	21	0	8	7.40	8.59
Rb	52	9	78	10	32	36.20	29.33
Sr	167	294	992	267	561	456.20	333.09
Th	0	0	12	0	23	7.00	10.34
U	0	0	9	0	11	4.00	5.52
W*	76	1	20	1	75	34.60	38.14
Y	18	14	36	20	35	24.60	10.19
Zn	68	67	104	77	96	82.40	16.77
Zr	136	113	744	213	392	319.60	261.30

Results indicated with a * should be considered semi-quantitative.

Table B5: Major and Trace Elements, XRF Results at Mooiplaas for Basalt Rock Samples.

XRF (wt %)	Rock Samples									
Test pit	NB14	NB17	NB29	NB27	Outcrop 4	Outcrop 5	Average	Standard Deviation	Maximum	Minimum
Depth (m)	Surface	Surface	Surface	1.00-1.50	Surface	Surface				
SiO_2	39.15	48.55	51.00	50.43	44.95	45.77	46.64	4.40	51.00	39.15
TiO_2	2.66	3.10	3.55	3.59	2.40	2.42	2.95	0.54	3.59	2.40
Al_2O_3	12.89	8.43	9.79	11.77	11.65	10.59	10.86	1.59	12.89	8.43
Fe_2O_3	12.08	12.79	11.99	11.07	12.73	13.07	12.29	0.73	13.07	11.07
MnO	0.22	0.17	0.15	0.14	0.19	0.21	0.18	0.03	0.22	0.14
MgO	5.70	15.01	10.50	5.04	6.83	7.22	8.38	3.76	15.01	5.04
CaO	9.72	7.74	7.76	7.72	9.43	10.46	8.81	1.21	10.46	7.72
Na_2O	7.25	1.39	1.86	1.30	6.54	4.50	3.81	2.67	7.25	1.30
K_2O	0.90	1.39	1.59	3.03	1.43	1.02	1.56	0.77	3.03	0.90
P_2O_5	1.10	0.38	0.54	0.44	0.39	0.38	0.54	0.28	1.10	0.38
Cr_2O_3	0.01	0.15	0.12	0.06	0.01	0.01	0.06	0.06	0.15	0.01
NiO	0.02	0.10	0.06	0.05	0.02	0.02	0.04	0.03	0.10	0.02
V_2O_5	0.06	0.05	0.06	0.06	0.06	0.06	0.06	0.00	0.06	0.05
ZrO_2	0.03	0.04	0.05	0.05	0.02	0.02	0.03	0.02	0.05	0.02
CuO	0.04	0.01	0.01	0.01	0.03	0.03	0.02	0.01	0.04	0.01
LOI	8.02	0.35	0.55	4.48	2.57	3.53	3.25	2.85	8.02	0.35
TOTAL	99.84	99.66	99.59	99.24	99.26	99.31	99.49	0.25	99.84	99.24

ppm										
As	4	0	5	0	0	0	1.50	2.35	5.00	0.00
Cu	289	108	107	82	218	216	170.00	82.63	289.00	82.00
Ga	27	19	21	16	16	11	18.33	5.43	27.00	11.00
Mo	11	15	16	14	11	11	13.00	2.28	16.00	11.00
Nb	100	23	18	19	70	69	49.83	34.57	100.00	18.00
Ni	26	726	364	555	51	82	300.67	295.02	726.00	26.00
Pb	19	8	8	6	12	15	11.33	4.97	19.00	6.00
Rb	30	29	40	43	43	34	36.50	6.35	43.00	29.00
Sr	1453	929	1238	501	1162	998	1046.83	325.26	1453.00	501.00
Th	26	30	25	21	22	28	25.33	3.44	30.00	21.00
U	16	10	15	7	9	9	11.00	3.63	16.00	7.00
W*	80	178	263	35	124	78	126.33	82.68	263.00	35.00
Y	29	35	38	34	19	20	29.17	8.04	38.00	19.00
Zn	132	118	121	106	123	126	121.00	8.76	132.00	106.00
Zr	278	386	462	465	213	213	336.17	117.17	465.00	213.00

Results indicated with a * should be considered semi-quantitative.

Table B6a: Major Elements, XRF Results at Nhlowa.

XRF (wt%)	Colluvium				Residual Basalt						Highly Weathered Basalt				Rock Samples			
Test pit	SB02	SB17	Average	Standard Deviation	SB02	SB16	SB17	SB29	Average	Standard Deviation	SB16	SB23	Average	Standard Deviation	SB10A	SB10J	Average	Standard Deviation
Depth (m)	0.00-0.12	0.00-0.64			0.12-0.55	0.38-0.65	0.64-0.84	0.81-1.3			0.65-1.03	0.12-0.40			Surface	Surface		
SiO_2	57.76	49.22	53.49	6.04	47.55	56.20	39.46	50.02	48.31	6.93	53.15	50.21	51.68	2.08	49.99	51.79	50.89	1.27
TiO_2	3.34	3.63	3.49	0.21	3.02	3.47	2.56	3.17	3.06	0.38	3.27	2.44	2.86	0.58	3.29	1.13	2.21	1.53
Al_2O_3	11.32	11.82	11.57	0.35	13.49	11.85	11.54	11.62	12.13	0.92	12.98	13.24	13.11	0.18	14.58	14.62	14.60	0.03
Fe_2O_3	14.48	22.26	18.37	5.51	18.74	13.79	16.18	16.11	16.21	2.02	13.00	15.28	14.14	1.62	12.46	12.41	12.43	0.04
MnO	0.19	0.23	0.21	0.03	0.43	0.14	0.28	0.24	0.27	0.12	0.18	0.22	0.20	0.03	0.12	0.20	0.16	0.05
MgO	1.14	1.03	1.09	0.08	4.06	1.10	1.76	2.46	2.34	1.27	2.39	5.45	3.92	2.17	3.89	6.55	5.22	1.88
CaO	0.85	0.74	0.80	0.07	1.79	1.22	10.72	6.29	5.01	4.44	3.74	9.71	6.72	4.22	6.91	8.50	7.71	1.12
Na_2O	0.41	0.73	0.57	0.23	0.40	0.98	0.67	1.56	0.90	0.50	1.73	1.98	1.85	0.17	3.52	3.12	3.32	0.28
K_2O	1.53	1.48	1.51	0.03	1.62	2.00	1.31	1.70	1.66	0.29	2.52	0.86	1.69	1.18	2.98	1.35	2.16	1.15
P_2O_5	0.16	0.26	0.21	0.07	0.20	0.27	0.14	1.28	0.47	0.54	0.47	0.30	0.38	0.12	0.66	0.13	0.40	0.37
Cr_2O_3	0.08	0.06	0.07	0.02	0.13	0.03	0.03	0.01	0.05	0.05	0.01	0.01	0.01	0.00	0.01	0.03	0.02	0.01
NiO	0.02	*<0.01*	0.02	0.01	0.06	*<0.01*	*<0.01*	*<0.01*	0.06	0.03	*<0.01*	*<0.01*	*<0.01*	0.00	*<0.01*	*<0.01*	*<0.01*	0.00
V_2O_5	0.06	0.08	0.07	0.02	0.06	0.06	0.06	0.04	0.05	0.01	0.06	0.08	0.07	0.01	0.05	0.05	0.05	0.00
ZrO_2	0.05	0.04	0.04	0.01	0.03	0.05	0.03	0.04	0.04	0.01	0.04	0.02	0.03	0.01	0.05	0.01	0.03	0.03
CuO	*<0.01*	*<0.01*	*<0.01*	0.00	*<0.01*	*<0.01*	*<0.01*	*<0.01*	*<0.01*	0.00	*<0.01*	*<0.01*	*<0.01*	0.00	*<0.01*	*<0.01*	*<0.01*	0.00
LOI	9.21	9.59	9.40	0.27	9.40	9.15	15.82	5.72	10.02	4.22	7.19	1.18	4.19	4.25	2.76	1.97	2.36	0.56
TOTAL	100.57	101.18	100.88	0.43	101.00	100.31	100.55	100.25	100.53	0.34	100.73	100.97	100.85	0.17	101.27	101.85	101.56	0.42

Table B6b: Trace Elements, XRF Results at Nhlowa.

XRF (ppm)	Colluvium				Residual Basalt						Highly Weathered Basalt				Rock Samples			
Test pit	SB02	SB17	Average	Standard Deviation	SB02	SB16	SB17	SB29	Average	Standard Deviation	SB16	SB23	Average	Standard Deviation	SB10A	SB10J	Average	Standard Deviation
Depth (m)	0.00-0.12	0.00-0.64			0.12-0.55	0.38-0.65	0.64-0.84	0.81-1.3			0.65-1.03	0.12-0.40			Surface	Surface		
As	22.97	25.91	24.44	2.08	31.05	28.15	23.42	21.15	25.94	4.48	16.62	26.62	21.62	7.07	22.98	18.50	20.74	3.17
Cu	136.14	225.76	180.95	63.37	144.39	131.86	189.27	195.68	165.30	31.90	97.24	224.15	160.69	89.74	136.56	133.64	135.10	2.06
Ga	22.47	22.33	22.40	0.10	27.91	21.46	22.73	24.38	24.12	2.80	21.78	23.83	22.80	1.45	27.85	20.82	24.33	4.98
Mo	2.16	4.90	3.53	1.94	3.85	1.30	3.81	4.03	3.25	1.30	7.57	3.90	5.74	2.59	3.71	2.03	2.87	1.19
Nb	21.25	27.43	24.34	4.37	20.40	23.31	19.87	31.95	23.88	5.58	25.80	17.53	21.66	5.85	31.44	8.02	19.73	16.56
Ni	191.47	100.18	145.83	64.55	579.00	74.92	89.17	57.12	200.05	252.97	68.49	54.44	61.47	9.93	61.44	72.33	66.89	7.70
Pb	10.29	8.91	9.60	0.98	17.83	16.49	5.36	8.70	12.09	6.03	12.54	4.75	8.64	5.51	11.78	9.00	10.39	1.97
Rb	50.56	56.72	53.64	4.36	49.30	51.83	46.38	45.38	48.22	2.93	53.00	22.18	37.59	21.79	68.89	50.39	59.64	13.08
Sr	141.64	137.40	139.52	3.00	225.13	350.92	174.59	414.66	291.33	110.71	505.61	301.60	403.60	144.26	902.17	460.98	681.57	311.97
Th	4.58	11.84	8.21	5.13	8.32	6.96	7.93	14.01	9.31	3.19	9.53	11.38	10.46	1.30	12.56	7.42	9.99	3.63
U	3.00	9.77	6.39	4.79	6.62	3.00	7.21	8.45	6.32	2.34	7.43	9.27	8.35	1.30	13.37	5.17	9.27	5.80
W*	229.33	101.20	165.26	90.60	6.00	94.56	6.00	90.08	49.16	49.87	6.00	6.00	6.00	0.00	6.00	91.15	48.58	60.21
Y	30.62	47.79	39.20	12.14	26.17	32.64	58.43	59.92	44.29	17.40	48.54	51.61	50.08	2.17	46.07	26.06	36.07	14.15
Zn	89.05	100.81	94.93	8.32	94.81	103.06	94.78	130.53	105.80	16.94	110.40	104.53	107.46	4.15	130.08	95.14	112.61	24.71
Zr	383.92	365.08	374.50	13.32	337.61	386.08	267.73	371.63	340.76	52.76	374.67	240.94	307.81	94.56	474.66	89.79	282.23	272.15
Cl*	7.58	7.58	7.58	0.00	7.58	7.58	7.58	7.58	7.58	0.00	7.58	7.58	7.58	0.00	7.58	7.58	7.58	0.00
Co	118.64	82.03	100.33	25.88	142.29	67.44	57.72	64.71	83.04	39.71	45.91	42.71	44.31	2.26	33.09	57.70	45.39	17.40
Cr	613.66	451.13	532.40	114.92	990.10	194.81	227.88	73.63	371.61	417.63	84.38	71.71	78.05	8.96	69.64	181.60	125.62	79.17
F*	100.00	100.00	100.00	0.00	100.00	100.00	100.00	100.00	100.00	0.00	100.00	100.00	100.00	0.00	100.00	100.00	100.00	0.00
S*	16.00	55.18	35.59	27.70	16.55	16.00	52.54	16.00	25.27	18.18	16.00	16.00	16.00	0.00	16.00	16.00	16.00	0.00
Sc	29.17	35.22	32.20	4.27	29.31	26.25	32.66	29.84	29.51	2.63	24.04	37.63	30.84	9.61	16.36	31.23	23.80	10.51
V	328.26	532.50	430.38	144.42	356.82	344.54	412.98	215.32	332.42	83.55	376.72	387.70	382.21	7.76	258.26	258.91	258.59	0.46
Cs	14.22	16.29	15.26	1.46	14.05	21.75	28.74	24.87	22.35	6.23	19.04	26.25	22.64	5.10	35.83	33.78	34.81	1.45
Ba	557.04	674.82	615.93	83.28	878.87	856.84	745.00	890.16	842.72	66.60	1460.58	531.71	996.14	656.81	1271.40	270.12	770.76	708.01
La	4.26	4.53	4.39	0.19	21.34	5.90	34.70	30.79	23.18	12.81	34.36	4.26	19.31	21.28	33.67	4.35	19.01	20.74
Ce	105.59	107.23	106.41	1.16	303.92	127.64	133.30	152.81	179.42	83.70	187.53	69.19	128.36	83.68	186.58	24.94	105.76	114.29

Results indicated with a * should be considered semi-quantitative.

Table B7a: Major Elements, XRF Results for the Sibasa Basalt at Siloam.

XRF (wt%)	Colluvium					Reworked Pebble Marker/ Residuum	Residual Basalt								
Test pit	TP01	TP03	TP05	Average	Standard Deviation	TP01	TP01	TP03	TP05	TP05	TP08	TP08	TP08	Average	Standard Deviation
Depth (m)	0.0-0.7	0.0-1.0	0.0-0.6			1.0-1.4	1.5-2.5	1.5-2.0	0.8-1.2	1.7	0.7-1.1	2.0-2.5	2.5-3.0		
SiO_2	45.85	49.73	48.59	48.06	2.00	69.98	51.37	51.12	41.65	48.08	48.18	49.02	47.65	48.15	3.23
TiO_2	2.18	1.82	1.87	1.95	0.19	0.60	1.63	1.53	1.69	1.69	1.69	1.38	1.49	1.59	0.12
Al_2O_3	6.76	16.24	16.86	13.29	5.66	7.80	15.05	14.12	15.53	14.78	14.17	14.50	15.45	14.80	0.57
Fe_2O_3	8.37	15.50	16.00	13.29	4.27	15.04	14.54	14.35	17.18	14.13	13.79	12.88	14.26	14.45	1.32
MnO	0.12	0.24	0.19	0.18	0.06	0.48	0.20	0.31	0.44	0.21	0.21	0.18	0.24	0.26	0.09
MgO	13.13	1.08	0.91	5.04	7.01	0.31	2.75	2.14	2.15	5.82	1.38	5.08	5.93	3.61	1.93
CaO	11.54	4.04	3.39	6.32	4.53	0.41	6.16	6.20	8.91	10.05	6.63	3.30	3.22	6.35	2.56
Na_2O	1.07	0.65	0.48	0.73	0.31	0.26	1.46	0.71	0.66	1.82	0.71	2.53	3.45	1.62	1.06
K_2O	1.19	0.42	0.32	0.65	0.48	0.20	0.16	0.29	0.23	0.44	0.41	0.81	0.92	0.46	0.29
P_2O_5	0.12	0.07	0.08	0.09	0.03	0.07	0.08	0.06	0.07	0.18	0.06	0.11	0.14	0.10	0.05
Cr_2O_3	0.08	0.03	0.03	0.05	0.03	0.03	0.02	0.02	0.03	0.03	0.03	0.02	0.02	0.02	0.00
NiO	0.04	0.01	0.01	0.02	0.02	0.01	0.01	0.02	0.02	0.03	0.01	0.01	0.02	0.02	0.00
V_2O_5	0.08	0.06	0.06	0.07	0.01	0.04	0.05	0.05	0.06	0.05	0.06	0.04	0.05	0.05	0.00
ZrO_2	0.04	0.03	0.03	0.03	0.01	0.01	0.02	0.02	0.02	0.02	0.03	0.02	0.02	0.02	0.00
CuO	0.00	0.02	0.02	0.01	0.01	0.01	0.02	0.02	0.02	0.02	0.02	0.02	0.02	0.02	0.00
LOI	9.36	10.08	11.14	10.20	0.90	4.69	7.15	8.70	12.21	2.84	11.64	10.23	6.60	8.48	3.27
TOTAL	99.95	100.01	99.99	99.98	0.03	99.94	100.69	99.66	100.87	100.20	99.01	100.14	99.48	100.01	0.67

Table B7b: Trace Elements, XRF Results for the Sibasa Basalt at Siloam.

XRF (ppm)	Colluvium					Reworked Pebble Marker/ Residuum	Residual Basalt								
Test pit	TP01	TP03	TP05	Average	Standard Deviation	TP01	TP01	TP03	TP05	TP05	TP08	TP08	TP08	Average	Standard Deviation
Depth (m)	0.0-0.7	0.0-1.0	0.0-0.6			1.0-1.4	1.5-2.5	1.5-2.0	0.8-1.2	1.7	0.7-1.1	2.0-2.5	2.5-3.0		
As	0	0	0	0.00	0.00	0	0	0	0	0	0	0	0	0.00	0.00
Cu	177	207	197	193.67	15.28	164	256	210	244	233	169	196	184	213.14	32.36
Ga	21	22	22	21.67	0.58	15	21	20	20	20	19	16	18	19.14	1.68
Mo	2	3	3	2.67	0.58	2	2	2	1	1	3	0	0	1.29	1.11
Nb	10	11	10	10.33	0.58	4	10	10	9	10	9	6	7	8.71	1.60
Ni	103	119	113	111.67	8.08	120	133	159	168	138	99	119	136	136.00	23.18
Pb	12	11	11	11.33	0.58	14	6	10	5	1	8	2	0	4.57	3.74
Rb	47	34	29	36.67	9.29	16	9	20	16	13	30	25	24	19.57	7.37
Sr	128	127	129	128.00	1.00	24	227	160	216	271	123	100	79	168.00	71.91
Th	2	0	0	0.67	1.15	0	0	1	0	0	0	0	0	0.14	0.38
U	0	0	0	0.00	0.00	0	0	0	0	0	0	0	0	0.00	0.00
W*	70	17	182	89.67	84.24	89	21	44	25	48	20	13	2	24.71	16.35
Y	32	37	35	34.67	2.52	8	34	30	32	29	32	23	27	29.57	3.69
Zn	91	74	68	77.67	11.93	26	91	74	75	118	58	93	101	87.14	19.84
Zr	199	195	195	196.33	2.31	68	155	153	167	156	184	115	119	149.86	24.84

Results indicated with a * should be considered semi-quantitative.

Table B8: Major and Trace Elements, XRF Results for the Springbok Flats Basalt at Codrington

XRF (wt %)	Residual Basalt		Highly Weathered Basalt	Slightly Weathered Basalt
Test pit	S01	S01	S01	SR
Depth (m)	0.00-0.30	0.30-1.00	1.00-2.00	Surface
SiO_2	46.40	52.94	47.00	50.52
TiO_2	2.49	0.86	0.93	0.97
Al_2O_3	11.50	13.22	14.33	14.85
Fe_2O_3	14.80	9.07	10.70	11.09
MnO	0.23	0.16	0.16	0.16
MgO	5.09	3.13	5.84	6.21
CaO	8.32	6.51	10.08	9.86
Na_2O	1.97	1.11	1.91	2.12
K_2O	0.62	0.61	0.51	0.46
P_2O_5	0.27	0.10	0.15	0.16
Cr_2O_3	0.01	0.03	0.03	0.03
NiO	0.01	0.01	0.01	0.01
V_2O_5	0.06	0.03	0.04	0.04
ZrO_2	0.02	0.02	0.01	0.01
CuO	0.02	0.01	0.01	0.01
LOI	9.19	10.59	6.92	2.81
TOTAL	101.01	98.39	98.62	99.31

ppm				
As	0	0	0.00	0.00
Cu	76	85	90.00	96.00
Ga	14	15	19.00	18.00
Mo	2	1	0.00	2.00
Nb	10	9	8.00	8.00
Ni	61	63	67.00	71.00
Pb	9	8	6.00	6.00
Rb	47	30	9.00	11.00
Sr	54	129	240.00	241.00
Th	0	0	0.00	0.00
U	0	0	0.00	0.00
W*	28	19	21.00	32.00
Y	26	24	21.00	23.00
Zn	71	74	85.00	84.00
Zr	202	146	107.00	105.00

Results indicated with a * should be considered semi-quantitative.

Appendix C

XRD Results

Table C1: XRD Results for Colluvium and Alluvium Horizons of the Mooiplaas Site

XRD (wt %)	Colluvium				Alluvium					
Sample nr	NB01	NB03	Average	Standard Deviation	NB30	NB30	NB31	NB32	Average	Standard Deviation
Depth (m)	0.00-0.40	0.00-0.25			0.00-0.38	0.38-0.61	0.00-0.90	0.00-0.24		
Augite	0.00	0.00	0.00	0.00	0.00	0.00	0.00	0.00	0.00	0.00
Diopside	9.93	8.22	9.08	1.21	6.39	8.06	7.76	0.00	5.55	3.77
Chlorite	0.00	0.00	0.00	0.00	0.00	0.00	0.00	0.00	0.00	0.00
Muscovite	0.00	0.00	0.00	0.00	0.00	0.00	0.00	0.00	0.00	0.00
Enstatite	0.00	0.00	0.00	0.00	0.00	0.00	0.00	0.00	0.00	0.00
Goethite	0.00	0.00	0.00	0.00	0.00	0.00	0.00	0.00	0.00	0.00
Kaolinite	0.00	0.00	0.00	0.00	0.00	0.00	0.00	0.00	0.00	0.00
Ilmenite	0.00	0.00	0.00	0.00	2.23	2.32	1.64	1.50	1.92	0.41
Magnetite	0.00	0.00	0.00	0.00	0.00	0.00	0.00	0.00	0.00	0.00
Hematite	6.12	0.00	3.06	4.33	0.00	0.00	0.00	0.00	0.00	0.00
Hornblende	0.00	3.85	1.93	2.72	0.00	0.00	0.00	0.00	0.00	0.00
Forsterite	0.00	0.00	0.00	0.00	0.00	0.00	0.00	0.00	0.00	0.00
Microcline	10.06	0.00	5.03	7.11	0.00	0.00	0.00	0.00	0.00	0.00
Orthoclase	0.00	0.00	0.00	0.00	6.14	6.75	0.00	0.00	3.22	3.73
Plagioclase	23.00	23.66	23.33	0.47	0.00	0.00	0.00	0.00	0.00	0.00
Quartz	50.88	14.59	32.74	25.66	16.10	14.93	7.28	24.29	15.65	6.96
Smectite	0.00	49.68	24.84	35.13	0.00	0.00	0.00	0.00	0.00	0.00
Titanite	0.00	0.00	0.00	0.00	0.00	0.00	0.00	0.00	0.00	0.00
Calcite, magnesian	0.00	0.00	0.00	0.00	6.63	13.98	3.56	4.07	7.06	4.80
Talc	0.00	0.00	0.00	0.00	0.00	0.00	0.00	0.00	0.00	0.00
Rutile	0.00	0.00	0.00	0.00	0.00	0.00	0.00	0.00	0.00	0.00
Palygorskite	0.00	0.00	0.00	0.00	62.50	53.95	79.76	45.88	60.52	14.51
Dolomite	0.00	0.00	0.00	0.00	0.00	0.00	0.00	24.26	6.07	12.13
Anatase	0.00	0.00	0.00	0.00	0.00	0.00	0.00	0.00	0.00	0.00
Analcime	0.00	0.00	0.00	0.00	0.00	0.00	0.00	0.00	0.00	0.00
Actinolite	0.00	0.00	0.00	0.00	0.00	0.00	0.00	0.00	0.00	0.00
Natrolite	0.00	0.00	0.00	0.00	0.00	0.00	0.00	0.00	0.00	0.00
Nepheline	0.00	0.00	0.00	0.00	0.00	0.00	0.00	0.00	0.00	0.00
Laumonite	0.00	0.00	0.00	0.00	0.00	0.00	0.00	0.00	0.00	0.00
Total	99.99	100.00	100.00	0.01	99.99	99.99	100.00	100.00	100.00	0.01

Average and Standard deviation calculations include samples with zero values

0.00 Zero Values are greyed out to accentuate quantitative values

Table C2: XRD Results for Reworked Residual Basalt Horizon of the Mooiplaas Site.

XRD (wt %)	Reworked Residual Basalt																	
Sample nr	**NB06**	**NB07**	**NB11**	**NB11**	**NB12**	**NB15**	**NB17**	**NB19**	**NB20**	**NB22**	**NB24**	**NB29**	**NB31**	**NB33**	**NB34**	**NB34**	**Average**	**Standard Deviation**
Depth (m)	**0.00-0.48**	**0.00-0.30**	**0.00-0.24**	**0.24-0.32**	**0.00-0.31**	**0.00-0.40**	**0.00-0.30**	**0.00-0.44**	**0.00-0.44**	**0.00-0.47**	**0.00-0.35**	**0.00-0.21**	**0.90-1.20**	**0.00-0.25**	**0.00-0.30**	**0.30-0.60**		
Augite	0.00	0.00	14.71	0.00	5.98	0.00	0.00	0.00	0.00	0.00	0.00	0.00	0.00	0.00	30.55	37.50	5.55	11.83
Diopside	4.83	2.58	0.00	18.74	0.00	8.03	4.97	2.47	16.43	6.69	3.98	1.16	6.11	14.12	0.00	0.00	5.63	5.99
Chlorite	0.00	0.00	0.00	0.00	0.00	0.00	0.00	0.00	0.00	0.00	0.00	0.00	0.00	0.00	0.00	0.00	0.00	0.00
Muscovite	0.00	0.00	0.00	4.50	1.71	0.00	0.00	0.00	0.00	0.00	0.00	0.00	0.00	0.00	0.00	0.00	0.39	1.18
Enstatite	0.00	0.00	0.00	0.00	0.00	0.00	0.00	0.00	0.00	0.00	0.00	6.96	0.00	20.57	0.00	0.00	1.72	5.32
Goethite	0.00	0.00	0.00	0.00	0.00	0.00	0.00	0.00	0.00	0.00	0.00	0.00	0.00	0.00	0.00	0.00	0.00	0.00
Kaolinite	0.00	0.00	0.00	0.00	0.00	0.00	0.00	0.00	0.00	0.00	0.00	0.00	0.00	0.00	0.00	0.00	0.00	0.00
Ilmenite	0.00	0.00	2.15	1.90	2.11	0.00	2.64	3.31	4.02	4.51	4.70	2.98	0.00	0.00	4.78	1.68	2.17	1.79
Magnetite	0.00	0.00	0.00	0.00	0.00	0.00	0.00	0.00	0.00	0.00	0.00	0.00	0.00	0.00	0.00	0.00	0.00	0.00
Hematite	1.93	0.00	0.00	0.00	0.00	0.00	0.00	0.00	0.00	0.00	0.00	0.00	0.00	0.00	0.00	0.00	0.12	0.48
Hornblende	0.00	0.00	0.00	0.00	0.00	0.00	0.00	0.00	0.00	0.00	0.00	0.00	0.00	0.00	4.74	0.00	0.30	1.19
Forsterite	0.00	0.00	0.00	0.00	0.00	0.00	0.00	0.00	0.00	0.00	0.00	0.00	0.00	0.00	0.00	0.00	0.00	0.00
Microcline	0.00	0.00	0.00	0.00	0.00	0.00	0.00	0.00	0.00	0.00	0.00	0.00	0.00	0.00	0.00	0.00	0.00	0.00
Orthoclase	0.00	0.00	0.00	0.00	0.00	17.08	0.00	0.00	0.00	18.13	16.24	6.97	5.45	0.00	19.24	15.09	6.14	7.99
Plagioclase	14.22	6.43	9.44	11.71	9.09	4.72	7.49	7.03	12.06	0.00	0.00	0.00	0.00	21.34	12.63	30.66	9.18	8.30
Quartz	16.51	14.43	7.14	5.84	20.93	9.23	18.98	12.19	19.37	19.89	15.00	19.97	12.01	30.39	23.37	8.46	15.86	6.61
Smectite	62.50	38.83	55.31	47.67	60.17	60.94	65.92	49.20	48.12	50.77	60.09	61.95	0.00	0.00	0.00	0.00	41.34	25.61
Titanite	0.00	0.00	0.00	0.00	0.00	0.00	0.00	0.00	0.00	0.00	0.00	0.00	0.00	0.00	0.00	0.00	0.00	0.00
Calcite, magnesian	0.00	27.64	0.00	0.00	0.00	0.00	0.00	2.08	0.00	0.00	0.00	0.00	2.10	13.58	4.68	6.58	3.54	7.40
Talc	0.00	0.00	0.00	2.70	0.00	0.00	0.00	0.00	0.00	0.00	0.00	0.00	0.00	0.00	0.00	0.00	0.17	0.68
Rutile	0.00	0.00	0.00	0.00	0.00	0.00	0.00	0.00	0.00	0.00	0.00	0.00	0.00	0.00	0.00	0.00	0.00	0.00
Palygorskite	0.00	10.09	11.25	6.94	0.00	0.00	0.00	23.71	0.00	0.00	0.00	0.00	53.55	0.00	0.00	0.00	6.60	14.17
Dolomite	0.00	0.00	0.00	0.00	0.00	0.00	0.00	0.00	0.00	0.00	0.00	0.00	20.77	0.00	0.00	0.00	1.30	5.19
Anatase	0.00	0.00	0.00	0.00	0.00	0.00	0.00	0.00	0.00	0.00	0.00	0.00	0.00	0.00	0.00	0.00	0.00	0.00
Analcime	0.00	0.00	0.00	0.00	0.00	0.00	0.00	0.00	0.00	0.00	0.00	0.00	0.00	0.00	0.00	0.00	0.00	0.00
Actinolite	0.00	0.00	0.00	0.00	0.00	0.00	0.00	0.00	0.00	0.00	0.00	0.00	0.00	0.00	0.00	0.00	0.00	0.00
Natrolite	0.00	0.00	0.00	0.00	0.00	0.00	0.00	0.00	0.00	0.00	0.00	0.00	0.00	0.00	0.00	0.00	0.00	0.00
Nepheline	0.00	0.00	0.00	0.00	0.00	0.00	0.00	0.00	0.00	0.00	0.00	0.00	0.00	0.00	0.00	0.00	0.00	0.00
Laumonite	0.00	0.00	0.00	0.00	0.00	0.00	0.00	0.00	0.00	0.00	0.00	0.00	0.00	0.00	0.00	0.00	0.00	0.00
Total	99.99	100.00	100.00	100.00	99.99	100.00	100.00	99.99	100.00	99.99	100.01	99.99	99.99	100.00	99.99	99.97	99.99	0.01

Average and Standard deviation calculations include samples with zero values

0.00 Zero Values are greyed out to accentuate quantitative values

Table C3: XRD Results for Residual Basalt Horizon of the Mooiplaas Site.

XRD (wt %)	Residual Basalt																	
Sample nr	NB01	NB03	NB06	NB07	NB11	NB12	NB12	NB17	NB19	NB20	NB22	NB23	NB24	NB24	NB29	NB34	Average	Standard Deviation
Depth (m)	0.40-0.50	0.25-0.50	0.48-0.88	0.30-0.73	0.32-0.58	0.31-0.50	0.50-1.48	0.30-0.42	0.44-0.95	0.44-1.07	0.47-0.96	0.59-0.87	0.35-0.70	0.70-0.80	0.21-0.64	0.60-0.80		
Augite	0.00	0.00	0.00	0.00	0.00	3.65	7.84	0.00	0.00	0.00	0.00	0.00	0.00	0.00	0.00	20.07	1.97	5.26
Diopside	6.16	21.53	12.82	3.86	24.20	0.00	0.00	0.00	5.09	11.08	13.29	16.83	17.78	6.89	11.14	0.00	9.42	7.93
Chlorite	0.00	0.00	25.67	0.00	0.00	0.00	0.00	0.00	0.00	0.00	0.00	0.00	0.00	0.00	0.00	0.00	1.60	6.42
Muscovite	0.00	4.77	0.00	1.82	0.00	0.00	0.00	0.00	0.00	0.00	0.00	0.00	0.00	0.00	0.00	0.00	0.41	1.25
Enstatite	0.00	0.00	0.00	0.00	0.00	0.00	0.00	0.00	0.00	0.00	0.00	0.00	0.00	0.00	0.00	0.00	0.00	0.00
Goethite	0.00	0.00	0.00	0.00	0.00	0.00	0.00	0.00	0.00	0.00	0.00	0.00	0.00	0.00	0.00	0.00	0.00	0.00
Kaolinite	0.00	0.00	0.00	0.00	0.00	0.00	0.00	0.00	0.00	0.00	0.00	0.00	0.00	0.00	0.00	0.00	0.00	0.00
Ilmenite	0.00	0.00	0.00	0.00	2.54	0.97	0.00	1.21	2.81	2.57	3.61	2.36	5.26	2.13	2.43	3.30	1.82	1.59
Magnetite	0.00	0.00	0.00	0.00	0.00	0.00	0.00	0.00	0.00	0.00	0.00	0.00	0.00	0.00	0.00	0.00	0.00	0.00
Hematite	2.97	0.00	0.00	0.00	0.00	0.00	0.44	0.00	0.00	0.00	0.00	0.00	0.00	0.00	0.00	0.00	0.21	0.74
Hornblende	3.94	3.46	0.00	0.00	0.00	0.00	0.00	0.00	0.00	0.00	0.00	0.00	0.00	0.00	0.00	0.00	0.46	1.27
Forsterite	0.00	0.00	0.00	0.00	0.00	0.00	0.00	0.00	0.00	0.00	0.00	0.00	0.00	0.00	0.00	0.00	0.00	0.00
Microcline	0.00	0.00	0.00	0.00	0.00	0.00	0.00	0.00	0.00	0.00	0.00	0.00	0.00	0.00	0.00	0.00	0.00	0.00
Orthoclase	0.00	0.00	0.00	0.00	0.00	0.00	0.00	0.00	0.00	8.75	20.59	14.36	20.08	9.20	0.00	10.60	5.22	7.62
Plagioclase	23.18	31.46	19.14	2.40	18.91	6.92	9.73	0.00	5.13	0.00	0.00	0.00	0.00	0.00	5.89	10.00	8.30	9.86
Quartz	20.86	6.00	1.34	8.79	0.71	10.54	3.77	7.39	2.51	4.65	4.92	2.46	11.04	7.47	4.71	0.00	6.07	5.16
Smectite	42.89	22.11	41.03	25.72	44.20	39.07	50.32	0.00	57.47	47.00	36.25	40.96	45.84	22.05	37.60	34.67	36.70	13.77
Titanite	0.00	0.00	0.00	0.00	0.00	0.00	0.00	0.00	0.00	0.00	0.00	0.00	0.00	0.00	0.00	0.00	0.00	0.00
Calcite, magnesian	0.00	10.68	0.00	0.00	9.44	32.20	27.90	90.17	0.00	25.93	21.34	16.65	0.00	52.26	38.22	21.37	21.64	24.10
Talc	0.00	0.00	0.00	0.00	0.00	0.00	0.00	0.00	0.00	0.00	0.00	6.38	0.00	0.00	0.00	0.00	0.40	1.60
Rutile	0.00	0.00	0.00	0.00	0.00	0.00	0.00	1.23	0.00	0.00	0.00	0.00	0.00	0.00	0.00	0.00	0.08	0.31
Palygorskite	0.00	0.00	0.00	57.41	0.00	6.65	0.00	0.00	26.99	0.00	0.00	0.00	0.00	0.00	0.00	0.00	5.69	15.38
Dolomite	0.00	0.00	0.00	0.00	0.00	0.00	0.00	0.00	0.00	0.00	0.00	0.00	0.00	0.00	0.00	0.00	0.00	0.00
Anatase	0.00	0.00	0.00	0.00	0.00	0.00	0.00	0.00	0.00	0.00	0.00	0.00	0.00	0.00	0.00	0.00	0.00	0.00
Analcime	0.00	0.00	0.00	0.00	0.00	0.00	0.00	0.00	0.00	0.00	0.00	0.00	0.00	0.00	0.00	0.00	0.00	0.00
Actinolite	0.00	0.00	0.00	0.00	0.00	0.00	0.00	0.00	0.00	0.00	0.00	0.00	0.00	0.00	0.00	0.00	0.00	0.00
Natrolite	0.00	0.00	0.00	0.00	0.00	0.00	0.00	0.00	0.00	0.00	0.00	0.00	0.00	0.00	0.00	0.00	0.00	0.00
Nepheline	0.00	0.00	0.00	0.00	0.00	0.00	0.00	0.00	0.00	0.00	0.00	0.00	0.00	0.00	0.00	0.00	0.00	0.00
Laumonite	0.00	0.00	0.00	0.00	0.00	0.00	0.00	0.00	0.00	0.00	0.00	0.00	0.00	0.00	0.00	0.00	0.00	0.00
Total	100.00	100.01	100.00	100.00	100.00	100.00	100.00	100.00	100.00	99.98	100.00	100.00	100.00	100.00	99.99	100.01	100.00	0.01

Average and Standard deviation calculations include samples with zero values

0.00 Zero Values are greyed out to accentuate quantitative values

Table C4: XRD Results for Highly Weathered Basalt Horizon and Rocks of the Mooiplaas Site.

XRD (wt %)	Highly weathered Basalt							Rock samples							
Sample nr	NB01	NB12	NB15	NB19	NB34-4	Average	Standard Deviation	NB14	NB17	NB29	NB27	Outcrop 4	Outcrop 5	Average	Standard Deviation
Depth (m)	0.50-0.80	1.48-1.72	0.40-0.45	0.95	0.80-0.90			Surface	Surface	Surface	0.40-0.60				
Augite	0.00	8.22	0.00	0.00	26.71	6.99	11.59	26.49	44.16	47.83	26.34	46.57	61.51	42.15	13.61
Diopside	16.98	0.00	28.55	6.29	0.00	10.36	12.31	0.00	0.00	0.00	0.00	0.00	0.00	0.00	0.00
Chlorite	0.00	0.00	0.00	0.00	0.00	0.00	0.00	0.00	0.00	0.00	0.00	0.00	0.00	0.00	0.00
Muscovite	3.75	0.00	1.78	0.00	0.00	1.11	1.67	0.00	0.00	0.00	0.00	1.42	4.15	0.93	1.68
Enstatite	0.00	0.00	0.00	0.00	0.00	0.00	0.00	0.00	0.00	0.00	0.00	0.00	0.00	0.00	0.00
Goethite	0.00	0.00	0.00	0.00	0.00	0.00	0.00	0.00	0.00	0.00	0.00	0.00	0.00	0.00	0.00
Kaolinite	0.00	0.00	0.00	0.00	0.00	0.00	0.00	0.00	0.00	0.00	0.00	0.00	0.00	0.00	0.00
Ilmenite	0.00	0.60	3.88	2.47	2.83	1.96	1.61	0.00	3.03	4.52	0.00	0.00	0.00	1.26	2.01
Magnetite	0.00	0.00	0.00	0.00	0.00	0.00	0.00	9.07	0.00	0.00	0.00	5.48	5.84	3.40	3.93
Hematite	3.48	0.18	0.00	0.00	0.00	0.73	1.54	0.00	0.00	0.00	0.00	1.62	2.12	0.62	0.98
Hornblende	2.79	0.00	0.87	0.00	0.00	0.73	1.21	0.00	0.00	0.00	0.00	7.22	0.00	1.20	2.95
Forsterite	0.00	0.00	0.00	0.00	0.00	0.00	0.00	0.00	22.96	10.45	0.00	0.00	0.00	5.57	9.49
Microcline	0.00	0.00	0.00	0.00	0.00	0.00	0.00	0.00	0.00	0.00	0.00	0.00	0.00	0.00	0.00
Orthoclase	0.00	0.00	0.00	0.00	9.76	1.95	4.36	0.00	0.00	0.00	9.52	0.00	0.00	1.59	3.89
Plagioclase	32.88	9.74	22.92	8.49	12.09	17.22	10.44	0.00	29.86	37.20	0.00	0.00	0.00	11.18	17.47
Quartz	14.26	2.93	2.57	2.41	0.00	4.43	5.61	0.00	0.00	0.00	0.00	0.00	0.00	0.00	0.00
Smectite	25.85	40.87	39.44	52.43	25.86	36.89	11.26	0.00	0.00	0.00	56.29	0.00	0.00	9.38	22.98
Titanite	0.00	0.00	0.00	0.00	0.00	0.00	0.00	0.00	0.00	0.00	0.00	0.00	0.00	0.00	0.00
Calcite, magnesian	0.00	37.46	0.00	27.90	22.75	17.62	16.93	4.94	0.00	0.00	0.00	0.00	0.00	0.82	2.02
Talc	0.00	0.00	0.00	0.00	0.00	0.00	0.00	0.00	0.00	0.00	0.00	0.00	0.00	0.00	0.00
Rutile	0.00	0.00	0.00	0.00	0.00	0.00	0.00	0.00	0.00	0.00	0.00	0.00	0.00	0.00	0.00
Palygorskite	0.00	0.00	0.00	0.00	0.00	0.00	0.00	0.00	0.00	0.00	0.00	0.00	0.00	0.00	0.00
Dolomite	0.00	0.00	0.00	0.00	0.00	0.00	0.00	0.00	0.00	0.00	0.00	0.00	0.00	0.00	0.00
Anatase	0.00	0.00	0.00	0.00	0.00	0.00	0.00	0.00	0.00	0.00	0.00	0.00	0.00	0.00	0.00
Analcime	0.00	0.00	0.00	0.00	0.00	0.00	0.00	0.00	0.00	0.00	3.35	11.53	11.98	4.48	5.79
Actinolite	0.00	0.00	0.00	0.00	0.00	0.00	0.00	9.22	0.00	0.00	0.00	0.00	0.00	1.54	3.76
Natrolite	0.00	0.00	0.00	0.00	0.00	0.00	0.00	50.28	0.00	0.00	0.00	12.25	14.40	12.82	19.49
Nepheline	0.00	0.00	0.00	0.00	0.00	0.00	0.00	0.00	0.00	0.00	0.00	13.92	0.00	2.32	5.68
Laumonite	0.00	0.00	0.00	0.00	0.00	0.00	0.00	0.00	0.00	0.00	4.50	0.00	0.00	0.75	1.84
Total	99.99	100.00	100.01	99.99	100.01	100.00	0.01	100.00	100.01	100.00	100.00	100.01	100.00	100.00	0.01

Average and Standard deviation calculations include samples with zero values

0.00 Zero Values are greyed out to accentuate quantitative values

Table C5: XRD results for the Nhlowa site.

XRD (wt %)	Colluvium				Residual Basalt						Highly Weathered Basalt				Rock Sample			
Sample nr	SB02	SB17	Average	Standard Deviation	SB02	SB16	SB17	SB29	Average	Standard Deviation	SB16	SB23	Average	Standard Deviation	SB10A	SB10J	Average	Standard Deviation
Depth (m)	0.00-0.12	0.00-0.64			0.12-0.55	0.38-0.65	0.64-0.84	1.30			0.65-1.03	0.12-0.40			Surface	Surface		
Augite	0.00	0.00	0.00	0.00	0.00	0.00	0.00	0.00	0.00	0.00	0.00	0.00	0.00	0.00	0.00	0.00	0.00	0.00
Diopside	3.60	4.43	4.02	0.59	4.75	0.00	0.00	0.00	1.19	2.38	2.19	33.72	17.96	22.30	0.00	31.30	15.65	22.13
Chlorite	0.00	0.00	0.00	0.00	3.56	0.00	0.00	0.00	0.89	1.78	0.00	3.91	1.96	2.76	22.80	18.21	20.51	3.25
Muscovite	0.00	0.00	0.00	0.00	0.00	0.00	16.07	11.04	6.78	8.09	0.00	0.00	0.00	0.00	0.00	8.14	4.07	5.76
Enstatite	0.00	0.00	0.00	0.00	0.00	5.90	0.00	0.00	1.48	2.95	0.00	0.00	0.00	0.00	0.00	4.18	2.09	2.96
Goethite	0.00	48.04	24.02	33.97	0.00	0.00	0.00	0.00	0.00	0.00	0.00	0.00	0.00	0.00	0.00	0.00	0.00	0.00
Kaolinite	0.00	0.00	0.00	0.00	0.00	0.00	0.00	0.00	0.00	0.00	0.00	0.00	0.00	0.00	0.00	0.00	0.00	0.00
Ilmenite	8.88	4.65	6.77	2.99	6.55	6.10	5.01	5.02	5.67	0.78	0.00	0.00	0.00	0.00	0.00	0.00	0.00	0.00
Magnetite	0.00	0.00	0.00	0.00	0.00	0.00	3.18	0.00	0.80	1.59	0.00	0.00	0.00	0.00	0.00	0.00	0.00	0.00
Hematite	0.00	0.00	0.00	0.00	0.00	0.00	0.00	0.00	0.00	0.00	0.00	0.00	0.00	0.00	1.42	0.00	0.71	1.00
Hornblende	0.00	0.00	0.00	0.00	0.00	0.00	0.00	0.00	0.00	0.00	0.00	0.00	0.00	0.00	0.00	4.46	2.23	3.15
Forsterite	0.00	0.00	0.00	0.00	0.00	0.00	0.00	0.00	0.00	0.00	0.00	0.00	0.00	0.00	0.00	0.00	0.00	0.00
Microcline	9.37	4.44	6.91	3.49	8.23	0.00	8.00	5.59	5.46	3.83	8.39	0.00	4.20	5.93	31.92	0.00	15.96	22.57
Orthoclase	0.00	0.00	0.00	0.00	0.00	18.36	0.00	0.00	4.59	9.18	0.00	0.00	0.00	0.00	0.00	0.00	0.00	0.00
Plagioclase	14.98	5.60	10.29	6.63	10.90	18.50	7.11	14.99	12.88	4.94	19.45	58.03	38.74	27.28	28.73	33.70	31.22	3.51
Quartz	63.17	32.84	48.01	21.45	66.01	51.14	22.44	45.14	46.18	18.10	10.63	4.34	7.49	4.45	4.31	0.00	2.16	3.05
Smectite	0.00	0.00	0.00	0.00	0.00	0.00	0.00	18.22	4.56	9.11	59.34	0.00	29.67	41.96	0.00	0.00	0.00	0.00
Titanite	0.00	0.00	0.00	0.00	0.00	0.00	0.00	0.00	0.00	0.00	0.00	0.00	0.00	0.00	10.83	0.00	5.42	7.66
Calcite, magnesian	0.00	0.00	0.00	0.00	0.00	0.00	38.19	0.00	9.55	19.10	0.00	0.00	0.00	0.00	0.00	0.00	0.00	0.00
Total	100.00	100.00	100.00	0.00	100.00	100.00	100.00	100.00	100.00	0.00	100.00	100.00	100.00	0.00	100.01	99.99	100.00	0.01

Average and Standard deviation calculations include samples with zero values

0.00 Zero Values are greyed out to accentuate quantitative values

Table C6: XRD results for the Sibasa Basalts at Siloam

XRD (wt %)	Colluvium					Reworked Pebble Marker/ Residuum	Residual Basalt								
Sample nr	TP01	TP03	TP05	Average	Standard Deviation	TP01	TP01	TP03	TP05	TP05	TP08	TP08	TP08	Average	Standard Deviation
Depth (m)	0.0-0.7	0.0-1.0	0.0-0.6			1.0-1.4	1.5-2.5	1.5-2.0	0.8-1.0	1.7	0.7-1.1	2.0-2.5	2.5-3.0		
Augite	0.00	0.00	0.00	0.00	0.00	0.00	0.00	0.00	0.00	0.00	0.00	1.51	4.01	0.79	1.53
Actinolite	0.00	0.00	0.00	0.00	0.00	0.00	0.00	0.00	0.00	3.25	0.00	0.00	5.05	1.19	2.09
Diopside	0.00	0.00	0.00	0.00	0.00	0.00	0.00	0.00	0.00	21.63	0.00	0.00	0.00	3.09	8.18
Epidote	10.91	10.28	17.18	12.79	3.81	0.00	18.89	12.78	13.80	23.57	10.56	5.10	0.00	12.10	7.95
Chlorite	4.43	7.52	0.00	3.98	3.78	0.00	5.62	3.37	7.98	27.71	4.03	8.63	8.98	9.47	8.34
Muscovite	3.24	0.00	0.00	1.08	1.87	0.00	0.00	0.00	0.00	0.00	0.00	0.00	0.00	0.00	0.00
Enstatite	0.00	0.00	0.00	0.00	0.00	0.00	0.00	0.00	0.00	0.00	0.00	0.00	0.00	0.00	0.00
Goethite_	0.00	0.00	14.93	4.98	8.62	20.75	0.00	0.00	0.00	0.00	0.00	0.00	0.00	0.00	0.00
Kaolinite	0.00	0.00	20.95	6.98	12.10	0.00	0.00	0.00	0.00	0.00	0.00	0.00	0.00	0.00	0.00
Ilmenite	0.00	0.00	0.00	0.00	0.00	0.00	0.00	0.00	0.00	0.00	0.00	0.00	0.00	0.00	0.00
Magnetite_	0.00	0.00	0.00	0.00	0.00	0.00	0.00	0.00	0.00	0.00	0.00	0.00	0.00	0.00	0.00
Hematite	4.58	0.00	3.89	2.82	2.47	4.94	0.00	0.00	0.00	0.00	2.25	0.00	0.00	0.32	0.85
Hornblende	0.00	0.00	0.00	0.00	0.00	0.00	0.00	0.00	0.00	0.00	0.00	0.00	0.00	0.00	0.00
Microcline	0.00	0.00	0.00	0.00	0.00	0.00	0.00	0.00	0.00	0.00	0.00	6.20	6.98	1.88	3.22
Orthoclase	0.00	0.00	0.00	0.00	0.00	0.00	0.00	0.00	0.00	0.00	0.00	0.00	0.00	0.00	0.00
Plagioclase	6.52	18.24	6.37	10.38	6.81	0.00	13.86	3.20	4.41	11.10	6.53	16.81	26.54	11.78	8.20
Quartz	30.50	28.50	36.68	31.89	4.26	74.32	21.45	27.37	14.36	12.74	20.50	12.71	3.77	16.13	7.67
Smectite	39.82	32.95	0.00	24.26	21.29	0.00	40.18	53.28	51.69	0.00	46.51	49.04	44.67	40.77	18.51
Titanite	0.00	0.00	0.00	0.00	0.00	0.00	0.00	0.00	0.00	0.00	0.00	0.00	0.00	0.00	0.00
Calcite, magnesian	0.00	2.51	0.00	0.84	1.45	0.00	0.00	0.00	7.77	0.00	9.62	0.00	0.00	2.48	4.28
Total	100.00	100.00	100.00	100.00	0.00	100.01	100.00	100.00	100.01	100.00	100.00	100.00	100.00	100.00	0.00

Average and Standard deviation calculations include samples with zero values

0.00 Zero Values are greyed out to accentuate quantitative values

Table C7: XRD results for the Springbok Flats Basalt at Codrington

XRD (wt %)	Residual Basalt		Highly Weathered Basalt	Slightly Weathered Basalt
Sample nr	**S01**	**S01**	**S01**	**SR**
Depth (m)	**0.0-0.3**	**0.3-1.0**	**1.0-2.0**	**Surface**
Augite	0.00	14.52	19.59	24.73
Actinolite	0.00	0.00	0.00	0.00
Diopside	0.00	0.00	0.00	0.00
Epidote	0.00	0.00	0.00	0.00
Chlorite	0.00	0.00	0.00	0.00
Muscovite	0.00	0.00	0.00	0.00
Enstatite	0.00	8.54	0.00	0.00
Goethite_	0.00	0.00	0.00	0.00
Kaolinite	0.00	0.00	0.00	0.00
Ilmenite	0.00	0.00	0.00	0.00
Magnetite_	0.00	0.00	0.00	0.00
Hematite	0.00	0.00	0.00	2.24
Hornblende	0.00	0.00	0.00	0.00
Microcline	6.90	11.18	0.00	0.00
Orthoclase	0.00	0.00	0.00	0.00
Plagioclase	6.96	11.23	41.42	43.95
Quartz	34.95	20.39	3.14	5.13
Smectite	51.19	26.37	35.85	23.96
Titanite	0.00	0.00	0.00	0.00
Calcite, magnesian	0.00	7.77	0.00	0.00
Total	100.00	100.00	100.00	100.01

Average and Standard deviation calculations include samples with zero values

0.00 Zero Values are greyed out to accentuate quantitative values